CHARACTERIZATION OF THE BETA-SUBUNIT OF THE MAMMALIAN SRP RECEPTOR AND ITS ROLE IN ASSEMBLY OF THE SRP RECEPTOR

By

KYLE R. LEGATE, B. Sc.

A Thesis
Submitted to the School of Graduate Studies
In Partial Fulfillment of the Requirements
for the Degree
Doctor of Philosophy

McMaster University

CHARACTERIZATION OF THE TRANSLOCATION GTPASE SRβ

Doctor of Philosophy (2003)
(Biochemistry)

McMaster University
Hamilton, Ontario

TITLE: Characterization of the beta-subunit of the mammalian SRP receptor and its role in assembly of the SRP receptor

AUTHOR: Kyle R. Legate, B. Sc. (McMaster University)

SUPERVISOR: Dr. David W. Andrews

NUMBER OF PAGES:

ABSTRACT

The eukaryotic signal recognition particle (SRP) receptor is a heterodimeric complex present on the endoplasmic reticulum (ER) membrane, and is required for the targeting and translocation of nascent polypeptide chains across the ER. Both SRP receptor subunits, SRα and SRβ, are GTP-binding proteins. The role of the SRα subunit in the nascent chain targeting reaction is well understood, but the function of the SRβ subunit has not been determined.

This thesis demonstrates that a complete and functional GTP-binding domain of SRβ is necessary to bind SRα, and that the integrity of the SRα-SRβ dimer is regulated by the SRβ GTPase. Further analysis of SRβ revealed functional characteristics that are not shared with other GTPases. Most significantly, whereas other GTPases purify in the GDP-bound inactive state, SRβ purified in the GTP-bound active state. Furthermore, SRβ bound specifically to ribosomes, but ribosome-binding did not influence the activity of SRβ.

The recently solved structure of the SRα-SRβ complex from yeast allows for the discussion of my results from a structural perspective. The results of this work in combination with the published literature allow me to update the existing model for protein targeting and translocation in higher eukaryotes. In this new model SRβ plays a greater role than previously appreciated.

ACKNOWLEDGEMENTS

I would like to acknowledge the guidance and patience of my supervisor, Dr. David W. Andrews, and the members of my supervisory committee, Drs. Gerber, Whyte and Nodwell. Thank you for forcing me onto the straight and narrow.

I would like to thank the following colleagues for stimulating discussion at various stages of this work: Jason, Jon, Peter, Mina, Matt, Iain, Martin, Felicia, Matthew; I would like to thank the rest for comic relief.

Thank you to my friends in various branches of science and engineering, for lengthy discussions from different perspectives; and to all my friends, from whatever discipline, for allowing me to maintain a semblance of sanity.

Thank you to the always influential forces of Chaos, for keeping everything interesting.

I would like to thank my family, particularly my Mother Joan and brother Kris for pretending to understand what I was talking about while I described the SRP pathway using a plate of spaghetti, and for their support.

Finally I would like to thank Aline Fiebig for her love and support. You are my foundation.

TABLE OF CONTENTS

LIST OF ABBREVIATIONS

ATP	Adenosine 5'-triphosphate
BMH	*bis*-maleimidohexane
DMSO	Dimethyl sulfoxide
DNA	Deoxyribonucleic acid
DTT	Dithiothreitol
E. coli	*Escherichia coli*
EDTA	(ethylenedinitrolo)-tetraacetic acid
EK	Enterokinase
ER	Endoplasmic reticulum
FPLC	Fast performance liquid chromatography
GAP	GTPase activating protein
GDP	Guanosine 5'-diphosphate
GFP	Green fluorescent protein
GMP	Guanosine 5'-monophosphate
GMPPNP	Guanosine 5'-[β,γ-imido]triphosphate
GRF	Guanine nucleotide release factor
GTP	Guanosine 5'-triphosphate
HA	Hemagglutinin
HPLC	High performance liquid chromatography
K_d	Affinity of dissociation
KRM	Salt washed rough microsomes
mant-	2'-(or 3')-*O*(*N*-methylanthraniloyl)-
NEM	*N*-ethylmaleimide
Ni-NTA	Nickel-nitrilotriacetic acid
OAc	Acetate
PMSF	Phenylmethylsulfonyl fluoride
RET	Resonance energy transfer
RNA	Ribonucleic acid
RNC	Ribosome-nascent chain
S. cerevisiae	*Saccharomyces cerevisiae*
SDS-PAGE	sodium dodecyl sulfate-polyacrylamide gel electrophoresis
SR	SRP receptor
SRα	SRP receptor, alpha subunit
SRβ	SRP receptor, beta subunit
SRP	Signal recognition particle
SRX(2)	SRβ-binding region of SRα
TCA	Trichloroacetic acid
TLC	Thin layer chromatography
TX100	Triton X-100 (nonionic detergent)

XDP	Xanthosine 5'-diphosphate
XTP	Xanthosine 5'-triphosphate
XMPPNP	Xanthosine 5'-[β,γ-imido]triphosphate

LIST OF TABLES

LIST OF FIGURES

PREFACE

Data presented in Chapter 2 originally appeared in the following publications:

1. Young JC, Ursini J, Legate KR, Miller JD, Walter P, Andrews DW. An amino-terminal domain containing hydrophobic and hydrophilic sequences binds the signal recognition particle receptor alpha subunit to the beta subunit on the endoplasmic reticulum membrane. (1995) *J. Biol. Chem.* **270**:15650-15657.
2. Legate KR, Falcone D, Andrews DW. Nucleotide-dependent binding of the GTPase domain of the signal recognition particle receptor beta-subunit to the alpha-subunit. (2000) *J. Biol. Chem.* **275**:27439-27446.

Data presented in Chapter 3 originally appeared in the following publication:

3. Legate KR, Andrews DW. The β subunit of the SRP receptor is a novel GTP binding protein without intrinsic GTPase activity. (2003) *J. Biol. Chem.* in press.

The following figures contain data from experiments performed by Mina Falcone:

Figure 2.3, Figure 2.9.

1. INTRODUCTION

All life, from the simplest cells to the most complex organisms, consists of a series of chemical reactions that are concentrated and sequestered from the environment by biological membranes. The simplest forms of life are defined by a single cell membrane enclosing all materials required for reproduction and growth. More complicated cells contain systems of biological membranes, defining the boundaries of organelles, which in turn are surrounded by an outer cell membrane to provide a protective barrier from the environment.

Biological membranes display selective permeability by allowing the passage of distinct sets of molecules. The properties of biological membranes are largely determined by the proteins that reside on and within them; these proteins determine the selectivity and directionality of transmembrane transport. Without these proteins, biological membranes would be impermeable lipid bilayers, unable to accept the passage of hydrophilic molecules. One of the most difficult molecules to transport across a membrane is a polypeptide chain due to its large size and significant hydrophilic character. For this reason, cells have developed specific, evolutionarily-conserved mechanisms by which proteins are inserted into, and transported across, biological membranes. This process is referred to as protein translocation.

Bacteria, for which *E. coli* is a model organism, possess three mechanisms for the transport of proteins across the plasma membrane: a post-translational pathway used for general secretion (the Sec pathway), a post-translational pathway for the transport of folded, cofactor-containing proteins (the twin-arginine translocation (Tat) pathway) and a pathway for the co-translational integration of proteins containing hydrophobic transmembrane sequences (the SRP pathway). Lower eukaryotes, for which *S. cerevisiae* is a model organism (hereafter referred to as yeast), have retained a post-translational pathway analogous to the *E. coli* Sec pathway, and a co-translational SRP pathway. Both pathways converge at the endoplasmic reticulum (ER), the organelle from which the cell membrane, Golgi apparatus and transport vesicles are derived. Higher eukaryotes appear to possess only a co-translational SRP pathway operating at the ER.

This introduction will describe each pathway that has developed to translocate proteins into and across the *E. coli* cell membrane and eukaryotic ER, but will focus mainly on the most highly conserved pathway, the SRP pathway. The first section will introduce the protein factors involved in each pathway; the second section will outline the mechanistic details of the SRP pathway; the third section will provide a closer examination of the translocation GTPases that maintain the directionality and fidelity of protein translocation; and the final section will outline my studies on the beta subunit of the SRP receptor (SRβ), a translocation GTPase.

1.1 Protein translocation systems in higher eukaryotes: the SRP pathway

With few exceptions (Watts et al., 1983; Zimmermann and Mollay, 1986; Klappa et al., 1994), protein translocation across the ER in higher eukaryotes occurs co-

translationally (Klappa et al., 1994). The vast majority of proteins destined for insertion into, and translocation across the ER membrane are distinguished from cytoplasmic proteins by an amino-terminal signal sequence. Signal sequences from different proteins demonstrate no sequence homology, but all share a hydrophobic core of at least six amino acids (von Heijne, 1985). A class of proteins called tail-anchor proteins do not depend on the presence of a signal peptide and therefore provide the exception to this rule. Distinguished by a carboxyl-terminal transmembrane domain, they are directed to their target membrane by carboxyl-terminal sequences and therefore must be targeted and inserted post-translationally (reviewed in (Wattenberg and Lithgow, 2001)).

When a secretory or integral membrane protein is synthesized, one of the first elements to exit the ribosome is the signal sequence. When a signal sequence emerges from a ribosome it is recognized and bound in the cytoplasm by signal recognition particle (SRP) (Walter and Blobel, 1981; Walter et al., 1981; Ogg and Walter, 1995). SRP is an 11S ribonucleoprotein composed of six polypeptides (named according to their molecular weights: SRP9, 14, 19, 54, 68, 72) arranged on a 300 nucleotide 7SL RNA scaffold (see Table 1.1) (Walter and Blobel, 1980; Walter and Blobel, 1982; Walter and Blobel, 1983a). Like other ribonucleoproteins, SRP is primarily assembled in the nucleolus; the addition of SRP54 occurs once pre-SRP exits the nucleus and enters the cytoplasm (Pederson and Politz, 2000; Politz et al., 2000; Ciufo and Brown, 2000). The incorporation of SRP54 into SRP depends on the presence of SRP19 (Walter and Blobel, 1983a; Romisch et al., 1990). The binding of SRP19 to SRP-RNA causes structural changes in the RNA that allow binding of SRP54 (Kuglstatter et al., 2002).

SRP54 is the subunit responsible for binding signal sequences but the precise determinants of signal sequence recognition and binding are not clear. Mutagenesis, crystal structure and crosslinking studies provide conflicting results, with evidence both for and against signal sequence-binding by all three domains of SRP54 (Zopf et al., 1990; Gowda et al., 1997; Newitt and Bernstein, 1997; Batey et al., 2000; Cleverley and Gierasch, 2002; Huang et al., 2002).

Regardless of the details of signal sequence binding by SRP54, once SRP has recognised and bound a signal sequence it stimulates a transient pause in translation, mediated by the SRP9/14 subunits and SRP RNA (Chang et al., 1997; Thomas et al., 1997). The ribosome-nascent chain (RNC)-SRP ternary complex is then targeted to the ER by an interaction between SRP and an ER-bound SRP receptor (SR) (Gilmore et al., 1982a; Meyer et al., 1982b; Gilmore et al., 1982b; Gilmore and Blobel, 1983).

SR is a heterodimer consisting of an alpha subunit (SRα) and a beta subunit (SRβ) (Tajima et al., 1986). SRα is localized to the ER membrane through a high affinity interaction with SRβ, a type I integral membrane protein (Andrews et al., 1989; Young et al., 1995; Miller et al., 1995; Legate et al., 2000). A detailed description of the assembly of SR on the ER membrane is presented in Chapter 2.

Once the RNC has become bound to the ER the ribosome is then transferred to a proteinaceous pore, or translocon, through which the nascent chain can traverse the

Table 1.1: SRP pathway components for *E. coli*, *S. cerevisiae*, and higher eukaryotes

	Higher Eukaryotes	*S. cerevisiae*	*E. coli*
SRP	SRP72	Srp72p	
	SRP68	Srp68p	
	SRP54	Srp54p	Ffh
	SRP19	Sec65p	
	SRP14	Srp14p	
	SRP9	Srp9p	
	SRP RNA*	SRP RNA (scR1)	4.5S RNA
		Srp21p	
SRP Receptor	SRα	Srp101p	FtsY
	SRβ	Srp102p	
Translocon	Sec61α	Sec61p/Ssh1p	SecY
	Sec61β	Sbh1p/Sbh2p	
	Sec61γ	Sss1p	SecE
	BiP	Kar2p	
		(Sec63p)	
			SecG
			YidC

*originally 7SL RNA

membrane. The environment of this pore ensures that the nascent chain remains exposed to aqueous solvent throughout its passage across the membrane (Simon and Blobel, 1991; Crowley et al., 1993; Crowley et al., 1994). This pore is primarily composed of a multi-protein complex called the Sec61 complex. In addition to the Sec61 complex, some of the proteins that are associated with the translocon are TRAM (Gorlich et al., 1992a), the TRAP complex, oligosaccharyltransferase (Wang and Dobberstein, 1999), signal peptidase (Kalies et al., 1998), and the lumenal chaperone BiP (Hamman et al., 1998).

The minimal components of a functional translocon *in vitro* are the heterotrimeric Sec61 complex, consisting of Sec61α, β and γ (Gorlich and Rapoport, 1993; Hartmann et al., 1994). Sec61α is a multispanning membrane protein that binds the ribosome and contacts the nascent chain as it traverses the membrane (High et al., 1991; Gorlich et al., 1992b; High et al., 1993a; High et al., 1993b; Kalies et al., 1994; Nicchitta et al., 1995; Laird and High, 1997; Raden et al., 2000). Nascent membrane proteins and some secreted proteins have also been crosslinked to another transmembrane protein called TRAM that may have a role in discriminating hydrophobic sequences in transmembrane domains from those in secretory signal sequences (High et al., 1993b; Do et al., 1996). TRAM may assist in the partitioning of transmembrane segments into the lipid bilayer, particularly if the transmembrane segment is not sufficiently hydrophobic to spontaneously equilibrate into the bilayer (Do et al., 1996; Heinrich et al., 2000).

Studies based on electron microscopy revealed that Sec61α forms the bulk of the central pore of the engaged translocation complex (Menetret et al., 2000). Purified reconstituted Sec61 complexes are arranged as oligomers containing 3-4 copies of the trimeric complex, in a pentagonal configuration (Hanein et al., 1996). The central pore of these oligomers has been measured at ~20 Å across but may increase to 40-60 Å across during a translocation event, demonstrating that the architecture of the complex may be significantly influenced by the ribosome (Hamman et al., 1997).

Sec61β and γ were identified as subunits of the Sec61 complex because they fractionate biochemically with Sec61α after solubilization in non-ionic detergent (Gorlich and Rapoport, 1993). Crosslinks between Sec61β and Sec61α have been observed, suggesting that these subunits are tightly associated (Kalies et al., 1998; Meyer et al., 2000). Sec61β may have a regulatory role in the recruitment of peripheral components and gating of the translocon (Kalies et al., 1998). Sec61β is indispensable at physiologic temperature, as biochemical removal of this component has been shown to abrogate translocation activity in a system reconstituted from detergent extract. Slowing down the ribosome-binding step by chilling the reaction to 0°C partially restores translocation, suggesting that Sec61β is involved in, but not essential for, the translocation process, possibly by recruiting signal peptidase to the translocon (Kalies et al., 1998). Recently a fluorescent approach as used to provide evidence that Sec61β may function as a guanine nucleotide release factor (GRF) for SRβ (Helmers et al., 2003). Data on the Sec61γ subunit are lacking and any insight into its role in translocation is purely speculative at this time.

Recent biochemical fractionation and crosslinking experiments have identified two additional proteins, Sec62 and Sec63, that associate with translocons in the absence of bound ribosomes (Meyer et al., 2000). These proteins are homologous to the yeast proteins Sec62p and Sec63p, both of which are involved in post-translational translocation (see below). Since mammalian ER does not appear to support a post-translational translocation pathway to a significant extent, the purpose for these proteins in the mammalian system cannot be predicted based on their function in yeast. Although a requirement for Sec63p in SRP-dependent translocation has been suggested in yeast (Young et al., 2001) the inability to isolate Sec63-containing complexes in the presence of bound ribosomes suggests that both mammalian Sec62 and Sec63 are not likely to be involved in SRP-mediated protein translocation in mammals. Based on mutational analysis in yeast, these proteins may form part of the pore involved in ER-assisted protein degradation, a pathway used to extrude substrates from the ER lumen for degradation in the cytoplasm via the ubiquitin pathway (Plemper et al., 1997).

1.2 Protein translocation systems in *S. cerevisiae*

1.2.1 Post-translational translocation

In yeast many secretory precursors are translocated across the ER membrane in a post-translational fashion. Translocation precursors maintain translocation-competence by binding to cytoplasmic chaperones prior to ER targeting (Deshaies et al., 1988; Chirico et al., 1988; Plath and Rapoport, 2000). The pore involved in post-translational translocation consists of Sec61p, Sbh1p and Sss1p, homologues of Sec61α, β and γ, respectively (see Table 1.1) (Gorlich et al., 1992b; Hartmann et al., 1994; Panzner et al., 1995) as well as the tetrameric Sec62-Sec63 complex, which also contains Sec71p and Sec72p and the lumenal chaperone Kar2p (BiP) (Deshaies et al., 1991; Panzner et al., 1995). In the absence of ATP, secretory precursors can be targeted to the ER and can crosslink to Sec62p, Sec71p and Sec72p, implying that these proteins may serve as members of a secretory precursor recognition complex (Musch et al., 1992; Lyman and Schekman, 1997). In the presence of ATP, the secretory precursor is transferred to the translocon, where it can crosslink to Sec61p (Musch et al., 1992; Sanders et al., 1992). The transfer of the secretory precursor to Sec61p, and subsequent completion of translocation, depends on localization of Kar2p to the translocon via binding to Sec63p (Sanders et al., 1992; Lyman and Schekman, 1995; Lyman and Schekman, 1997), as well as the other ER lumenal chaperones Lhs1p and Sil1p (Craven et al., 1996; Tyson and Stirling, 2000).

1.2.2 Co-translational translocation: the SRP pathway

While many secretory precursors can be translocated across the ER membrane once they have completed synthesis, a post-translational mode of translocation for transmembrane proteins and secretory proteins with large hydrophobic domains is inefficient. Moreover, accumulation of these proteins in the cytoplasm, due to their low solubility in aqueous solutions, is toxic. The co-translational SRP-mediated pathway is used to accommodate these substrates that are recognized based on the hydrophobicity of the signal peptide. In general, proteins with more hydrophobic signal sequences are

translocated via the SRP pathway whereas proteins with less hydrophobic signal sequences are translocated post-translationally (NG et al., 1996).

Yeast SRP contains orthologues to all six mammalian SRP protein subunits and the RNA scaffold, plus an additional 21 kDa polypeptide that is not found in mammalian SRP (see Table 1.1) (Hann et al., 1989; Hann and Walter, 1991; Stirling and Hewitt, 1992; Brown et al., 1994). Furthermore, orthologues of both subunits of mammalian SR have been identified in yeast (Ogg et al., 1992; Ogg et al., 1998).

The core translocon used for co-translational translocation consists of Sec61p, Sbh1p and Sss1p. Sec61p, like the mammalian orthologue, binds ribosomes with high affinity (Beckmann et al., 1997; Prinz et al., 2000a; Morrow and Brodsky, 2001). Furthermore, electron microscopy of ribosome-Sec61p complexes revealed that the nascent-chain exit tunnel within the ribosome aligns with the central pore of Sec61p, implying that Sec61p serves as the channel through which the nascent chain spans the membrane (Beckmann et al., 1997).

A combination of biochemical and genetic approaches identified a second translocon consisting of Ssh1p (a homologue of Sec61p), Sbh2p (a homologue of Sbh1p) and Sss1p (Finke et al., 1996). This complex binds tightly to ribosomes *in vitro* (Prinz et al., 2000a) but plays a minor role to Sec61p in determining the total ribosome-binding capacity of yeast ER (Prinz et al., 2000b). Unlike the Sec61p complex the Ssh1p complex is believed to be dedicated to co-translational translocation since it does not associate with the Sec62-Sec63 complex (Finke et al., 1996; Wittke et al., 1999), and cannot complement a *Δsec61* mutant. Further evidence that the Ssh1p complex is involved in SRP-mediated translocation comes from the observation that a *Δssh1* mutation is synthetically lethal when combined with a *sec65-1* mutation, affecting a subunit of SRP (Wilkinson et al., 2001). Finally, deletion of Ssh1 results in deficiencies in protein translocation that can be suppressed by slowing the rate of translation, indicating that the Ssh1p complex helps to determine the total translocation capacity of the yeast ER membrane (Wilkinson et al., 2001).

1.3 Protein translocation systems in *E. coli*

E. coli possess a single cell membrane where all protein translocation pathways converge. To accommodate the wide variety of protein substrates that must be integrated into the membrane or translocated into the periplasmic space, three translocation pathways have evolved:

1.3.1 Post-translational translocation: the twin-arginine translocation (Tat) pathway

Protein substrates that fold and bind cofactor molecules in the cytoplasm must be translocated across the inner membrane in a folded state. A specific translocation apparatus has been identified that can translocate folded substrates in a Sec-independent manner (reviewed in Yen et al., 2002). Called the twin arginine translocation pathway, or Tat pathway, after a pair of arginine residues in the targeting sequence (Stanley et al., 2000), it appears to be functionally analogous to the ΔpH-driven system in chloroplasts and peroxisomes (Robinson and Bolhuis, 2001). Although five Tat proteins have been

identified in *E. coli* three of these--TatA, TatB and TatC--are sufficient to reconstitute the Tat system *in vitro* (Yahr and Wickner, 2001). Furthermore, the *in vitro* system confirms that *E. coli* Tat, like the chloroplast and peroxisome ΔpH-driven system, requires a membrane potential for activity (Yahr and Wickner, 2001).

1.3.2 Post-translational translocation: the Sec pathway

Periplasmic proteins and many outer membrane proteins are translocated across the inner cell membrane by the post-translational Sec pathway (Qi and Bernstein, 1999; Qi et al., 2002). This pathway can be reconstituted *in vitro* with four proteins (SecA, SecB, SecY, SecE), and ATP (Brundage et al., 1990). SecB is a cytoplasmic chaperone that maintains translocation competence by binding to large domains of secretory precursors in an ATP-independent manner (Kumamoto, 1991; Topping and Randall, 1997). This complex is targeted to the membrane by a high affinity interaction between SecB and membrane-bound SecA, which is localized to the translocon (Hartl et al., 1990). SecA also binds the signal sequence and mature portions of the secretory precursor (Lill et al., 1990). Once translocation is initiated SecB dissociates and returns to the cytoplasm (Fekkes et al., 1997). Translocation is initiated by ATP-dependent conformational changes within SecA that physically drive the amino terminus of the preprotein across the membrane (Schiebel et al., 1991; Economou and Wickner, 1994; Economou et al., 1995). Once the amino terminus has spanned the membrane, the membrane potential ($\Delta\mu_H+$) is sufficient to achieve translocation of the remainder of the secretory protein (Schiebel et al., 1991).

The translocon consists of the SecYEG complex, with SecY showing homology to Sec61α/Sec61p and SecE showing homology to Sec61γ/Sss1p (see Table 1.1) (Gorlich et al., 1992b; Hartmann et al., 1994). SecG shows no sequence homology to translocon components in either yeast or mammals; its role appears to be to facilitate the membrane insertion/deinsertion of SecA (Matsumoto et al., 1998; Suzuki et al., 1998). SecG is a non-essential protein. A genetic deletion of *SecG* resulted in a modest translocation defect *in vivo*, in several different strains of *E. coli* (Flower et al., 2000). *In vivo*, deletion of *SecG* was compensated for by overexpression of the SecYE complex (Duong and Wickner, 1997).

SecE is an essential protein (Schatz et al., 1989). Depletion of SecE leads to a severe translocation defect *in vivo* (Traxler and Murphy, 1996), although the efficient translocation of a subset of secretory and membrane proteins using SecE-depleted vesicles *in vitro* has been reported (Yang et al., 1997; Cristobal et al., 1999). Depletion of SecE or overexpression of SecY in *E. coli* leads to rapid degradation of SecY by the protease FtsH (Kihara et al., 1995; Akiyama et al., 1996). Simultaneous overexpression of SecE and SecY completely protects SecY from protease digestion (Taura et al., 1993). Therefore, one function of SecE may be to stabilize SecY in the *E. coli* inner membrane.

The structural arrangement of the bacterial translocation pore is controversial. Electron microscopic studies of purified SecYE revealed a quasi-pentagonal arrangement of 3-4 dimers that resembled the eukaryotic complex (Meyer et al., 1999). However,

electron microscopy of purified SecYEG clearly showed a dimeric arrangement of SecYEG complexes (Breyton et al., 2002). Other data suggested that addition of SecA assembles SecYEG into a tetrameric arrangement resembling the eukaryotic translocation pore in both shape and size (Manting et al., 2000).

Biochemical approaches have not clarified the nature of the oligomeric state of active SecYEG. A crosslinking approach employing epitope-tagged versions of SecE and SecY in a solubilized reconstituted system of SecYEG suggested that the pore operates as a monomer (Yahr and Wickner, 2000). Upon reconstituting translocation pores containing equal amounts of tagged and untagged subunits the authors were unable to detect crosslink products that would suggest an oligomeric arrangement. However, their data cannot rule out the possibility that crosslinks between subunits of the SecYEG trimer were favoured over crosslinks to neighbouring trimeric complexes. Also, the immunoprecipitation conditions that were used to detect a physical interaction between a proOmpA secretory precursor polypeptide and components of the translocation pore may have resulted in the disassembly of multimeric complexes while maintaining the interaction of proOmpA with one of the SecYEG trimers. In this case mixed complexes of tagged and untagged SecYEG might not be detected, leading to the conclusion that SecYEG functions as a monomer.

A more recent crosslinking and blue native PAGE approach demonstrated that SecYEG is a dynamic structure, with 1-4 copies associating with one another (Bessonneau et al., 2002). Using a secretory precursor that became arrested in translocation it was shown that preproteins were trapped by dimers of SecYEG or SecYE, providing the best biochemical evidence to date that SecYEG functions as a dimer.

1.3.3 Co-translational translocation: the SRP pathway

Multi-spanning membrane proteins, by virtue of the high degree of hydrophobicity of the transmembrane segments, are only efficiently translocated into the bacterial inner membrane concomitant with translation. For this reason bacteria retain a SRP pathway that functions in much the same way as the eukaryotic SRP pathway. However, *E. coli* have a simplified SRP, consisting of a homologue of SRP54, called Ffh (fifty-four homologue) and 4.5S RNA (Romisch et al., 1989; Bernstein et al., 1989; Ribes et al., 1990; Poritz et al., 1990). *E. coli* SRP, like the eukaryotic counterpart, binds signal sequences of nascent presecretory chains as they emerge from the ribosome (Luirink et al., 1992). The requirements for signal sequence recognition are determined by the hydrophobicity and alpha helical character of the signal sequence. Decreasing either the hydrophobicity or alpha helical character decreases the reliance on the SRP pathway and increases the probability that the preprotein will be translocated by the post-translational Sec pathway (Lee and Bernstein, 2001; Adams et al., 2002). Once Ffh binds the signal peptide, the ribosome-nascent chain-Ffh complex binds to the *E. coli* SRP receptor.

In *E. coli* the SRP receptor differs from the eukaryotic counterpart in two ways. First, it is a single polypeptide, called FtsY, bearing functional homology to SRα (Table 1.1)(Luirink et al., 1994). Second, FtsY is a peripheral membrane protein that is equally

distributed between the cytoplasm and the plasma membrane (Luirink et al., 1994). The gene for FtsY was isolated using a genetic screen to identify genes involved in cell division (Gill et al., 1986). Consistent with a role in cell division the gene for FtsY is located in an operon containing two other genes implicated in cell division. A direct role for FtsY in cell division has not been forthcoming and it is now widely thought that the cell division defect associated with inactivation of FtsY is an indirect result of its role in protein targeting.

Assembly of FtsY onto the *E. coli* plasma membrane occurs independently of any established targeting pathway. Instead, FtsY binds to the cell membrane through a direct interaction with phospholipids (Millman et al., 2001). The lipid binding domain has been mapped to the amino-terminus of FtsY and is composed of a region rich in acidic amino acids (the A region) and a small independently folded domain (the N region)(Millman and Andrews, 1999). Recently, the membrane binding domain of FtsY was shown to bind specifically to phosphatidylethanolamine, a major component of the *E. coli* inner membrane(Millman et al., 2001). However, experiments with phosphatidylethanolamine-depleted strains of *E. coli* suggest that FtsY also binds to a trypsin sensitive component on the inner membrane (Millman et al., 2001). The identity and characteristics of this component are unknown at this time.

Since a significant proportion of FtsY is found in the cytoplasm, it is not clear whether Ffh binds to FtsY while they are both in the cytoplasm, or if Ffh binds to membrane-bound FtsY. Both proteins can functionally interact with each other in the absence of membranes (Miller et al., 1994), demonstrating that the structural changes that occur within FtsY upon membrane binding (De Leeuw et al., 2000; Millman et al., 2001) are not required for Ffh-FtsY complex formation. Since *E. coli* has only one distinct membrane system there is no requirement for a membrane-bound SR to distinguish the correct membrane for protein targeting. Therefore, the order of the Ffh-FtsY binding step and the membrane targeting step may not be important in bacteria.

Cotranslational substrates use the SecYEG translocon to traverse the plasma membrane. A genetic screen for mutants deficient in membrane protein assembly revealed that SecA is also required for the translocation of an SRP-dependent substrate *in vivo* (Tian et al., 2000). *In vitro* a subset of SRP-dependent proteins appear to require SecA to translocate large periplasmic domains across the membrane (Valent et al., 1998; Qi and Bernstein, 1999; Neumann-Haefelin et al., 2000).

The integration of membrane proteins into the lipid bilayer involves the participation of a translocon-associated protein called YidC. During the translocation of inner membrane proteins YidC is in close proximity to transmembrane segments at the lipid-protein boundary, suggesting that YidC functions during the lateral transfer step of transmembrane segments from the translocon to the lipid bilayer (Beck et al., 2001; Urbanus et al., 2001). Furthermore, depletion of YidC causes a defect in membrane protein assembly, with only a minor effect on secretory protein translocation (Samuelson et al., 2000). Although there are no ER-associated homologues to YidC (see Table 1.1),

there is significant homology, however, between YidC and the mitochondrial protein translocation protein Oxa1p (Scotti et al., 2000).

1.4 The mechanism of SRP-mediated protein targeting and nascent-chain transfer to the translocon

1.4.1 Eukaryotes

The process of co-translational protein translocation can be divided into three stages: 1) targeting of secretory precursors to the ER membrane, 2) transfer of the RNC to the translocon, and 3) translocation of the nascent chain across the membrane (Figure 1.1). To ensure that translocation is a unidirectional process, the coordinated action of three GTPases is required: The 54 kDa subunit of SRP (SRP54), SRα and SRβ. SRP54 and SRα define a unique family of GTPases called SRP GTPases, and SRβ is a member of the Ras superfamily of small molecular weight GTPases (see Section 1.5). GTPases function as 'switches' to allow molecular events to occur in a temporally discrete and regulated fashion (Vetter and Wittinghofer, 2001).

The involvement of the first GTPase, SRP54, occurs during signal sequence recognition. When SRP is not engaged in targeting, SRP54 displays low affinity for GTP, and is likely empty (Miller et al., 1993). Upon recognition of the signal sequence by SRP, the affinity of SRP54 for GTP is moderately increased, but the active site is not in a 'locked' conformation since bound GTP remains exchangeable with cytoplasmic GTP (Bacher et al., 1996; Rapiejko and Gilmore, 1997). The SRP-nascent chain complex is targeted to the membrane via the affinity of SRP for its receptor. SRα also readily exchanges bound GTP for free GTP and is probably empty when it is not engaged in targeting (Rapiejko and Gilmore, 1997). Once SRP54 contacts SRα the affinity of both molecules for GTP greatly increases such that bound GTP can no longer exchange with solution GTP, and both proteins become tightly bound to each other (Connolly et al., 1991; Connolly and Gilmore, 1993; Rapiejko and Gilmore, 1997). *In vitro* the half life of this interaction is >6 hours, therefore this step alone is sufficient to make targeting unidirectional (Rapiejko and Gilmore, 1992). Coincubation of SRP54 and SRα *in vitro* stimulates hydrolysis of GTP by both proteins, demonstrating that these proteins also function as reciprocal GTPase activating proteins (GAPs) (Miller et al., 1993; Connolly and Gilmore, 1993). GTP hydrolysis releases SRP54 from SRα, allowing SRP to return to the cytoplasm (Connolly et al., 1991). The presence of a nascent chain bound to SRP54 inhibits the GTPase activity of both proteins (Miller et al., 1993).

Once tethered to the ER via a physical interaction between SRP54 and SRα, the ribosome must then be transferred to the translocon. However, a direct interaction between SR and the translocon has not been unambiguously demonstrated. Using a split ubiquitin technique whereby the amino-terminal half of ubiquitin was fused to both yeast Sec61p and its homologue Ssh1p and the carboxyl-terminal half of ubiquitin was fused to SRβ, Wittke et al. demonstrated that SRβ was in close proximity to both Sec61α homologues *in vivo* (Wittke et al., 2002). The close proximity was detected by reconstitution of both halves of ubiquitin, and the subsequent release and degradation of a

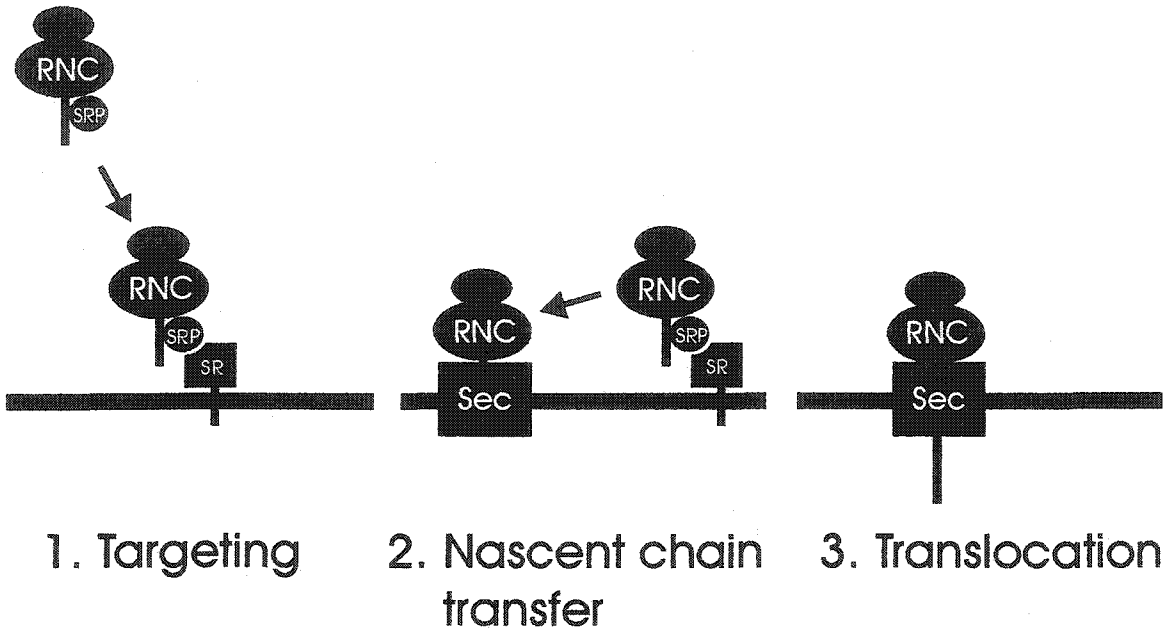

Figure 1.1: A simplified model of SRP-mediated protein translocation. A schematic diagram of protein translocation, illustrating the three main stages: ribosome-nascent chain targeting to the ER/*E. coli* plasma membrane, transfer of the ribosome-nascent chain to the translocon, and nascent chain translocation. All components are not displayed to scale. Abbreviations are as follows: RNC, ribosome-nascent chain; SRP, signal recognition particle; SR, SRP receptor; Sec, Sec61/SecYEG complex, translocon.

reporter protein from the carboxyl-terminus of the reconstituted ubiquitin (Johnsson and Varshavsky, 1994). However, since SRβ contains an amino-terminal transmembrane domain it must insert into the ER via the translocon. Degradation of the reporter protein may be detected if reconstitution of ubiquitin was allowed to precede the release of SRβ from the translocon; therefore this observation could lead to the erroneous conclusion that SRβ remained in close proximity to the translocon following its synthesis.

The group of Dobberstein and colleagues have presented data that they claim provides evidence that SRβ controls the transfer of the RNC to Sec61. By using a modified version of SRβ that recognised the purine biosynthesis intermediate xanthosine triphosphate (XTP) this group detected the transfer of nascent chains from SRP to the translocon when they included the non-hydrolyzable XTP analogue XMPPNP in their assay, but no transfer was observed in the presence of XDP (Fulga et al., 2001). This group also detected a crosslink between SRβ and a ribosomal protein in the absence of nucleotide or in the presence of GDP, but not in the presence of GTP. From these data they concluded that the binding of GTP to SRβ regulates the transfer of the RNC from SR to the translocon. Data will be presented in this thesis that exposes serious flaws in their interpretation of the data, and therefore their conclusions regarding the role of SRβ in the nascent chain transfer step. To date the precise steps governing the transfer of the nascent chain to the translocon remain unresolved.

The Sec61 complex itself appears to govern the release of the nascent chain from SRP. Using a combination of proteolysis approaches and partial reconstitution of translocation pathway components Song and colleagues discovered that the nascent chain remained bound to SRP/SR in the absence of Sec61 (Song et al., 2000). This data supports the notion that in the absence of available translocons, targeted RNCs can remain bound to the membrane as a post-targeting intermediate. Once targeting was achieved, digestion of SRα by proteolysis did not release RNCs from the membrane, demonstrating that the post-targeting intermediate does not involve a series of protein-protein interactions consisting of RNC-SRP-SRα-SRβ (Murphy, III et al., 1997). There are no clear candidates for the post-targeting RNC receptor at this time.

1.4.2 *E. coli*

The bacterial SRP pathway is similar to the eukaryotic SRP pathway in many respects. In *E. coli*, the steps controlling targeting and nascent chain transfer to the translocon also involve the concerted action of GTPases. Since *E. coli* lack a homologue for the mammalian SRβ, there are only two GTPases involved in translocation: Ffh (SRP54) and FtsY (SRα).

It was demonstrated *in vitro* that Ffh and FtsY, like their eukaryotic counterparts, bind and hydrolyze GTP as reciprocal GAPs, and that this activity is inhibited by synthetic signal peptides (Miller et al., 1994; Powers and Walter, 1995). However, there are two important differences between the prokaryotic and eukaryotic SRP pathway mechanisms with respect to SR. The first difference concerns the initial targeting step. It is not known whether binding of Ffh to FtsY occurs in the cytoplasm, followed by

targeting of the RNC-Ffh-FtsY complex to the plasma membrane or, like the eukaryotic SRP pathway, the high affinity interaction between Ffh and FtsY occurs at the membrane. The second difference became apparent when gel filtration chromotography was used to study the membrane binding characteristics of *E. coli* FtsY. It was discovered that some FtsY molecules underwent a proteolytic cleavage event between the membrane binding AN domain and the catalytic G domain when FtsY was bound to inverted vesicles (Millman and Andrews, 1999). Binding of FtsY to inverted vesicles was shown to cause a conformational change within FtsY that exposed the protease-sensitive site (Millman et al., 2001). It is not known whether cleavage of FtsY is coupled to targeting of RNCs to the membrane, transfer of nascent polypeptides to the translocon, or whether it occurs independent of these processes. The identity of the protease that cleaves FtsY is also unknown, although it is almost certain to be a component of the bacterial inner membrane (Millman and Andrews, 1999). The fact that cleavage of FtsY was also detected in Western blots of exponentially growing cultures demonstrated that it is a genuine biological event (Millman and Andrews, 1999).

If the cleavage event is coupled to translocation, the GTP binding site may in part regulate an additional conformational change in FtsY to facilitate access to the protease. Fluorescence measurements using a tryptophan residue within the effector region of the G domain revealed significant structural changes within the FtsY GTPase upon binding Ffh and GTP (Jagath et al., 2000). Such a structural change may present the cleavage site to the protease. Cleavage of FtsY upon binding Ffh/GTP would serve to make targeting unidirectional at the expense of destroying FtsY.

1.5 Characterization of translocation GTPase family members

SRα/FtsY and SRP54/Ffh define their own family of SRP GTPases. In contrast, SRβ belongs to the Ras superfamily of small molecular weight GTPases.

1.5.1 SRP-type GTPases

The SRP-type GTPases are distinguished from other types of GTPases in three ways. First, they demonstrate unusual stability in the empty state. GTPases are usually bound to either GTP or GDP; the empty state is transient and is stabilized by an interaction with a guanine nucleotide exchange protein (Boguski and McCormick, 1993; Sprang, 1997). Biochemical data suggest that both SRP54 and SRα can freely exchange nucleotide in solution, and switch to the activated GTP-bound forms once they bind each other (Rapiejko and Gilmore, 1997). The fact that several bacterial SRP GTPases have been crystalized in the apo-form bears testament to their stability in the absence of nucleotide (Freymann et al., 1997; Montoya et al., 1997; Montoya et al., 2000).

There is a wealth of structural data from bacterial orthologues that explains why these GTPases are stable in the absence of bound nucleotide. (Freymann et al., 1997). In both Ffh and FtsY structures the key nucleotide-binding side chains are either displaced relative to the corresponding side chains in the Ras structure, or are sequestered by a network of side chain interactions, preventing collapse of the structure and necessitating significant reorientation of the side chains to facilitate GTP-binding (Freymann et al.,

1997). An insertion between the G1 and G2 consensus regions, called the I box, has also been predicted to contribute to the stability of the empty state (Montoya et al., 1997). The structure of *T. aquaticus* Ffh bound to the non-hydrolysable GTP analogue GMPPNP revealed that the nucleotide is kinked to exclude the β-phosphate from the binding pocket (Padmanabhan and Freymann, 2001), suggesting that Ffh is unable to bind GTP in a manner similar to other GTPases unless the binding pocket undergoes restructuring. Reorganization of the active site could result from an interaction between Ffh and FtsY, either through the I box or through the N domain, a unique amino terminal domain in these GTPases (Freymann et al., 1997; Montoya et al., 1997).

Sequence comparisons between SRP-type GTPases and other GTPases revealed the second difference that sets SRP-type GTPases apart from other GTPases. A search of the protein database revealed three consensus sequence elements specific to the GTPase superfamily (Table 1.2). SRP-type GTPases diverge from the consensus by containing a threonine in place of a conserved asparagine in the third consensus sequence (Table 1.2), a distinction that has not been noted previously. In Ras the aspargine hydrogen bonds to the guanine ring to aid in the recognition of the nucleotide (Pai et al., 1990). The threonine found in SRP-type GTPases likely serves a similar purpose since substitution of the threonine with asparagine in FtsY decreased GTP-binding (Kusters et al., 1995). The consensus sequence elements are separated by 40-80 amino acids of non-conserved sequence (Dever et al., 1987). The I box disrupts the spacing between the conserved sequence elements, further defining the SRP-type GTPases as a distinct family.

The third difference between the SRP-type GTPases and other GTPases is their ability to act as reciprocal GAPs. Alone, Ffh has a low basal GTPase activity, and hydrolysis arising from FtsY cannot be detected; however, when they are combined GTP hydrolysis increases dramatically (Miller et al., 1994). By modifying FtsY to bind and hydrolyse XTP it was discovered that nucleotide hydrolysis was only detected in the presence of FtsY, Ffh, GTP and XTP, thereby demonstrating that the nucleotide-bound forms of both proteins were required for costimulation of GTPase activity (Powers and Walter, 1995). A dramatic increase in GTP hydrolysis was also observed during coincubation of mammalian SR and either SRP or isolated SRP54/SRP RNA (Miller et al., 1993; Connolly and Gilmore, 1993).

1.5.2 Ras-type GTPases

SRβ is the only Ras-type GTPase involved in the SRP pathway. It conforms to the consensus sequences assigned by Dever (Dever et al., 1987) and displays the appropriate spacing between the sequence elements (Miller et al., 1995). Furthermore, the recently solved structure of yeast SRβ bears a close resemblance to Ras-type GTPases (Schwartz and Blobel, 2003). Consistent with the properties of other Ras-type GTPases SRβ is most stable when bound to nucleotide (see Chapter 3) (Schwartz and Blobel, 2003). The experimentally determined affinity of SRβ for GTP spans a wide range, from 1 μM for the detergent solubilized SR (Miller et al., 1995), to 20 nM for SR reconstituted into phospholipid vesicles (Bacher et al., 1999). The affinity of SRβ for GTP has not been

Table 1.2: G-box sequence homology among Ras-type and SRP-type GTPases

	G-1	G-2	G-3
Consensus sequence	**G**XXXX**GK**	**D**XX**G**	**NK**X**D**
Rat Ras	**G**AGGV**GK**	**D**TA**G**	**NK**C**D**
Human Arf-1	**G**LDAA**GK**	**D**VG**G**	**NK**Q**D**
Murine Sar-1	**G**LDNA**GK**	**D**LG**G**	**NK**I**D**
Ras $G_s\alpha$	**G**AGES**GK**	**D**VG**G**	**NK**Q**D**
Canine SRβ	**G**LCDS**GK**	**D**LP**G**	**NK**Q**D**
Human SRα	**G**VNGV**GK**	**D**TA**G**	**TK**F**D**
Human SRP54	**G**LQGS**GK**	**D**TS**G**	**TK**L**D**

determined in the absence of SRα so it is not known whether SRα influences the affinity of SRβ for GTP. Compared to other Ras-type GTPases, the properties of SRβ have remained relatively unexplored.

1.6 Project objectives

The original focus of this project was to study the assembly of the SRP receptor. To explore the unusually strong interaction between SRα and SRβ, the SRβ-binding domain of SRα was delineated through deletion mutation analysis. This approach identified an amino-terminal domain called SRX2 as the SRβ-binding domain of SRα (Young et al., 1995). My first objective was to use a complementary approach to identify the sequences in SRβ required for binding SRα. I extended this mutational analysis to include an analysis of the assembly of SRβ in the ER membrane. Furthermore, a series of amino acid substitutions within the SRβ GTP-binding pocket were used to study a putative role for the SRβ GTPase in regulating the assembly of the SRP receptor. This data is presented in Chapter 2. My second objective was to study the properties of the SRβ GTPase in the absence of SRα, to provide some data on this poorly understood member of the Ras-family of GTPases. To this end I expressed a soluble version of SRβ from *E. coli*, purified it, and compared its properties with those of a GTPase point mutant. This data is presented in Chapter 3. Interpretation of this data has allowed me to contribute insight into the role of SRβ in the RNC targeting and nascent chain transfer steps at the ER membrane.

2. MEMBRANE TOPOLOGY OF SRβ, AND CHARACTERIZATION OF THE SRα-SRβ INTERACTION

2.1 Introduction

SRP receptor (SR), or docking protein, was originally purified in 1982 as the membrane-bound component responsible for releasing SRP-mediated translation arrest (Meyer et al., 1982a; Gilmore et al., 1982b). Partial purification of proteins from solubilized ER membranes on a SRP-affinity column yielded an arrest-releasing activity that cofractionated with a 72 kDa protein on sucrose density gradients. A 30 kDa contaminating protein did not fractionate exactly with arrest releasing activity so it was excluded as a component of SR (Gilmore et al., 1982b). Based on this data and on the amino acid sequence of the encoded polypeptide SR was considered to be a single protein, anchored to the ER membrane by amino-terminal hydrophobic sequences (Gilmore et al., 1982b; Lauffer et al., 1985; Hortsch et al., 1985). Further research discovered that SR assembled onto membranes in a SRP-independent manner, as membrane association could be achieved post-translationally and in the absence of nucleotides (Andrews et al., 1989). Furthermore, SR assembled onto trypsin-treated ER membranes could be extracted by washing the membranes with urea, demonstrating that direct insertion of SR into the lipid bilayer is unlikely (Andrews et al., 1989). This data pointed to the likelyhood that SR assembles onto membranes via an interaction with another protein.

When an antibody was generated against the 72 kDa SR protein and used to purify SR a 30 kDa protein was also purified that bound tightly to the 72 kDa protein and cofractionated with it on sucrose density gradients. Since the two proteins were found in the same cellular compartment, bound tightly to each other throughout purification, and were present in roughly equimolar amounts on the ER membrane (the 30 kDa protein was present in 10% molar excess over the 72 kDa protein), the evidence suggested that SR is composed of two subunits: SRα (72 kDa) and SRβ (30 kDa) (Tajima et al., 1986). Furthermore, two proteins of 30 kDa molecular weight copurified with SRα on a SRP-affinity column: SRβ and a second polypeptide with no demonstrated role in translocation (Tajima et al., 1986). This explained the earlier finding that the 30 kDa protein noticed by Gilmore et al. did not fractionate exactly with translation arrest releasing activity on sucrose gradients (Gilmore et al., 1982b).

The amino acid sequence of SRβ suggests that it is a type I integral membrane protein with homology to Ras-type GTPases (Miller et al., 1995). The transmembrane character was confirmed by the discovery that SRβ partitioned from membranes into the detergent phase upon extraction with the non-ionic detergent Triton X-114 (Young et al., 1995; Miller et al., 1995). Initial interpretation of this data was confused by the observation that SRα-SRβ dimers partitioned into the aqueous phase; however, removal of the large soluble domain of SRα by mild digestion with trypsin moved SRβ into the detergent phase, as expected for an integral membrane protein (Bordier, 1981; Young et al., 1995). Genetic studies in *S. cerevisiae* revealed that the transmembrane domain of

SRβ provides the anchor for attaching SR to the ER membrane, since deletion of the transmembrane domain caused SR to fractionate predominantly in the cytoplasm (Ogg et al., 1998).

The binding between SRα and SRβ is unusually strong, compared to other protein-protein interactions. SRα remained bound to membranes following extraction with 500 mM KI or 2 M NaCl, demonstrating that the SRα-SRβ dimer is highly resistant to salt-induced disruption (Hortsch et al., 1985). Also, SRα could not be extracted from membranes with 2M urea, conditions that are usually sufficient to disrupt protein-protein interactions (Andrews et al., 1989). Furthermore, treatment of membranes with high pH (11.5), a condition usually sufficient to remove peripherally associated membrane proteins, did not remove SRα (Hortsch et al., 1985; Young et al., 1995; Miller et al., 1995). However by raising the pH further, to 13.0, SRα was completely extracted from the membrane, while SRβ was not (Miller et al., 1995). A soluble fragment of SRα lacking the amino-terminal 152 amino acids (SRα-EF) can bind to membranes in a biologically active conformation but is not resistant to treatment with urea or 500 mM salt, providing evidence that the tight interaction is mediated by the amino-terminus of SRα (Meyer and Dobberstein, 1980; Andrews et al., 1989).

To determine the minimum SRβ-binding unit within SRα a series of deletions were made within the amino-terminal domain of SRα that remains attached to SRβ following proteolytic digestion (Young et al., 1995; see Figure 2.7). Deletions within the amino-terminal 156 amino acids were unable to support an interaction with SRβ, as assayed by gel filtration experiments and immunoprecipitation assays. An *in vitro* translation experiment whereby reactions synthesizing SRα were terminated at various time points by the addition of cycloheximide revealed that an SRα fragment consisting of approximately the first 140 amino acids of SRα represented the minimum fragment size that could associate with vesicles in a salt-resistant manner (Young et al., 1995).

Further examination of the membrane assembly requirements of SRα revealed the presence of a mRNA-mediated pause in translation between the amino-terminal domain and the GTPase domain of SRα (Young and Andrews, 1996). Destabilizing a putative stem-loop structure within the mRNA, by introducing silent mutations into the DNA sequence encoding SRα, abolished the pause event and decreased the efficiency of SRα assembly onto the membrane. The theory developed from this data states that this pause event allows the amino-terminus of SRα to fold correctly, allowing SRα to target to the ER membrane via an interaction with SRβ (Young and Andrews, 1996). The relevance of an SRα pausing event *in vivo* has yet to be demonstrated.

In this chapter the interaction of SRβ with the ER membrane is further explored using an engineered glycosylation site as a readout for translocation into the lumen, proving that SRβ is a type I integral membrane protein. Membrane-binding and proteolysis experiments reveal the determinants of SRβ orientation within the membrane, and reveal the regions of SRβ that are available to bind SRα, by virtue of being on the

correct side of the membrane. Immunoprecipitation of SRα deletion mutants with SRβ confirm that the SRX2 domain comprises the minimum SRβ-binding domain within SRα, and a similar approach is used to establish the minimum SRα-binding requirements for SRβ. By mutation of the SRβ GTPase, the role of the GTPase in mediating a tight SRα-SRβ interaction is also assessed. By assaying each set of mutations it is established that an intact, functional GTPase domain of SRβ is all that is required to establish a tight binding interaction with SRα.

2.2 Materials and Methods

2.2.1 Materials and General Methods

General chemical reagents were obtained from either Fisher, Sigma or Life Technologies, Inc. SURE™ *Escherichia coli* cells used for plasmid construction were purchased from Stratagene. Except where specified, restriction enzymes and other molecular biology enzymes were from New England Biolabs or MBI Fermentas. ^{35}S-labeled methionine was from DuPont NEN. SP6 polymerase, *Taq* polymerase and RNAse inhibitor were from MBI Fermentas. Creatine kinase was from Boehringer Mannheim. A monoclonal antibody directed against a HA epitope was purchased from Berkeley Antibody Company.

Transcription reactions with SP6 polymerase were performed as described previously (Gurevich et al., 1991). Cell-free translation reactions were performed in rabbit reticulocyte lysate (RRL) and labeled with ^{35}S-methionine as described previously (Andrews et al., 1989); translation products were analyzed by SDS-PAGE and radiography. Canine pancreatic rough microsomes were prepared and either washed with 0.5 M KOAc (KRMs) or further purified by Sepharose CL-2B size exclusion chromatography (CRMs) as described (Walter and Blobel, 1983b).

Polyclonal antiserum directed against SRα was obtained as described (Young et al., 1995). Polyclonal antiserum against a synthetic peptide corresponding to the carboxyl-terminal 20 amino acids of SRβ was obtained from ExAlpha Biologicals.

2.2.2 Plasmids

Construction of plasmids, sequencing and site directed mutagenesis were performed using standard techniques. Unless otherwise stated, all SRβ constructs were inserted following the SP6 RNA polymerase promoter in pMAC334, a version of pGEM3 containing the 5'-untranslated region of pSPUTK (Falcone and Andrews, 1991) and the 3'-untranslated region of bovine preprolactin and all SRα constructs were inserted following the SP6 RNA polymerase promoter in pSPUTK (Falcone and Andrews, 1991). All deletion constructs are presented in tabular format as Table 2.1. pMAC191, encoding a modified full-length cDNA sequence of canine SRα; pMAC455, encoding $SR\beta_{md}$; pMAC690, encoding $SR\beta_{md}$ with an amino-terminal HA epitope-tag; pMAC55, encoding SRD4, a mutant of SRα in which the first hydrophobic series of amino acids are deleted; pMAC459, encoding SRD6, a mutant of SRα in which the second hydrophobic series of amino acids are deleted; pMAC494, encoding SRD7, a mutant of SRα in which the first highly charged series of amino acids are deleted; and pMAC205, encoding amino acids 1-

Table 2.1: Summary of plasmid constructs encoding deletions of SRα and SRβ

Plasmid designation	Polypeptide designation	Description
	SRα	
pMAC191	SRα	full-length canine SRα
pMAC55	SRD4	SRαΔ1-27
pMAC459	SRD6	SRαΔ38-79
pMAC494	SRD7	SRαΔ79-103
pMAC205	SRX2	amino acids 1-176 of SRα
	SRβ	
pMAC455	SRβmd	full-length murine-canine SRβ chimera
pMAC690	HA-SRβmd	HA-tagged SRβmd
pMAC853	SRβΔTM	SRβΔ1-58
pMAC747	SRβC1	SRβΔ260-265
pMAC1300	SRβC1ΔTM	SRβΔ1-58,260-265
pMAC1056	SRβD4	SRβΔ1-69
pMAC1057	SRβD5	SRβΔ1-82
pMAC1082	SRβΔloop	SRβΔ185-219
pMAC1363	SRβ-loop2	SRβ with scrambled amino acids 185-219
pMAC1200	SRβΔch	SRβΔ64-70

176 of SRα were previously reported (Young et al., 1995). pMAC507, encoding SpgPA, a chimeric protein that serves as a positive control for glycosylation, has also been previously reported (Janiak et al., 1994).

Plasmid pMAC853 encodes SRβΔTM, a fusion of the carboxyl-terminal 206 amino acids of canine SRβ with an amino-terminal HA epitope tag $(MYPYDVPDYAA)_2$. To assemble this plasmid the coding sequence for $SR\beta_{md}$ in pMAC690 was replaced by a PCR product generated by amplifying the appropriate region of the coding sequence from pMAC455 using a 5' sense primer CATGCCATGGCTAAGTTCATCCGGAGCAGA and a 3' antisense primer complementary to the T7 promoter. The PCR product was digested with *NcoI* and *EcoRI* and subcloned into the vector cut with the same enzymes.

pMAC747 encodes SRβC1, a version of $SR\beta_{md}$ lacking the carboxyl-terminal six amino acids. The coding region for SRβC1 was amplified by PCR from pMAC455 using a 5' sense primer complementary to the SP6 promoter, and a 3' antisense primer GCTCTAGACCTACTTCTCCAGGTCCTGGATG. The PCR product was cut with *NcoI* and *XbaI* and subcloned into pMAC690 in place of the coding sequence for $SR\beta_{md}$.

pMAC1300 encodes SRβC1ΔTM, and was created by digesting pMAC747 (encoding SRβC1) with *BspEI* and *BamHI*, and subcloning it into the corresponding region of pMAC853 (encoding SRβΔTM).

pMAC1056 encodes SRβD4, the carboxyl-terminal 195 amino acids of canine SRβ. The coding region for SRβ was amplified by PCR from pMAC853 using a 5' sense primer CATGCCATGGCTGTTCTTCTTGTTGGC and a 3' antisense T7 promoter primer. The PCR product was cut with *NcoI* and *BamHI* and used to replace the $SR\beta_{md}$ coding region in pMAC690 digested with the same enzymes.

pMAC1057 encodes SRβD5, the carboxyl-terminal 182 amino acids of canine SRβ. The appropriate coding region was amplified from pMAC853 using a 5' sense primer CATGCCATGGGATTACTGTTTGTCAGGTTGTTAAC and a 3' antisense T7 promoter primer. This fragment was cloned into pMAC690 using *NcoI* and *BamHI* as above.

pMAC1082 encodes SRβΔloop, a version of SRβΔTM containing a deletion of amino acids 185 to 219. To prepare the plasmid for PCR, an endogenous *HindIII* site was removed from a non-coding region of the plasmid by cutting pMAC853 with *HindIII*, treating with Klenow fragment and ligating. The resulting plasmid (pMAC853-*HindIII)* was amplified with a 5' sense primer AATTAAGCTTGGAAAGAAAGGCAAAGAATTTGAGT and a 3' antisense primer AATTAAGCTTTGCGGATTTTGCCATTGTAATG. The PCR product (the entire plasmid except for the deleted region) was digested with *HindIII* and ligated to yield pMAC1082.

pMAC1363 encodes SRβ-loop2, a version of SRβΔTM with amino acids 185-219 replaced with the pseudo-random sequence RSTISLQQASPLTGTPDKSGRSATVLAQQLALNKL. The corresponding DNA sequence was created as a pair of oligonucleotides containing a 5' *BglII* and a 3' *HindIII*

site. The oligos were ligated into pSPUTK to give pSPUTK-loop2. The carboxyl-terminal region of SRβ and T7 RNA polymerase promoter were amplified from pMAC853-*HindIII* using a 5' sense primer containing a *HindIII* site and a 3' antisense primer containing a *NheI* site, and ligated into pSPUTK, giving pSPSRβ3'. pSPUTK-loop2 was digested with *BglII* and *HindIII*, and the fragment was ligated into pSRSRβ3' to give pSPSRβ3'-loop2. The amino-terminal region of pMAC853 including the SP6 RNA polymerase promoter and coding regions for the HA tag and the amino-terminal part of SRβ were amplified using a 5' sense primer containing an *AflIII* site and a 3' antisense primer containing a *BglII* site, and ligated into pSPSRβ3'-loop2 to assemble the coding region for SRβ-loop2.

All of the plasmids encoding GTPase mutants were created by oligonucleotide-directed point mutation and PCR using a method described previously (Hughes and Andrews, 1996) using an *ApaI* site. All plasmids were sequenced to confirm the presence of the desired mutations.

2.2.3 Endoglycosidase H treatment

10 μL of translation products were diluted to 100 μL in 0.5% SDS, 1% β-mercaptoethanol, 50 mM Na Citrate, pH 5.5 and incubated for 10 minutes at 100°C for 10 minutes. Samples were split in half and 50 units of Endoglycosidase H (New England Biolabs) were added to one sample. Both samples were incubated at 37°C for 1 hour, at which time 10 μL were analysed by SDS-PAGE.

2.2.4 Quantification of *in vitro* translation products

1 μL of translation reaction products were added to 50 μL 200 mM NaOH and 2.5 μL H_2O_2, and spotted onto glass microfibre filters (Whatman). The filters were soaked in 10% w/v trichloroacetic acid (TCA) for 10 minutes, washed 3 times in 5% TCA, once in 95% ethanol, and allowed to dry. The dry filters were added to scintillation fluid, and the measured radioactivity was converted to fmoles of protein by the following equations:

$$Ci = \frac{\left(\frac{CPMx\%P}{M}\right)xEF}{2.2x10^{12}},$$

where Ci is the number of curies per sample, %P is the percentage of counts from the translated protein, M is the number of methionines in the protein, and EF is the efficiency factor of the scintillation counter.

$$fmoles\_protein = \left(\frac{\frac{Ci}{f}}{\frac{1}{SA_0} - \frac{(1-f)}{1494}}\right)x10^{12},$$

where f is the radioactive decay factor and SA_0 is the specific activity of the isotope. Periodically, 0.5 μL of reaction products were separated by SDS-PAGE and subjected to Phosphorimager analysis to determine the percentage of radioactivity arising from the product of interest (%P), as compared to non-specific translation products. The determination of fmoles of protein rather than simply measuring radioactivity and correcting for the number of methionines was used to permit repeat experiments to be performed with identical quantities of *in vitro* translation products irrespective of the specific activity of the ^{35}S methionine.

2.2.5 Immunoprecipitations and Proteolysis

To immunoprecipitate dimers consisting of SRα deletion mutants and HA-tagged $SR\beta_{md}$, SRα molecules were synthesized *in vitro* and $SR\beta_{md}$ was synthesized *in vitro* in the presence of KRMs. 5 μL of $SR\beta_{md}$ was incubated with 30 μL of the indicated SRα mutants for 30 minutes at 24°C. The mixture was loaded onto a 0.8 mL CL2B column equilibrated and eluted with buffer containing 250 mM NaCl, 100 mM KOAc, 10 mM Tris-OAc, pH 7.5, 2.5 mM $MgCl_2$, 1 mM DTT. Fractions containing the excluded volume of the column were pooled, adjusted to 350 mM NaCl, 5% glycerol and 1% Triton X-100, and $SR\beta_{md}$ was recovered using monoclonal antibodies against the HA epitope and Protein G Affi-Gel (Bio-Rad). Immunoprecipitates were washed three times in TXSWB (100 mM Tris-Cl, pH 8.0, 500 mM NaCl, 10 mM EDTA, 1% Triton X-100, 5% glycerol), and washed two times with IP wash buffer (100 mM Tris-Cl, pH 8.0, 100 mM NaCl), prior to addition of SDS-PAGE loading buffer.

To immunoprecipitate dimers consisting of SRα and the specified SRβ mutant (all lacking the transmembrane domain), equimolar amounts of the two molecules were incubated for 15 minutes at 24°C. The reactions were then diluted in TXSWB at 4°C and incubated rotating end over end for 8-12 hours with either a polyclonal antibody to SRα conjugated to CNBr-activated Sepharose (Pharmacia), or a polyclonal antibody to the HA epitope bound to Protein G Affi-Gel. Immunoprecipitates were washed three times in TXSWB, and washed two times with IP wash buffer prior to addition of SDS-PAGE loading buffer. For immunoprecipitation with anti-$SR\beta_{COOH}$, SRβ and SRα translations were mixed such that the proteins were present in a 2:1 ratio, respectively. Reactions were added to 500 μL of TXSWB with anti-$SR\beta_{COOH}$ and Protein G Affi-Gel and incubated with end over end rotation for 12 hours at 4° C. The beads were pelleted and the supernatant was recovered and used for immunoprecipitation with anti-HA antibodies to isolate the remaining SRβ molecules.

To determine the membrane topology and protease sensitivity of the mutants bound to membranes, microsomes were added to 20 μL translation reactions. After translation for 60 minutes the membranes and membrane-bound proteins were isolated by gel-filtration chromatography and analyzed by proteolysis as described previously (Falcone et al., 1999).

2.2.6 Membrane pelleting experiments

20 μL *in vitro* translation reactions were supplemented with 1 equivalent KRMs

(+KRMs) or 1 μL water (-KRMs) and allowed to proceed for 1 hour. Reactions were overlayed onto an 80 μL 0.5 M sucrose cushion in retic buffer (10 mM Tris-Ac, pH 7.5, 100 mM KOAc, 2.5 mM MgOAc2, 1 mM DTT) and membranes were separated from bulk reaction products by spinning for 15 minutes at 26 psi in a Beckman airfuge. Samples were separated into 50 μL top (T) and middle (M) fractions, and the membrane pellet was solubilized in 50 μL 100 mM Tris-Cl, pH 8.0, 1% SDS (B).

2.2.7 GTP depletion

Depletion of small molecules from translation reactions was performed essentially as described (Kim et al., 1997). Briefly, translation reactions were loaded onto a 20X bed volume of Sephadex G25 resin equilibrated in 250 mM sucrose, 25 mM HEPES-KOH, pH 7.5, 10 mM KOAc, 1 mM DTT, 5% glycerol and centrifuged at low speed at 4°C. The flow through was collected and the procedure was repeated. To determine how effectively this procedure removed nucleotides a control reaction containing ^{35}S labeled ATP was analyzed. For nucleotide titration experiments, the appropriate amount of nucleotide was added to 10 μL of depleted SRβ reaction products and incubated for 20 minutes on ice prior to mixing with translation reactions for SRα for 15 minutes at 24°C.

2.3 Results

2.3.1 Membrane topology of SRβ

2.3.1.1 Glycosylation analysis

The hypothesis that SRβ is an integral membrane protein is based on the following data: 1. Examination of the primary sequence of murine and canine SRβ predict a transmembrane sequence at the amino-terminus (Miller et al., 1995); 2. SRβ partitioned into the detergent phase in Triton X-114 experiments, consistent with the properties of an integral membrane protein (Young et al., 1995; Miller et al., 1995); 3. SRβ remained in the membrane fraction after extraction with high pH conditions sufficient for removal of SRα (Miller et al., 1995). The positive inside rule, which states that the amino acid sequence flanking the TM domain that contains the highest concentration of positive charge will orient towards the cytoplasm (von Heijne and Gavel, 1988), predicts that SRβ assembles into the ER membrane in a type I orientation; that is, with the amino-terminus within the ER lumen. Nevertheless, SRβ could adopt one of two possible topologies, outlined in Figure 2.1.A. Orientation "a" shows the transmembrane domain dipping into the membrane, anchoring SRβ to the surface of the ER. This orientation causes the amino-terminus to protrude into the cytosol, where it could contribute to SRα-binding. Orientation "b" depicts a typical type I orientation. The transmembrane domain spans the membrane and the amino-terminus resides within the lumen of the ER. In this orientation the amino-terminus is unable to contribute to the tight binding of SRα-SRβ.

To distinguish between each of these possibilities I added a glycosylation sequence (MGNAS) onto the extreme amino-terminus of murine SRβ ($gSR\beta_m$) or onto a chimera consisting of the first ten amino acids of murine SRβ followed by residues

Figure 2.1: Probing SRβ membrane assembly using an amino terminal glycosylation sequence. A.The two possible conformations of SRβ in the ER membrane. In conformation "a" the transmembrane sequence dips into the lipid bilayer, leaving the amino terminus in the cytoplasm. In conformation "b" the transmembrane sequence spans the membrane, placing the amino terminus into the lumen. **B.** $gSR\beta_{m}$, $gSR\beta_{md}$, $S_{p}gPa$ and unmutated $SR\beta_{md}$ were translated *in vitro* in the presence or absence of salt washed canine microsomes (KRM). Samples of translation reactions were treated with endoglycosidase H (EndoH) to remove sugars from glycosylation sites, and reactions were analysed by SDS-PAGE followed by autoradiography. The presence of a glycosylation event is proof that the amino terminus of SRβ resides within the lumen of the ER. Glycosylation events denoted by ● arise from the engineered glycosylation site, while glycosylation events denoted by ▲ arise from a glycosylation sequence elsewhere within $SR\beta_{md}$.

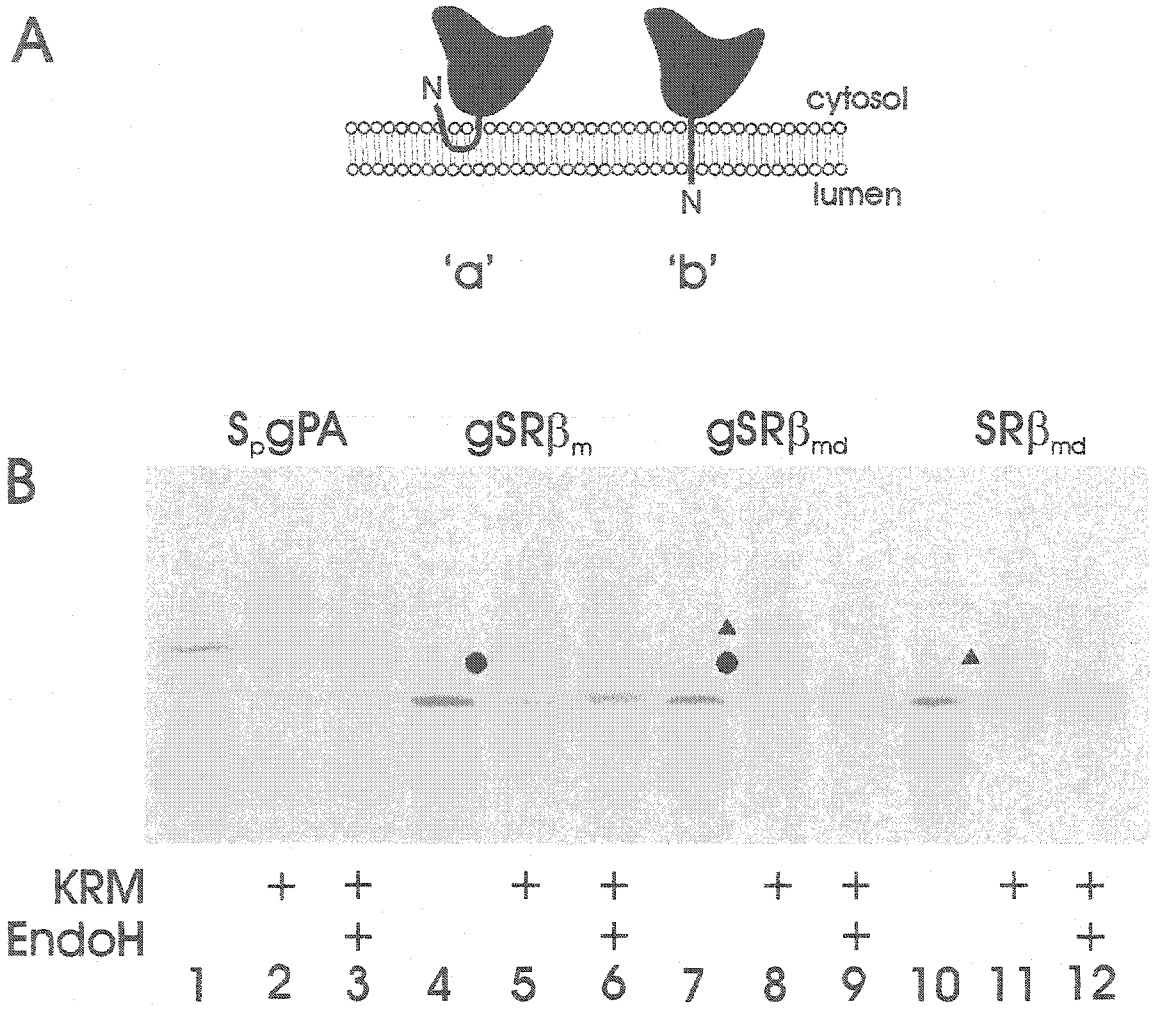
A
N
cytosol
N
lumen
'a'
'b'
B
SpgPA
gSRβm
gSRβmd
SRβmd
KRM
EndoH
1 2 3 4 5 6 7 8 9 10 11 12

10 to 265 of canine SRβ ($gSR\beta_{md}$). The detection of a glycosylation event, manifesting as an apparent increase in molecular weight on a SDS-PAGE gel, would prove that translocation into the ER lumen has occurred.

Both $gSR\beta_{m}$ and $gSR\beta_{md}$, as well as S_pgPA, a positive control molecule containing several glycosylation sites (Janiak et al., 1994), and unmodified $SR\beta_{md}$ were synthesized in a reticulocyte lysate cell free system including salt washed canine microsomes (KRMs) and assessed for the presence of a glycosylation event by SDS-PAGE (Figure 2.1.B). As expected, S_pgPA translocated into the lumen of ER vesicles, where it became glycosylated a number of times (lane 2). SRβ molecules containing the engineered glycosylation sequence were also efficiently glycosylated (lanes 5 and 8, ●), indicating that the amino-terminus was translocated into the lumen (orientation 'a' in Figure 2.1.A). A second glycosylation event was apparent within $SR\beta_{md}$ (lanes 8 and 11, ▲), probably arising from a glycosylation sequence between the G2 and G3 sequences in the GTP binding domain (amino acids 110-112). This sequence is not conserved within murine SRβ; therefore a second glycosylation event was not detected in $gSR\beta_{m}$. Since this glycosylation event and the engineered glycosylation event are additive, the second glycosylation event did not arise from a population of SRβ molecules adopting a reversed orientation in the membrane; rather it likely arose from a minor proportion of SRβ molecules that were translocated entirely across the membrane. Removal of carbohydrate from the glycosylation site by treatment with endoglycosidase H confirmed that the apparent shift in molecular weight on SDS-PAGE was due to the addition of carbohydrate and was not the result of an unexpected modification (lanes 3,6,9,12).

2.3.1.2 Deletion mutant analysis

To examine membrane assembly of SRβ, a series of sequence deletions were created (Figure 2.2). Selected molecules were synthesized in a reticulocyte lysate cell free system and assayed for correct assembly into ER membranes. As a starting point for this analysis the $SR\beta_{md}$ chimera was used. This chimera, referred to here as SRβ, was used because it was previously demonstrated to form heterodimers with canine SRα that were indistinguishable from the canine proteins found on microsomes (Young et al., 1995).

The chimeric amino-terminus and the transmembrane domain were deleted in SRβΔTM which therefore, comprises the cytoplasmic domain of canine SRβ. The additional sequences deleted in SRβD4 include a positively-charged region following the transmembrane domain. SRβC1 is a version of $SR\beta_{md}$ lacking only the carboxyl-terminal six amino acids. Finally, deletion of the SRβ cytoplasmic region adjacent to the putative transmembrane domain that is enriched in lysine and arginine residues yields SRβΔch. Preliminary immunoprecipitation studies (see Figure 2.6.D, lanes 3 and 4) determined that antibodies raised to a carboxyl-terminal peptide of SRβ precipitated only monomeric SRβ. Therefore, all SRβ constructs contain the well characterized HA epitope at the amino terminus, unless specified otherwise. Certain mutants in Figure 2.2 were not used to assay membrane assembly of SRβ but were required to identify the SRα-binding

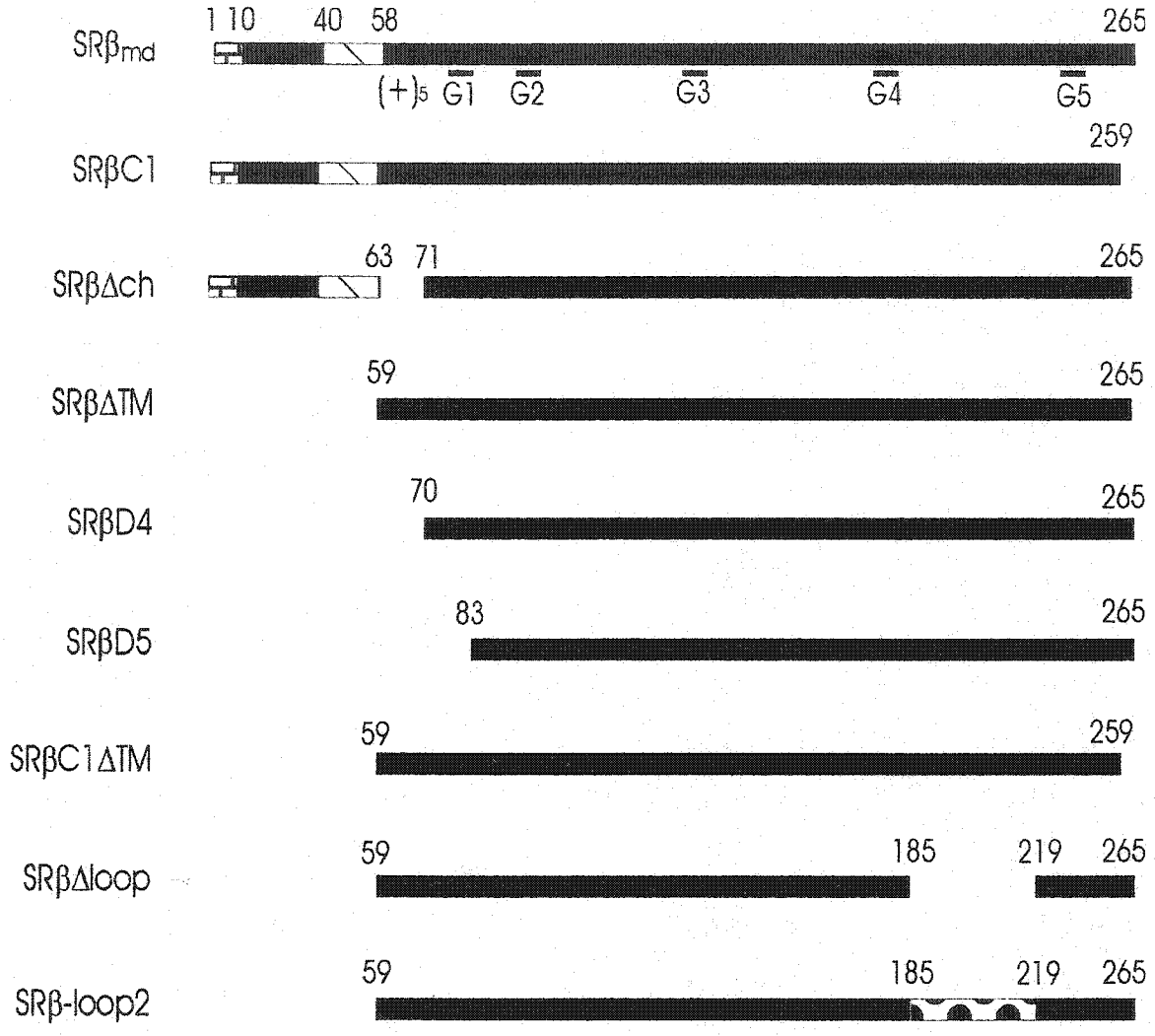

Figure 2.2: Amino acid sequence deletions of SRβ used in this study. All drawings depict a linear representation of SRβ with the canine sequence in black, murine sequence represented by a bricked bar, the transmembrane domain represented by hashed bar, and a scrambled amino acid sequence corresponding to a region of SRβ that does not align with Ras-family GTPases represented by a spotted bar. Positions of conserved regions defining SRβ as a member of the Ras family of small molecular weight GTPases are denoted beneath $SR\beta_{md}$ as G1-G5. A series of positive charges following the transmembrane domain is denoted as $(+)_5$. Numbering corresponds to the amino acid position that defines the border of the corresponding deletion or feature.

domain within SRβ. Description of these mutants appears in the appropriate section.

SRα is a cytoplasmic, peripheral ER protein. Therefore, it can only bind to those regions of SRβ that are on the cytoplasmic side of the membrane. Although Figure 2.1.B suggests that the amino-terminus of SRβ was translocated into the lumen leaving theremainder of SRβ to face the cytoplasm, the detailed topology of SRβ was verified experimentally by using a membrane binding and proteolysis assay (Figure 2.3). In the absence of membranes, a single primary translation product was obtained for SRβ. However, in agreement with an observation made from Figure 2.1.B, translation of SRβ in the presence of membranes resulted in two bands, each representing membrane bound proteins (Figure 2.3, lane 2). The upper band was glycosylated as after treatment with endoglycosidase H it co-migrated with the lower band (Figure 2.1.B and Figure 2.4). Since the one potential glycosylation site in SRβ was located within the GTP binding domain, the glycosylated band came from molecules oriented with the GTPase domain inside the endoplasmic reticulum. The glycosylated band was fully protected from protease digestion by the membrane (Figure 2.3, lane 3), suggesting that the entire molecule was translocated across the ER membrane.

Only SRβ that co-fractionated with membranes during gel-filtration chromatography are shown in lane 2 therefore, it is possible to calculate the fraction of molecules that adopt each topology. Greater than 60% of the membrane bound SRβ molecules were not glycosylated and co-migrated with SRβ synthesized in the absence of membranes, as expected for a membrane protein with type I transmembrane (amino-terminus lumenal) orientation. When membranes were treated with protease, the molecules that comigrated with SRβ were partially digested and therefore, migrated with lower apparent molecular weight (Figure 2.3, lane 3, ▲). This digestion pattern is typical of a type I molecule with a protease-resistant core structure. Some molecules were almost completely digested, resulting in the small band (Figure 2.3, *). This band resulted from protection of the amino-terminus and transmembrane domain of SRβ by the membrane. Upon solubilization of the membrane by Triton X-100 (lanes labelled TX100), the larger protease resistant fragment of SRβ was further digested by the protease (Figure 2.3, lane 4, ●) because the amino-terminus was no longer protected by the membrane.

These data confirm that SRβ spans the membrane as a typical type I integral membrane protein. Therefore, the amino acids at the amino-terminus of SRβ (approximately residues 1-58) reside within or span the ER membrane, where they are unlikely to come into contact with SRα. Thus, the sequence containing a series of positive charges (amino acids 58-70) following the transmembrane domain, is the most amino-terminal region of SRβ that is a candidate for binding to SRα.

Deletion of these residues from full length $SR\beta_{md}$ (SRβΔch) inverted the orientation of some of the type I molecules in the ER membrane. As a result, the topology of some of the glycosylated molecules were inverted as they were almost completely protected from the protease (Figure 2.3, lane 7). After proteolysis these molecules

Figure 2.3: Proteolysis of selected SRβ molecules. Deletion versions of SRβ were synthesized in the absence (lanes 1, 5, 9, 13) or presence (lanes 2-4, 6-8, 10-12, 14-16) of canine microsomes (RM). Membranes were isolated from the translation reactions by gel filtration chromatography and divided into three aliquots. Digestion with proteinase K (PK) was used to examine topology with respect to the membrane and to assay protein folding. Triton X-100, (TX100) was added to solubilize the membrane to permit digestion of protease sensitive fragments otherwise protected from the protease by the membrane. Triangles indicate type I transmembrane molecules including a protease resistant core (dots) and the transmembrane amino-terminus protected by the membrane. Asterisks indicate the transmembrane amino-terminus protected by the membrane. One microliter of total translation products were analyzed in lanes 1,5,9,13. All other lanes correspond to 7 microliters of the original translation reaction. The migration positions of molecular weight standards are indicated to the left of the panel. The data in this figure was prepared by Mina Falcone.

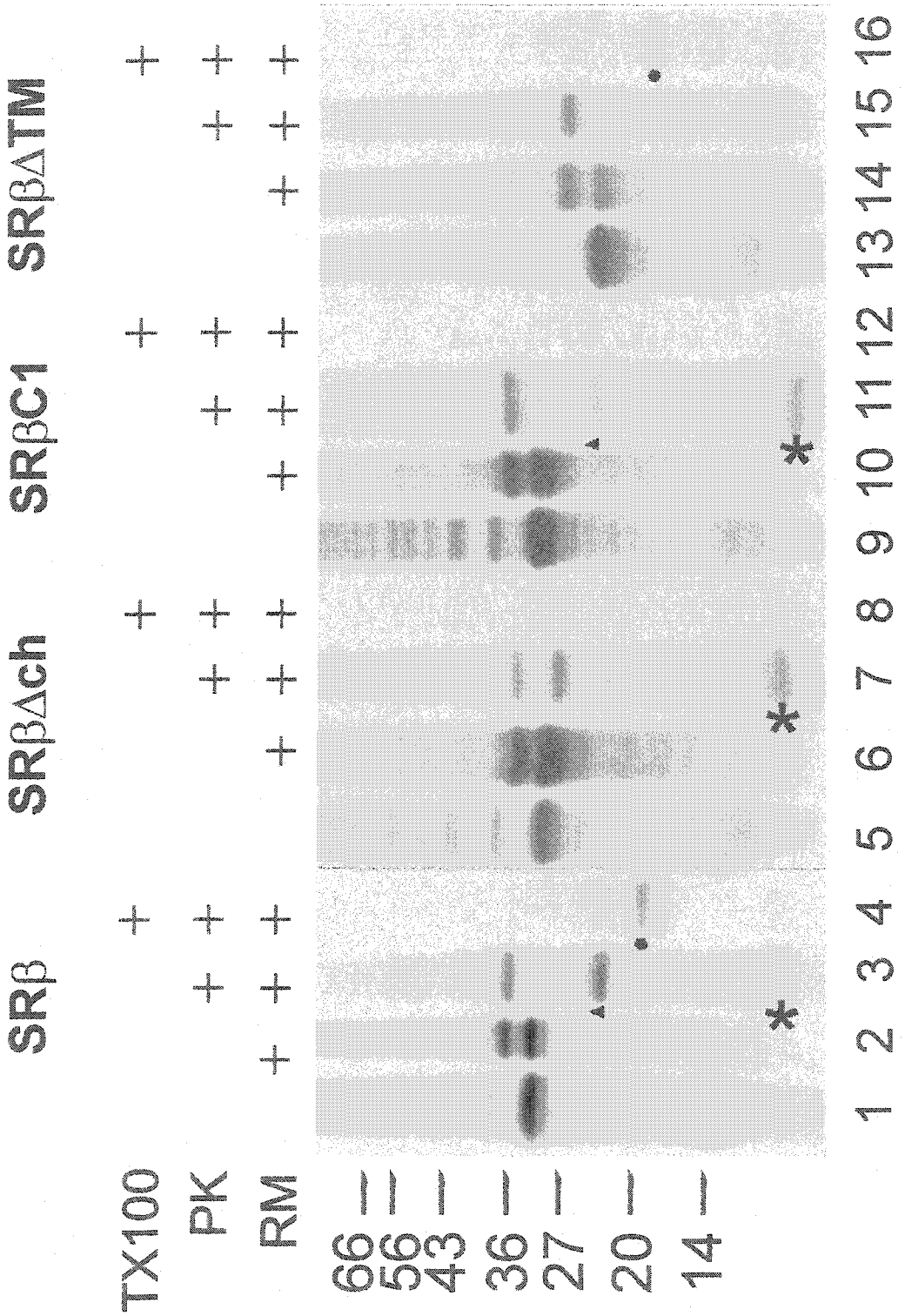
SRβ
SRβΔch
SRβC1
SRβΔTM
TX100
PK
RM
66
56
43
36
27
20
14
1 2 3 4 5 6 7 8 9 10 11 12 13 14 15 16

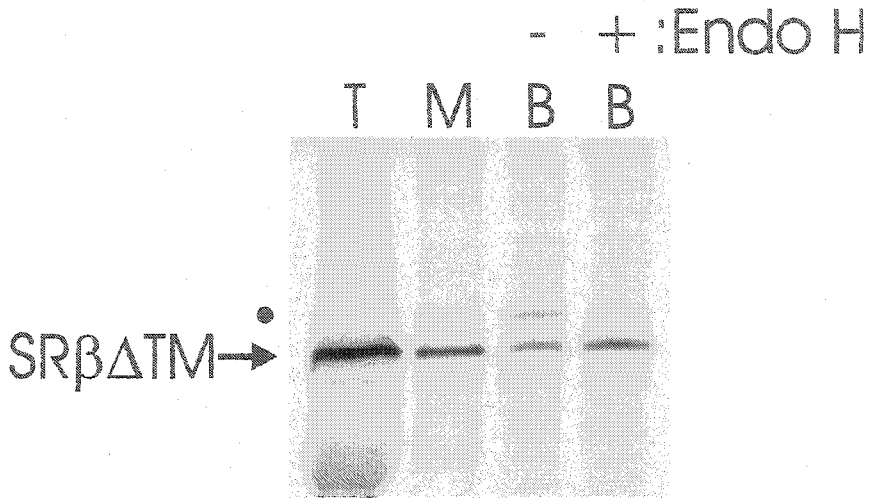

Figure 2.4: Binding of SRβΔTM to ER membranes. SRβΔTM was synthesized *in vitro* in the presence of salt washed canine microsomes and centrifuged over a 0.5M sucrose cushion to separate the microsome-bound products from unbound translation products. Following centrifugation the reaction was separated into a top (T) and middle (M) fraction, containing unbound material, and a bottom (B) fraction, containing the microsomes. Two bands are present in the bottom fraction; one migrating as unmodified SRβΔTM and one migrating with a higher apparent molecular weight. Treatment with endoglycosidase H, reveals that some of the membrane-associated SRβΔTM has undergone a glycosylation event. migrated slightly further due to proteolysis of the

amino-terminal HA tag and the approximately 40 amino acids that precede the transmembrane domain. These residues were susceptible to digestion because they were on the cytoplasmic side of the membrane, confirming an inverted topology for the protein. Neither these nor the non-glycosylated molecules folded into a protease resistant conformation as there was no protease resistant band in lane 8. As expected, the amino-terminus of that fraction of the molecules that still adopt the type I topology was protected from proteinase K by the membrane (Figure 2.3, * in lane 7). Thus, it appears that one function of the positively-charged region is to prevent translocation of the GTPase domain of SRβ during translocation of the transmembrane domain.

Surprisingly, deletion of the first 59 amino acids of SRβ which includes the transmembrane domain resulted in a molecule with reduced but not abolished interaction with membranes (Figure 2.3, compare lanes 1 and 2 with lanes 13 and 14; see also Figure 2.4). Both type I and type II membrane associated molecules were detected bound to ER membranes. The membrane protected amino-terminus of SRβΔTM was too small to detect by SDS-PAGE but the disappearance of the band that co-migrated with full length non-glycosylated SRβ–ΔTM upon addition of protease (Figure 2.3, compare lanes 14 and 15) is diagnostic for type I transmembrane molecules. In contrast, the lumenally disposed glycosylated SRβΔTM molecules were protected from added protease unless non-ionic detergent was added to solubilize the membranes (Figure 2.3, compare lanes 13-16) confirming that there is a cryptic signal sequence within SRβ that translocated the GTPase domain of SRβ across the ER membrane.

Of the 16 residues between the transmembrane segment and G1 consensus sequence in SRβ, 5 of the first 11 are positively charged. Although the next 5 residues are hydrophobic, signal peptides require a longer contiguous stretch of uncharged amino acids (von Heijne, 1985). Thus, the cryptic signal sequence must at least overlap the GTPase domain of SRβ. Consistent with this interpretation the first 6 residues of the GTPase domain are uncharged. As expected, membrane binding and translocation of SRβΔTM occurred only co-translationally, demonstrating that membrane binding was specific (Figure 2.5) and not due to aggregation on the surface of the ER. Finally, it is possible that deletion of residues 1-59 from SRβ impairs folding of the membrane bound molecules as less of the protease resistant core fragment was detected (Figure 2.3, lane 16).

To test the hypothesis that the residues between the transmembrane domain and the G1 consensus sequence can function as a cryptic signal sequence the membrane binding of SRβΔTM was compared to a molecule containing a further deletion of residues 59-70 (SRβD4) (Figure 2.6). Molecules were synthesized *in vitro* in the presence of ER membranes (lanes 1-3,7-9) or in the absence of membranes (lanes 4-6, 10-12) and membrane bound molecules were separated from unbound reaction products by pelleting the membranes through a sucrose cushion. Reactions were then fractionated into soluble (T, M) and membrane-bound (B) fractions. In agreement with results from Figures 2.3 and 2.4, SRβΔTM was translocated into vesicles, and a significant proportion of

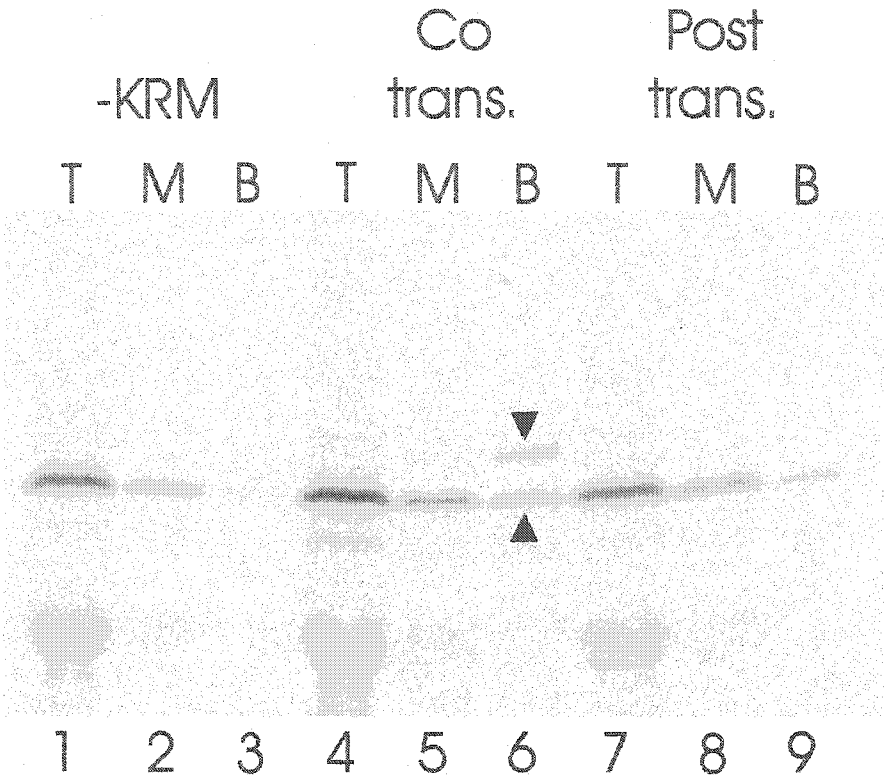

Figure 2.5: Targeting of SRβΔTM to membranes. SRβΔTM was synthesized *in vitro* in the absence of canine pancreatic microsomes (lanes 1-3), in the presence of microsomes (lanes 4-6), or in the presence of canine microsomes following synthesis of SRβΔTM (lanes 7-9). Reactions were centrifuged over sucrose cushions and divided into soluble (T, M) and membrane-bound (B) fractions. ▲: SRβΔTM that has been targeted to microsomes, ▼: SRβΔTM that has translocated across the ER membrane and glycosylated.

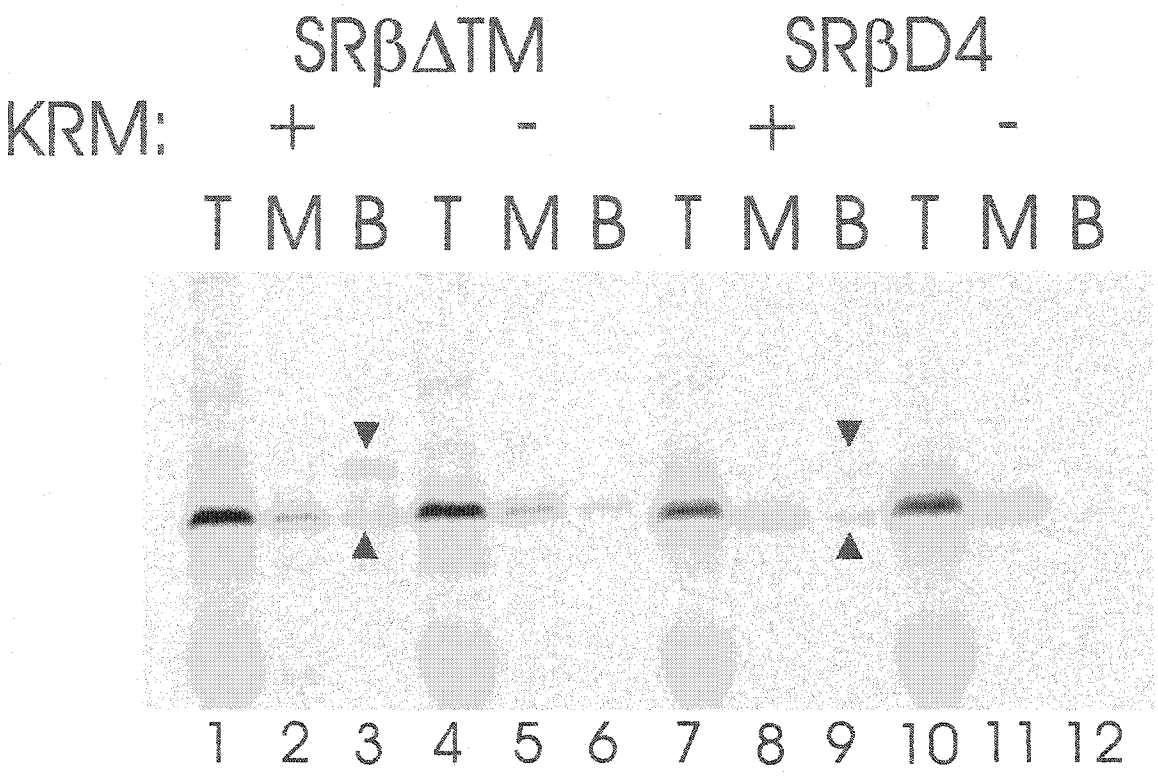

Figure 2.6: Membrane binding of SRβΔTM vs SRβD4. SRβΔTM or SRβD4 were synthesized *in vitro* in the presence (+) or absence (-) of salt washed canine microsomes (KRM). Translation reactions were then centrifuged over a 0.5M sucrose cushion to separate the microsomes from unassociated translation products, and separated into top (T), middle (M) and bottom (B) fractions. In the absence of KRMs nearly all SRβΔTM and SRβD4 fractionate in the top and middle fractions, while in the presence of KRMs, only SRβΔTM is detected in the bottom fraction, bound to microsomes. ▲: SRβΔTM that has been targeted to microsomes, ▼: SRβΔTM that has translocated across the ER membrane and glycosylated.

molecules became glycosylated (compare lane 3 with lane 6). This molecule did not contain the HA tag, so this result verified that the epitope sequence did not contribute significantly to the cryptic signal sequence. Removal of the charged residues following the transmembrane domain reduced binding of SRβ to membranes to background levels (compare lane 9 with lane 3), demonstrating conclusively that these residues directly contribute to the targeting of SRβΔTM to membranes.

Deletion of the last 6 amino-acids from the carboxyl-terminus of the SRβ GTPase domain resulted in a molecule (SRβC1) with primarily type I topology, similar to SRβ, (Figure 2.3, compare lanes 1-3 with lanes 9-11). However, this molecule was somewhat impaired for folding as the intensity of the band resulting from the protease resistant structure was substantially reduced (Figure 2.3, lane 11, ▲).

2.3.2 Dissecting the SRα/SRβ interaction

2.3.2.1 Deletion mutant analysis

Gel filtration analysis of a series of SRα deletions synthesized *in vitro* revealed that only those SRα molecules containing a complete amino-terminus eluted in the same fractions as canine pancreatic microsomes, presumably because SRα was binding to the microsomes through a physical interaction with SRβ (Young et al., 1995). To corroborate this data as well as to examine the SRα-SRβ interaction directly a coimmunoprecipitation approach was developed (Figure 2.7). To facilitate precipitation of SRβ the well characterized HA epitope was added to the amino-terminus of $SR\beta_{md}$ because antibody binding to the amino-terminus of SRβ was not expected to affect the SRα-SRβ interaction. By incubating SRα deletion mutants with HA-tagged $SR\beta_{md}$, and immunoprecipitating with an anti-HA antibody, SRα deletion mutants that bind to $SR\beta_{md}$ could be detected.

Full length SRα, and several deletion mutants within the amino-terminus were selected for immunoprecipitation with HA-tagged SRβ, using an anti-HA antibody (Figure 2.7.A). The SRD4, SRD6 and SRD7 deletions remove the first hydrophobic region, the second hydrophobic region and the first charged region of SRα, respectively. SRX2 is predicted to contain all of the sequence required to bind SRα to SRβ. All molecules were synthesized *in vitro* in the presence of ^{35}S-methionine to allow visualization by autoradiography, and incubated to allow binding to occur. Following immunoprecipitation full length SRα was efficiently precipitated with SRβ (Figure 2.7.B, lane 1), as expected. SRD4 and SRD6 did not precipitate well while SRD7 did not precipitate at all with SRβ (lanes 2-4). SRX2, consisting of the amino-terminal 176 amino acids of SRα precipitated efficiently with SRβ (lane 5), confirming that this domain is necessary and sufficient to bind SRα to SRβ. The band corresponding to SRX2 appeared lighter than full length SRα; this is because SRX2 contains three methionine residues compared to full length SRα, which contains 17 methionine residues. Therefore SRX2 will appear nearly six times lighter than an equivalent amount of SRα on an autoradiogram. The interaction between SRα and SRβ is specific, since no SRα was

Figure 2.7 Immunoprecipitation of SRα deletion products with SRβ. **A**: A diagram of full-length SRα and the SRα deletion products used in this experiment. Amino acid residues are numbered below the full-length SRα bar. Hydrophobic regions are shown in black and charged regions are shaded. The translated regions of each deletion product are black bars. **B**: Aliquots of *in vitro* translation reactions containing SRα deletions and HA-tagged $SR\beta_{md}$ were incubated together prior to immunoprecipitation. Samples were immunprecipitated with an anti-HA antibody to precipitate SRβ. Migration positions of SRα and SRβ are indicated to the left of the panel. The migration positions of S_LS_TgPA and SRX2 are indicated to the right of the panel. Both panels have been adapted from Young et al., 1995.

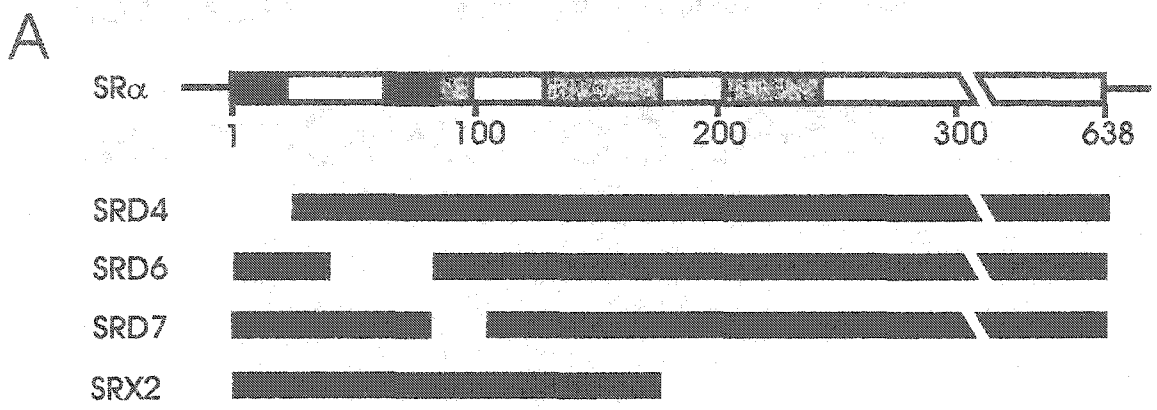
A
SRα
1
100
200
300
638
SRD4
SRD6
SRD7
SRX2

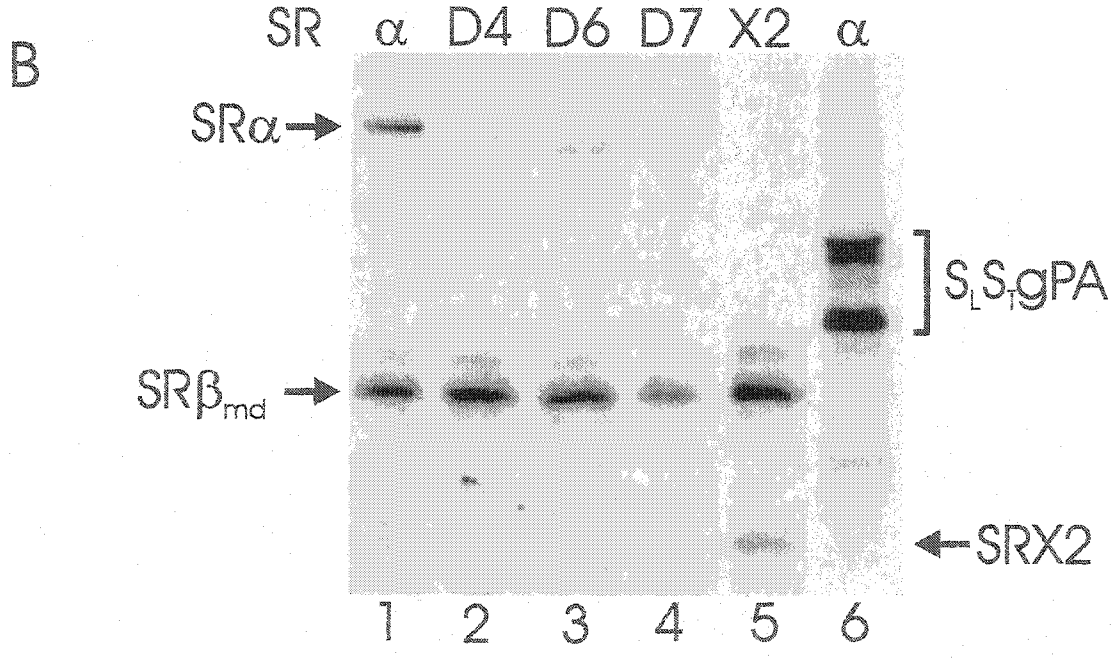
B
SR α D4 D6 D7 X2 α
SRα
SRβmd
SLSTgPA
SRX2
1 2 3 4 5 6

detected when a control molecule was immunoprecipitated with rabbit IgG (lane 6). The results of this experiment agreed with the gel filtration data, and confirm that SRX2 is the minimal SRβ-binding of SRα (Young et al., 1995).

To identify the SRα binding domain within SRβ the coimmunoprecipitation approach was used to assay a series of SRβ deletions for interaction with SRα (Figure 2.8). To precipitate the SRβ mutants the same anti-HA antibody was used as in Figure 2.7.B. To precipitate SRα I used an antibody directed against the linker region between the SRX2 domain of SRα that binds it to SRβ and the SRα GTPase domain.

I created additional truncations within SRβ to assay the requirements for SRα-binding (Figure 2.2). Sequences deleted in SRβD5 include the amino-terminus, transmembrane domain, positively-charged region and G1 GTPase consensus sequence. SRβC1ΔTM, like SRβC1, removed the carboxyl-terminal six amino acids, with the additional deletion of the amino-terminus and transmembrane domain. Alignment of SRβ with members of the Ras family of GTPases identified a putative insertion of 34 amino acids between the G4 and G5 consensus sequences (Miller et al., 1995). Deletion of this sequence from SRβΔTM yielded SRβΔloop, and replacement of the loop with a scrambled version of the sequence resulted in SRβ-loop2.

Since the positive charges following the transmembrane domain appear to dictate the membrane orientation of SRβ, this region is unlikely to be involved in binding to SRα. Therefore, the GTP-binding domain and the putative loop region are the main candidates for an SRα-binding motif. Consistent with the hypothesis that the amino-terminus of SRβ is not required for binding to SRα, dimerization of either SRβΔTM or SRβD4 with SRα was detected with both antibodies (Figures 2.8.B and 2.8.C, lanes 1 and 2, respectively). Deletion of the G1 region, (SRβD5) which comprises part of the SRβ GTPase domain, abolished binding to SRα (Figures 2.8.B and 2.8.C, lane 3). Deletion of as few as six amino acids from the carboxyl-terminus of SRβ also abolished binding to SRα (Figures 2.8.B and 2.8.C, lane 4). The last 6 amino acids of SRβ contribute to part of an alpha helix forming part of the GTPase domain (Miller et al., 1995). Thus, these results demonstrate that deletion of either end of the GTPase domain prevents dimer formation. In addition, both of these SRβ mutants (SRβD5 and SRβC1ΔTM) lacked the protease resistant fragment observed for SRβΔTM (Figures 2.3 and 2.9) suggesting that the protease resistant fragment probably resulted from correct folding of the SRβ GTPase domain. Taken together, these data imply that a properly folded SRβ GTPase domain is required for efficient binding of SRα.

Removal of the sequence from between G4 and G5 in SRβ that does not align with other Ras type GTPases (a putative loop, according to (Miller et al., 1995)) resulted in reduced but detectable binding of SRβΔloop to SRα, as did replacement of this sequence with a scrambled sequence (SRβ-loop2). SRα-binding to these deletion forms of SRβ was not efficient (arrowheads in Figure 2.8.B, lanes 5-6), therefore a darker exposure of these lanes of the autoradiogram is also shown (Figure 2.8.D, lanes 1-2).

Figure 2.8: Immunoprecipitation of SRα with SRβ deletions. Aliquots of *in vitro* translation reactions containing equimolar amounts of SRα and the specificed SRβ deletion molecules were incubated together prior to immunoprecipitation. **A**: Total products prior to immunoprecipitation, **B**: Immunoprecipitation with an anti-HA antibody to precipitate SRβ. SRα precipitates well with SRβΔTM and SRβD4, but precipitates poorly with SRβΔloop and SRβloop2 (upward arrowheads). No immunoprecipitation of SRα is detectable with SRβD5 or SRβC1, **C**: Immunoprecipitation with an anti-SRα antibody shows the reciprocal result. Again, SRβΔloop and SRβloop2 precipitate with SRα less efficiently than SRβΔTM (upward arrowheads). **D**: A darker exposure of panel B, lanes 5 and 6 (lanes 1 and 2), and immunoprecipitation of SRα-SRβΔTM complexes with an anti-$SR\beta_{COOH}$ antibody (lane 4) followed by immunoprecipitation with an anti-HA antibody (lane 4). The migration position of full length SRα is indicated by an arrow to the left of the panels. A SRα translation product that results from initiation of translation at an internal methionine is indicated by ●. The bracket indicates the migration positions of the SRβ deletions.

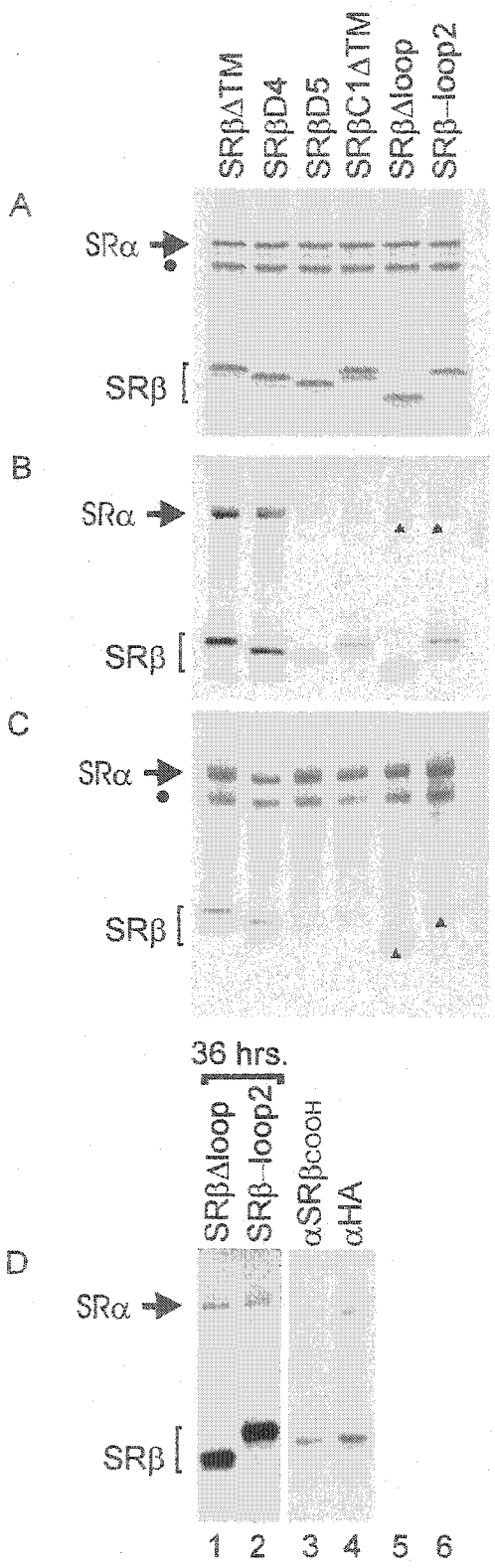
SRβΔTM
SRβD4
SRβD5
SRβC1ΔTM
SRβΔloop
SRβ–loop2
A
SRα
SRβ
B
SRα
SRβ
C
SRα
SRβ
36 hrs.
SRβΔloop
SRβ–loop2
αSRβCOOH
αHA
D
SRα
SRβ
1 2 3 4 5 6

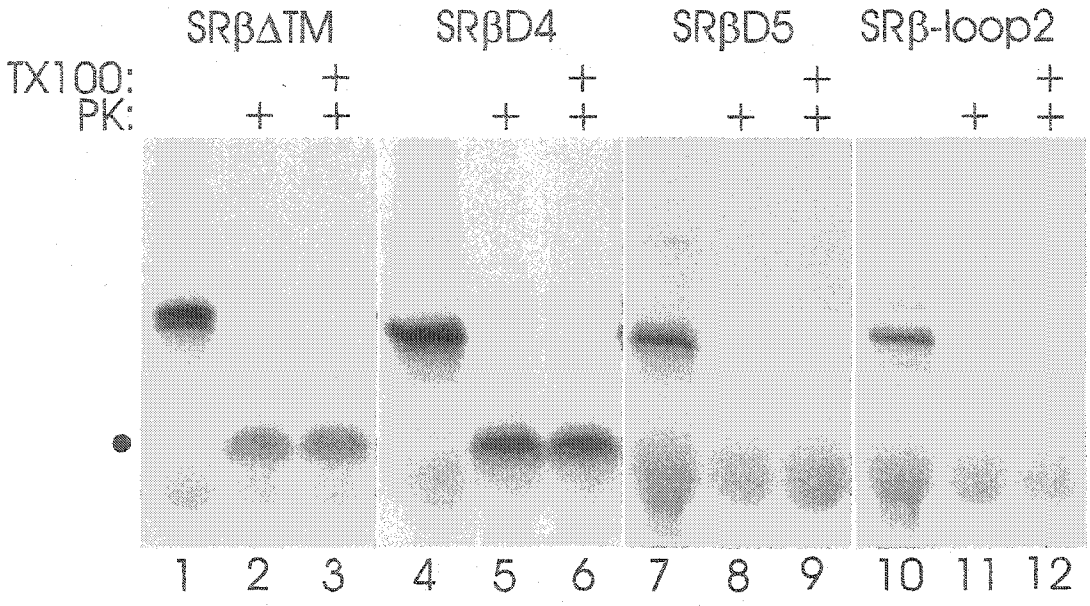

Figure 2.9: Proteolysis of selected SRβ deletions. *In vitro* translation reactions synthesizing SRβΔTM, SRβD4, SRβD5 and SRβ-loop2 were treated with proteinase K (PK) in the absence (lanes 2,5,8,11) and presence (lanes 3,6,9,12) of Triton X-100 (TX100), and analysed by SDS-PAGE followed by autoradiography. A protease resistant core fragment migrating above globin (a background product of the translation reaction) is indicated by ●. The data in this figure was prepared by Mina Falcone.

When the precipitation was performed using antibodies to SRα, binding of SRβΔloop was on average 30% that of binding to SRβΔTM while binding to SRβ-loop2 was about 15% that of binding to SRβΔTM (Figure 2.8.C, arrowheads in lanes 5 and 6, respectively). When synthesized *in vitro*, SRβ-loop2 was less resistant than SRβ was to added proteases (Figure 2.9, lanes 10-12) suggesting that the loop sequence contributes to the correct folding of the SRβ GTPase. Therefore, this sequence may contribute to, but is obviously not essential for, binding of SRβ to SRα.

An antibody was raised against the carboxyl-terminal twenty amino acids of SRβ to assay co-precipitation of SRβ and SRα with an antibody directed against another region of SRβ (anti-$SR\beta_{COOH}$) . However, consistent with the observation that the carboxyl-terminus of SRβ was required for SRα-SRβ dimerization, this antibody was unable to immunoprecipitate dimers (Figure 2.8.D, lanes 3-4). Instead, anti-$SR\beta_{COOH}$ immunoprecipitated only SRβΔTM from mixtures of SRβΔTM and SRα (Figure 2.8.D, lane 3). However, a second round of immunoprecipitation with anti-HA antibodies, following immunoprecipitation with anti-$SR\beta_{COOH}$ precipitated SR dimers that were not recognized by anti-$SR\beta_{COOH}$ (Figure 2.8.D, lane 4).

2.3.2.2 GTPase Mutant Analysis

Since the GTPase domain of SRβ appears to be both necessary and sufficient for binding to SRα, a series of GTPase point mutations (Table 2.2) were created in SRβΔTM to determine whether a functional GTPase domain is required for SR dimerization. Similar GTPase mutations were also examined for functional complementation of SRβ deletion in yeast (Ogg et al., 1998). Coimmunoprecipitation experiments performed with these GTPase mutants illustrated that only a subset were competent for SR dimerization (Figure 2.10 and Table 2.1). The mutants that bind to SRα include the G118L and H119L mutations believed to reduce the GTPase activity of GTP binding domains (Pai et al., 1990; Bourne et al., 1991; Jonak et al., 1994; Hwang et al., 1996) and D181N, a mutation that was shown to alter the nucleotide binding preference from GTP to XTP in other GTP-binding proteins (Figure 2.11)(Hwang and Miller, 1987; Weijland et al., 1994). Although the D181N mutation altered binding preference it did not eliminate GTP binding. Therefore, since our *in vitro* translation reactions contained at least 100 μM GTP it was likely that when synthesized *in vitro*, the D181N mutant was still primarily in the GTP bound form. Of the mutants that did not bind SRα, K75I is predicted to have much reduced nucleotide affinity based on data obtained from Ras (Sigal et al., 1986), whereas N187K is predicted to be structurally unstable based on data from the X-ray structure of Ras (Pai et al., 1990). Thus the common feature of all of the mutants that bound to SRα is that they are all expected to bind nucleotide.

SRX2, the previously identified minimum SRβ-binding domain of SRα (Young et al., 1995), bound to the GTPase domain of SRβ (Figure 2.12, lanes 1-2). In addition, the GTPase domain with the scrambled loop region (SRβ-loop2) also bound to SRX2 (Figure 2.12, lane 3). GTPase mutants that bound full-length SRα also bound to SRX2 (Figure

Table 2.2: Effect of SRβ mutations on the ability to bind SRα

Mutant	Coimmunoprecipitate	GTPase box	Phenotype in yeast[1]
SRβ-ΔTM	++++	N/A	wt
SRβD4	++++	N/A	nd
SRβD5	-	N/A	nd
SRβ1C1-ΔTM	-	N/A	nd
SRβ-Δloop	++	N/A	nd
SRβ-loop2	+	N/A	nd
K75I	-	G-1	ts
G118L	++++	G-3	ts
H119L	++++	G-3	wt
N178K	+	G-4	ts
D181N	++++	G-4	wt
K75I/H119L	-	G-1, G-3	null
G118L/D181N	+	G-3, G-4	nd

N/A = Not Applicable, nd = not determined, ts = temperature sensitive, wt = wild type
[1] Ogg et al., 1999

2.12, lanes 4-5). Since SRX2 bound to SRβ mutants in a manner identical to full length SRα, I conclude that no other sequences in SRα contribute to the interaction.

To determine whether the GTP-bound form, GDP-bound form or the empty form of SRβ binds to SRα, small molecules, including GTP, were removed from *in vitro* translation reactions by gel filtration chromatography. Since the *in vitro* translation reactions contained very small amounts of SRβ, (approximately 100 fmoles) there was a practical limit on the size of gel filtration column that could be used before there was unacceptable loss of SRβ due to non-specific binding. As a result, I was unable to reduce the amount of GTP in the reaction mixture to significantly less than 100 nM (Figure 2.13). Binding of SRβΔTM to SRα was not affected by gel-filtration chromatography (Figure 2.14, compare lane 5 with lane 7). Since SRβ has a measured K_d for GTP as low as 20 nM (Bacher et al., 1999) it is possible that SRβΔTM synthesized *in vitro* possessed a K_d low enough that gel-filtration chromatography was unable to remove nucleotides sufficiently to affect the nucleotide-bound status of SRβΔTM. However, gel filtration blocked dimerization of $SR\beta_{D181N}\Delta TM$ with SRα. $SR\beta_{D181N}\Delta TM$ was expected to possess a lower than wild-type affinity for GTP therefore gel filtration chromatography reduced the concentration of GTP sufficiently to unload $SR\beta_{D181N}\Delta TM$, which was then unable to bind SRα (Figure 2.14, compare lane 6 with lane 8). These data suggest that the empty form of the SRβ GTPase domain was unable to dimerize with SRα. To confirm this result and examine the nucleotide specificity for binding, this experiment was repeated and

Figure 2.10: Immunoprecipitation of SRα with SRβΔTM harbouring GTPase point mutations. Aliquots of *in vitro* translation reactions containing equimolar amounts of SRα and the specified SRβ GTPase point mutations were incubated together prior to immunoprecipitation. **A**: Total products prior to immunoprecipitation, **B**: Immunoprecipitation with an anti-HA antibody to precipitate the SRβ mutants. SRα precipitates well with $SR\beta_{G118L}$, $SR\beta_{H119L}$ and $SR\beta_{D181N}$ ($SR\beta_{XTP}\Delta TM$), but not with $SR\beta_{K75I}$ or $SR\beta_{N178K}$. **C**: Immunoprecipitation with anti-SRα demonstrates the reciprocal result. The migration position of full length SRα and SRβΔTM are indicated by arrows to the left of the panels. An SRα translation product that results from initiation of translation at an internal methionine is indicated by ●.

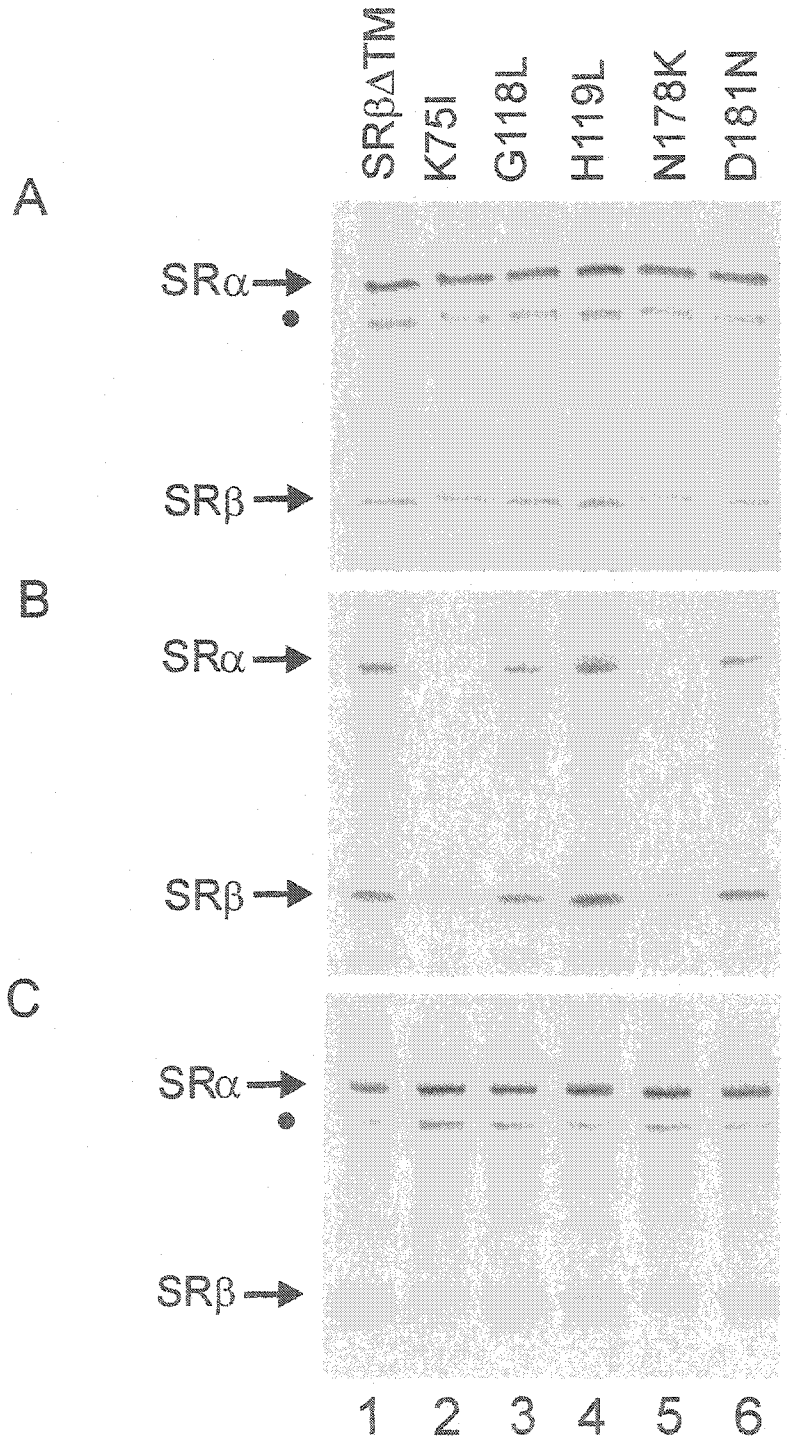
SRβΔTM
K75I
G118L
H119L
N178K
D181N
A
SRα
SRβ
B
SRα
SRβ
C
SRα
SRβ
1 2 3 4 5 6

A

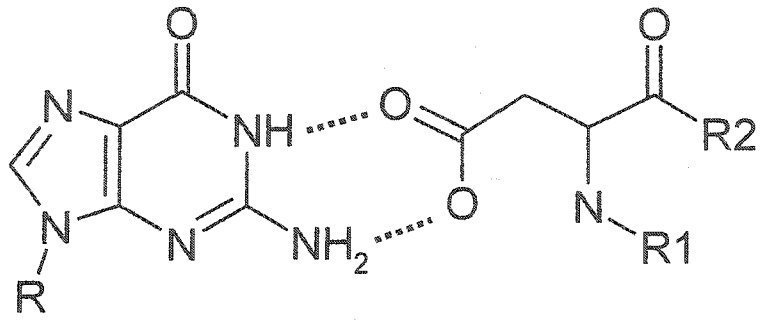

Guanosine Aspartic acid

B

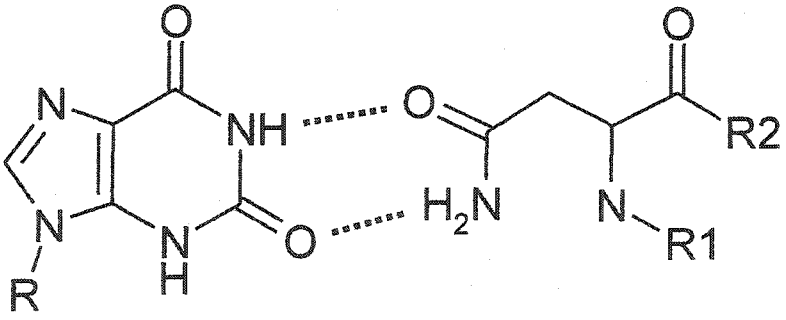

Xanthosine Asparagine

Figure 2.11: The rationale behind the Asp181 to Asn181 mutation. **A**: The interaction between the guanosine ring and Asp, as predicted from the crystal structure of Arf1 (Amor *et al.*, 1994) and H-*ras* p21 (Pai *et al.*, 1990). **B**: The predicted interaction between the xanthosine ring and Asn. The replacement of an amino group with a ketone in xanthosine disrupts a hydrogen bond between the nucleotide ring and Asp. Mutation of Asp to Asn restores the hydrogen bond. Hydrogen bonds are depicted as broken lines.

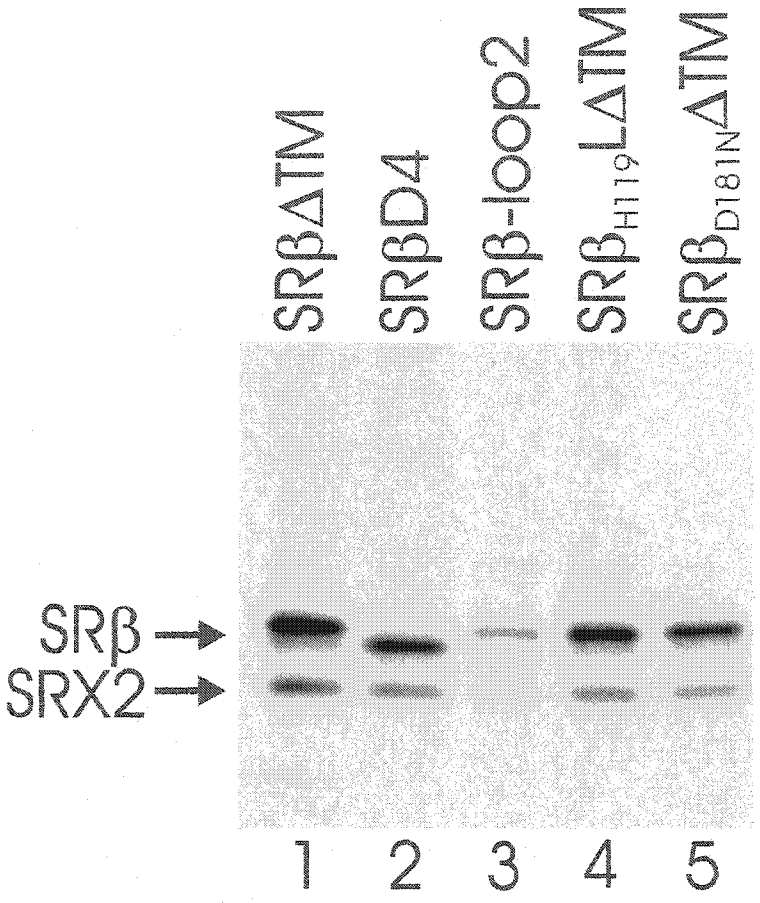

Figure 2.12: Immunoprecipitation of select SRβ molecules with SRX2. *In vitro* translation products of SRβ deletion mutations (lanes 1-3) and SRβ GTPase point mutations (lanes 4 and 5) were incubated with equimolar amounts of SRX2 and immunoprecipitated with an anti-HA antibody to precipitate SRβ. Mutants that precipitate full length SRα also precipitate SRX2. The positions of SRβ and SRX2 are indicated by arrows.

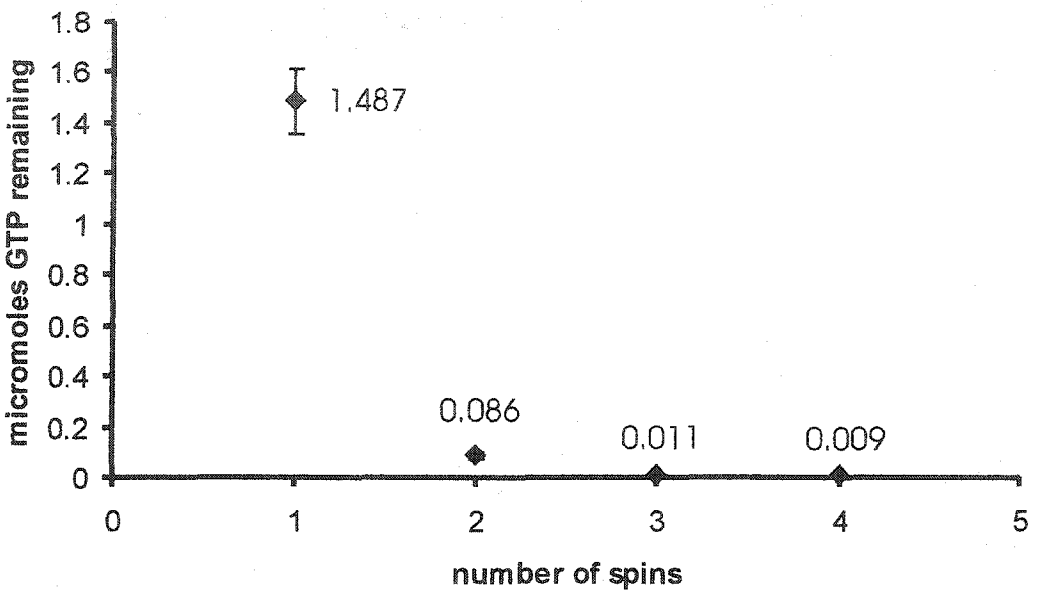

Figure 2.13: Removal of nucleotide by gel filtration. A 100 μM nucleotide solution containing ^{35}S-dATP as a tracer molecule was centrifuged over 20X bed volumes of Sephadex G-25, and the amount of nucleotide remaining in the filtrate was determined by scintillation counting. Error bars represent the standard deviation of three independent trials. The numerical value of the mean accompanies each data point. *In vitro* translation reactions could be centrifuged over two columns before the loss of radiolabelled protein became unacceptable.

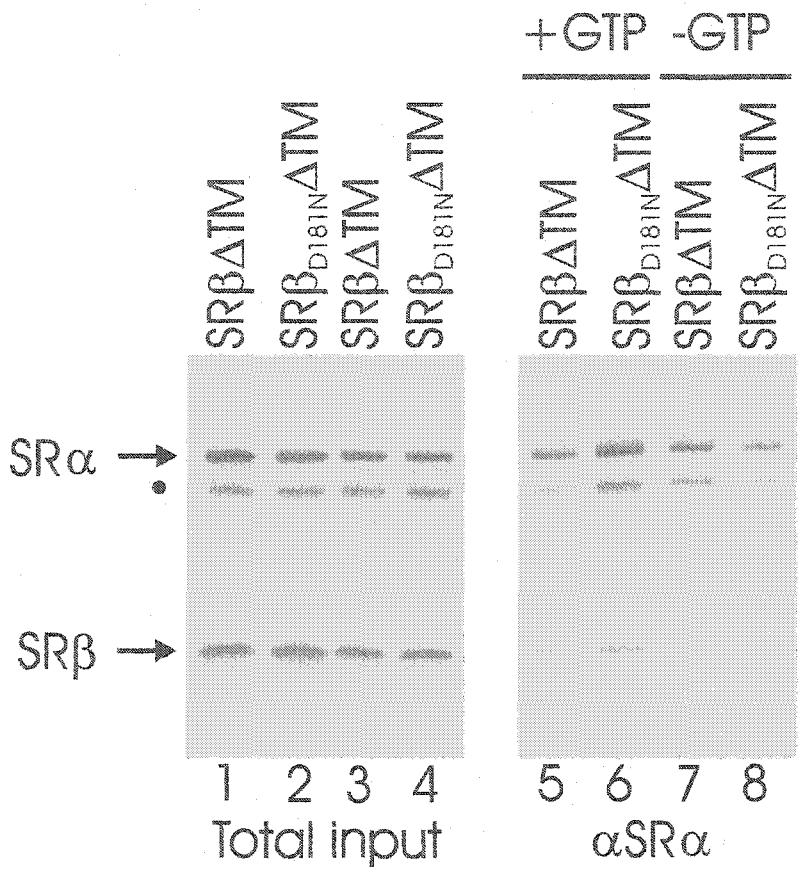

Figure 2.14: Immunoprecipitation of SRα with SRβΔTM and $SR\beta_{D181N}\Delta TM$ in depleted nucleotide conditions. Aliquots of *in vitro* translation reactions containing equimolar amounts of SRα and either SRβΔTM or $SR\beta_{D181N}\Delta TM$ were incubated together prior to immunoprecipitation. Some samples were processed by gel filtration to deplete nucleotides (-GTP). Reactions were then immunoprecipitated with an anti-SRα antibody. Both SRβΔTM and $SR\beta_{D181N}\Delta TM$ are precipitated when nucleotides are present; only SRβΔTM precipitates when nucleotides are depleted by gel filtration.

dimerization was assayed after adding back specific nucleotides.

When dimer formation was assayed with added ATP (up to 1 mM) co-precipitation of $SR\beta_{D181N}\Delta TM$ and SRα was not observed. In contrast, adding GTP, GDP, XTP or XDP restored some SRα-binding by $SR\beta_{D181N}\Delta TM$ (Figure 2.15). The effect of the xanthosine nucleotides was more pronounced than the guanosine nucleotides, consistent with the predicted preference of $SR\beta_{D181N}\Delta TM$ for XTP compared to GTP. *In vitro*, there seemed to be little preference for the di- or tri-phosphate forms of either nucleotide. Dimer formation could not be restored to the levels observed prior to nucleotide depletion suggesting that, similar to other small molecular weight GTPases, $SR\beta_{D181N}\Delta TM$ may be destabilized in the absence of bound nucleotide (Sprang, 1997). Taken together, these data reveal that an intact and nucleotide bound SRβ GTP binding domain is necessary for binding to the SRX2 region of SRα.

2.4 Discussion

We showed previously that SRα is anchored to the ER membrane through an interaction between the amino terminal SRX2 domain and SRβ ((Young et al., 1995); see Figure 2.7). Our current data demonstrate that the minimal GTPase domain of SRβ is necessary for binding to SRα via SRX2 (Figures 2.8 and 2.12), since removal of core GTPase sequences from SRβ (SRβD5) abolished binding of SRα to SRβ. Deletion of the carboxyl-terminal six amino acids also abolished SRα binding, demonstrating that this binding interaction cannot tolerate the removal of sequences (Figure 2.8). The carboxyl-terminal sequence of SRβ forms an alpha helix in the same relative location as the α5 helix of Ras-type GTPases (Figure 2.16.B) (Schwartz and Blobel, 2003). While this helix does not contribute residues to the GTP binding pocket, it packs tightly against the β sheet core structure of both Ras, Arf and Sar1 and is itself considered to be part of the core GTPase structure (Pai et al., 1989; Amor et al., 1994; Goldberg, 1998; Huang et al., 2001). Removal of part of this helix from SRβ greatly reduced the stability of a protease-resistant core fragment of SRβ, demonstrating that this helix is essential to the structure of the protein (Figure 2.3). How this alpha helix contributes to the stability of SRβ is not obvious from the X-ray structure; there are no hydrogen bonds between this helix and other regions of the protein.

According to the yeast SRX-SRβ structure (Figure 2.16.A) the carboxyl-terminal alpha helix of SRβ is not directly involved in the SRα-SRβ binding interface. This comes as a surprise considering that an anti-$SR\beta_{COOH}$ antibody could not coprecipitate dimers (Figure 2.8.D, lanes 3-4). Clearly the presence of bound SRα inhibited the formation of a high affinity antibody-SRβ interaction, but it did not appear to be due to competitive binding between SRα and the antibody.

Alignment of SRβ with related GTPases reveals the insertion of 34 amino acids between the G4 and G5 GTPase consensus sequences, that is absent from other GTPases (Miller et al., 1995). Removal of this insertion or replacement with a scrambled amino acid sequence of equal length resulted in decreased SRα binding (Figure 2.8). However,

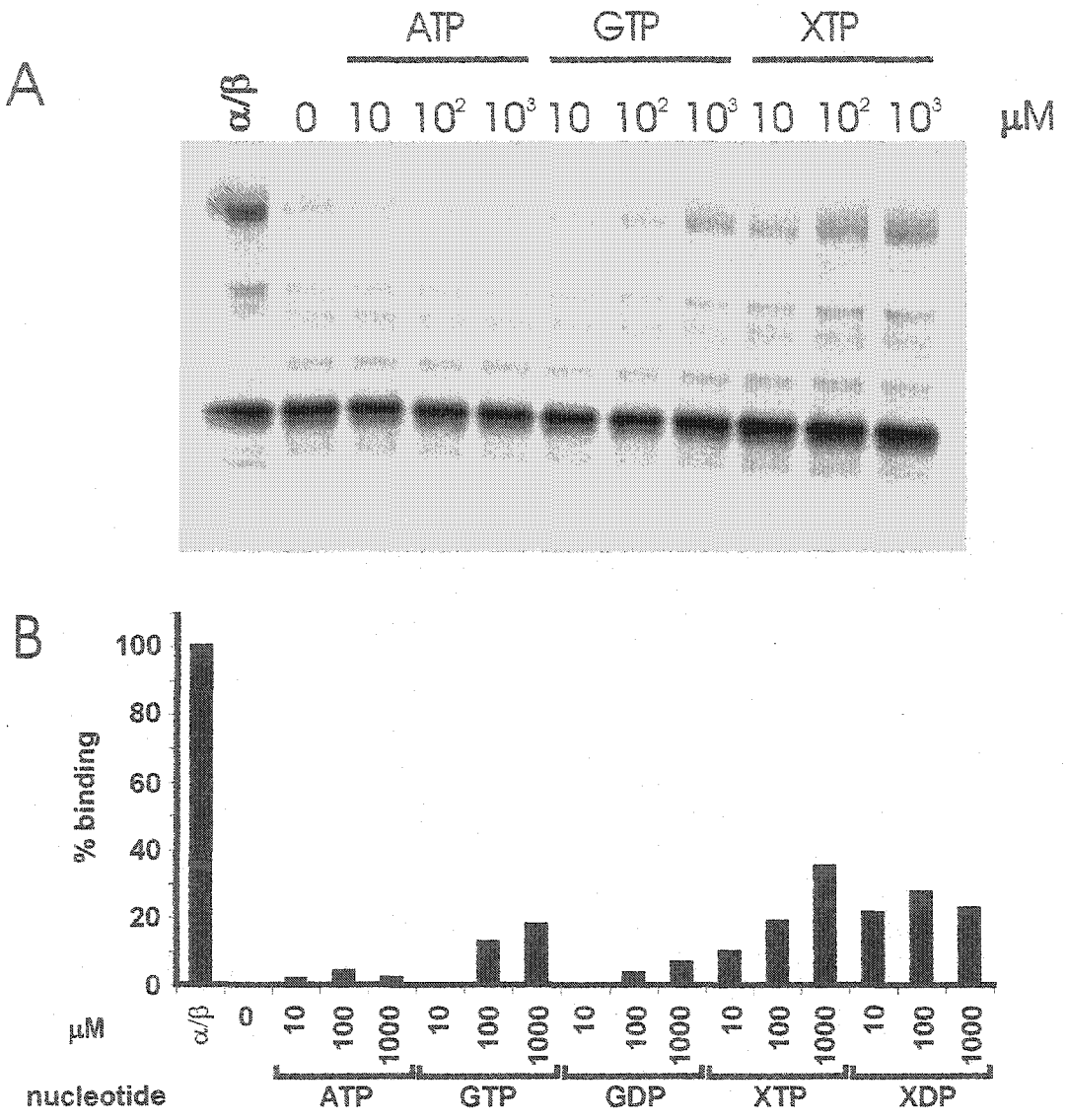

Figure 2.15: The effect of nucleotide titration on SRα-SRβ$_{D181N}$ΔTM immunoprecipitation. *In vitro* translation reactions were depleted of small molecules by gel filtration. Equimolar amounts of SRα and SRβ$_{XTP}$ΔTM were incubated together in the presence of increasing amounts of the indicated nucleotides and immunoprecipitated with an anti-HA antibody. **A**: Analysis by SDS-PAGE of the samples supplemented with triphosphates. **B**: The data was quantified by Phosphorimager analysis and plotted graphically. The amount of SRβ$_{D181N}$ΔTM that co-precipitated with SRα prior to nucleotide depletion was arbitrarily assigned a value of 100% (α/β) and is indicated for comparison. The results of one experiment (representative of three) are shown.

Figure 2.16: X-ray structure of SRX-SRβ from *S. cerevisiae*. Unless otherwise indicated all models were rendered using Protein Explorer. **A:** A carbon backbone trace of the SRβ-binding domain of SRα, SRX (blue) and SRβΔTM (green), with bound GTP shown as a space filling model. Amino acids involved in side chain protein-protein interactions are shown in red, and the amino-terminus, carboxyl-terminus and extended α4 helix of SRβΔTM are labelled. The flexible loop that does not appear in the structure has been drawn as a dotted line. **B:** Two different orientations of SRβΔTM are shown to illustrate the position of the carboxyl-terminal alpha helix relative to the rest of the structure. The carboxyl-terminal alpha helix is shown in black, the switch 1 region is coloured blue and the switch 2 region is coloured red. The amino-terminus, carboxyl-terminus and extended α4 helix are labelled. The Protein Data Dank (PDB) coordinates for these structures have been assigned the accession number 1NRJ.

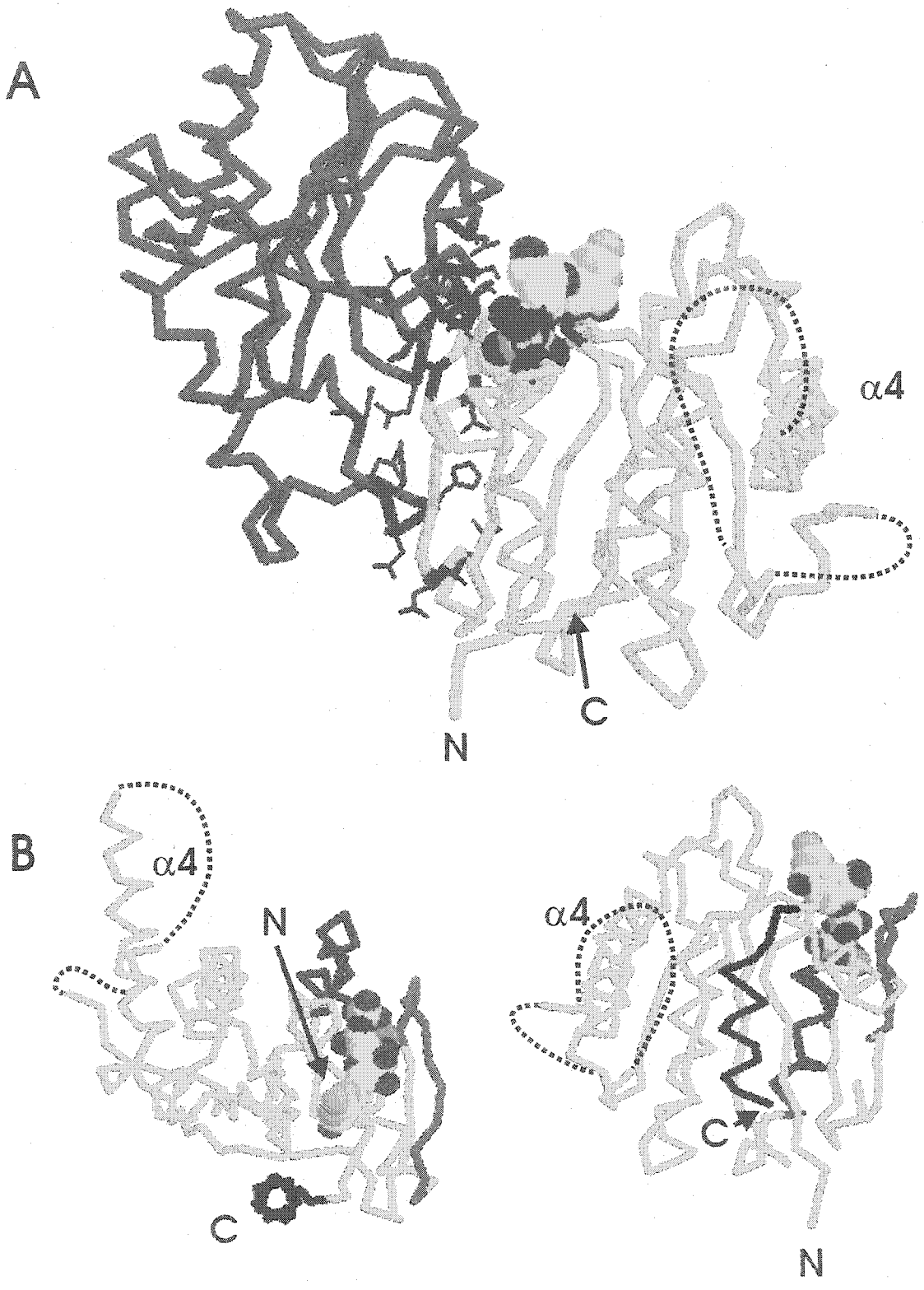
A
α4
C
N
B
α4
N
C
α4
C
N

this insertion appears to be necessary for a stable GTPase structure, since SRβ containing a scrambled insertion did not contain the protease-resistant fragment observed for the complete SRβ GTPase (Figure 2.9). This sequence in yeast SRβ extends the α4 helix beyond the length found in related GTPases, and contributes to an unstructured loop of unknown function (Figure 2.16) (Schwartz and Blobel, 2003). Therefore, the observed reduction in SRα binding likely results from a destabilized SRβ structure, rather than through the loss of a direct interaction with the insertion, which lies on the opposite side of SRβ from the SRX binding site (Schwartz and Blobel, 2003). Analysis of the structure of the yeast SRX-SRβ complex identified the amino acid side chains of both proteins that are responsible for maintaining the complex (Figure 2.16.A, Figure 2.17, red dots). A comparison between the sequences of yeast and mammalian SRX and SRβ reveal that the majority of these residues are not conserved (Figure 2.17). Therefore, while the binding face of the mammalian proteins may include the same structural regions as the yeast complex, the details of the binding interaction will be completely different.

Since the sequences necessary for heterodimerization were localized to the GTP binding domain of SRβ (Figure 2.8), a number of point mutations were introduced to determine the effect of GTP binding on SR dimerization. In each case the mutations were chosen based on structural data and functional characterization in related GTPases since the yeast SRβ structure was not known at the time. The subsequent publication of the crystal structure of yeast SRβ strengthens the hypothesis that each of the residues changed in canine SRβ performs the same function as corresponding residues in other GTPases.

A G118L mutation changes a glycine required for GTPase activity in Ras, and moderately decreases the affinity between Ras and effector molecules, but does not affect the nucleotide affinity or the ability to bind to GAPs (Sung et al., 1995; Hwang et al., 1996). A H119L mutation changes a residue predicted to orient a catalytic water molecule required for the hydrolysis of GTP. Ras contains a glutamine at this position, which is thought to position a water molecule for nucleophilic attack on the terminal phosphate group of GTP (Maegley et al., 1996; Scheffzek et al., 1997). Although SRβ contains a histidine in this position, the imidazole group is ideally positioned to orient the water molecule (Figure 2.18). Therefore, the H119L mutant is expected to be deficient in GTP hydrolysis but should still bind nucleotide. A similar histidine mutation within EF-Tu demonstrates reduced basal GTP hydrolysis *in vitro* (Jonak et al., 1994). Both G118L and H119L retained the ability to coprecipitate SRα (Figure 2.10), consistent with the hypothesis that nucleotide-bound SRβ binds SRα.

Also consistent with this hypothesis was the discovery that two mutations predicted to contain no bound nucleotide were unable to dimerize with SRα. K75I replaces a lysine residue that forms hydrogen bonds with both the β- and γ-phosphates in yeast SRβ (Schwartz and Blobel, 2003)and in the Ras-GTP crystal structure (Pai et al., 1989; Pai et al., 1990). Mutation of this residue in Ras decreased the affinity for both GTP and GDP by a factor of 100 (Sigal et al., 1986). Therefore SRβ K75I is predicted to exist predominantly in the empty state. N178K changes a residue that, according to the

Figure 2.17: Sequence alignment of SRβ and SRX(2). Sequence alignments of mouse, human, canine and yeast SRβ and human, canine and yeast SRX(2) were performed using T-Coffee (http://www.ch.embnet.org/software/TCoffee.html). Side chains participating in protein-protein interactions are denoted by red dots. Conserved GTPase consensus sequences are shaded purple, the switch 1 region of SRβ is shaded blue and the switch 2 region is shaded red, consistent with the carbon backbone traces in Figure 2.16.B. The switch 2 region overlaps with the second GTPase consensus sequence except for the amino-terminal aspartic acid, which does not form part of the switch 2 sequence.

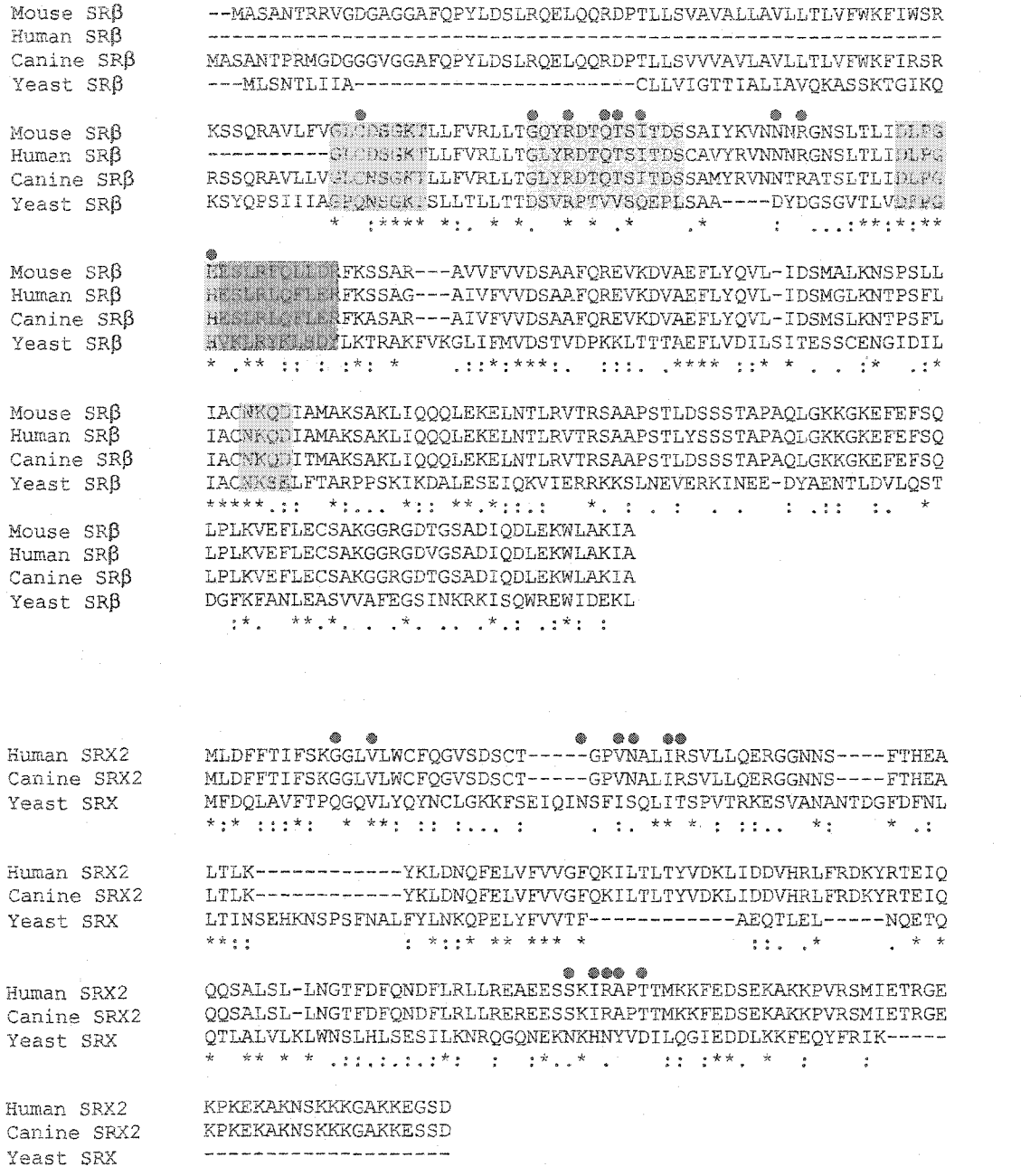
Mouse SRβ
Human SRβ
Canine SRβ
Yeast SRβ
Human SRX2
Canine SRX2
Yeast SRX

Figure 2.18: Detail of the GTP-binding site. A close up view of the active sites of Arf1-GMPPNP (A), Sar1-GMPPNP (B) and SRβ-GTP (C). The bound nucleotide is represented as a red ball-and-stick model, the coordinating Mg2+ is represented as a green dot and the catalytic water molecule is shown as a blue sphere extending as far as the van der Waals radius. The carbon backbone of the proteins is shown in grey, the activating glutamine (for Arf1) or histidine (for Sar1 and SRβ) is the green residue and the active site glutamic acid (for Arf1 and Sar1) or glutamine (for SRβ) is shown in purple. The PDB accession number for Sar1 bound to GMPPNP is 1M2O. The coordinates for Arf1-GMPPNP were provided by Jonathan Goldberg.

A

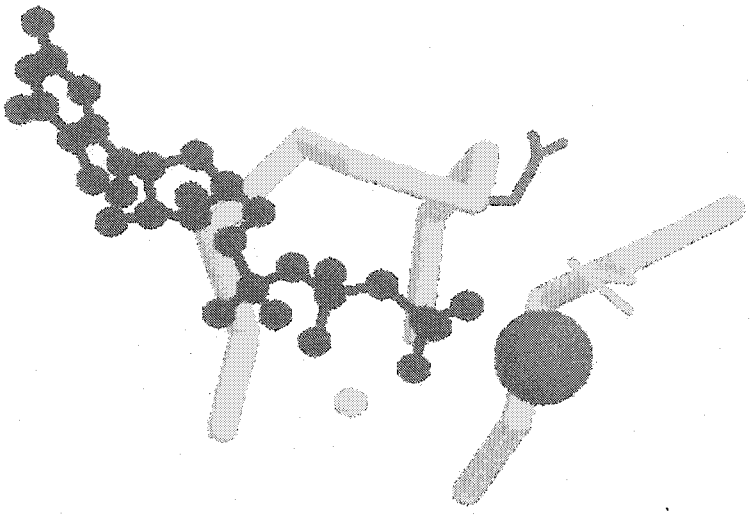

B

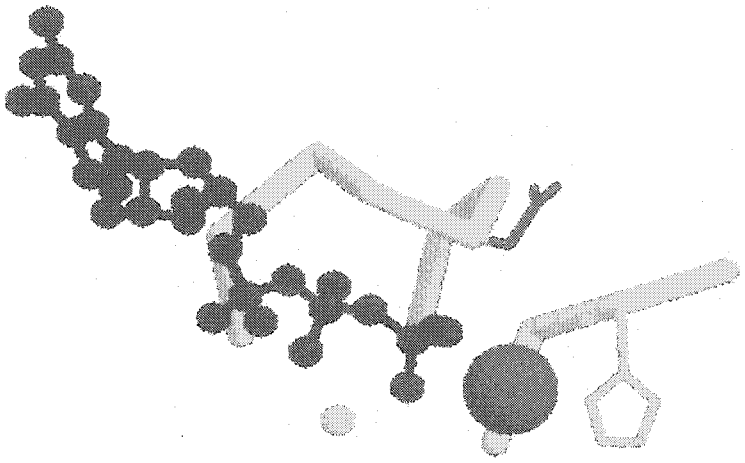

C

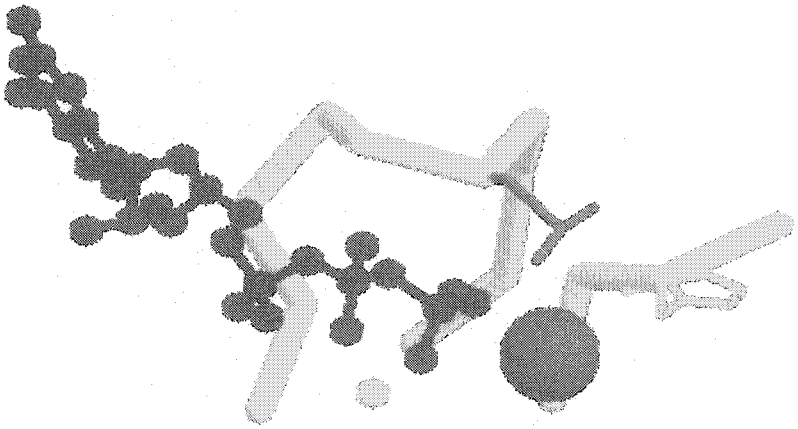

crystal structure of Ras, forms hydrogen bonds with a main chain oxygen in the G1 GTPase consensus and a threonine hydroxyl group in the G5 GTPase consensus sequence, and stabilizes the GTP binding pocket (Pai et al., 1990). Both hydrogen bonds are possible between the N178 residue of canine SRβ and the G1 and G5 GTPase consensus sequences; the hydrogen bond between this residue and G1 GTPase consensus is conserved in the yeast structure. Therefore this mutant is predicted to be structurally unstable and unable to bind nucleotide.

However, the most convincing evidence that dimerization is regulated by nucleotide binding comes from the mutant D181N. This mutant is expected to have reduced affinity for GTP but a preference to bind XTP and XDP. (Weijland et al., 1994; Powers and Walter, 1995) In the absence of nucleotide this mutant was no longer able to bind to SRα. However, replenishing the reaction mixture with nucleotide restored binding of SRβ to SRα. GTP, GDP, XTP and XDP all supported dimerization; the triphosphates supported the formation of a greater number of dimers, suggesting the relationship GTP>GDP>empty state with respect to the efficiency of dimer formation. Gel filtration of purified yeast SRβ and SRX2 also suggested that GTP promotes more efficient dimer formation than GDP (Schwartz and Blobel, 2003). Taken together, these data support the prediction that the ability of SRα to form a dimer with SRβ is contingent on the nucleotide-bound status of SRβ.

The SRβ-binding behaviour of SRα (ie. binding is most efficient when SRβ is bound to GTP) demonstrates that the SRα-SRβ interaction is analogous to the GTPase-effector interaction. However, the interaction of effectors with GTPases is usually transient, as the GTP-bound, 'active' state is transient (Sprang, 1997). However, since SRα resides solely on the ER membrane (Ogg et al., 1998), the SRα-SRβ dimer is not a transient complex. Attempts to map yeast protein-protein interactions on the proteome scale using a TAP-tag based purification approach identified SRβ as the only binding partner for TAP-tagged SRα, so it is unlikely that SRα is retained on the ER membrane by binding a protein other than SRβ (Gavin et al., 2002). The implication from these data is that SRβ, in contrast to other small GTPases, may spend the majority of the time in to the GTP-bound, active state to ensure that SRα remains bound to the ER membrane. The following section examines the properties of the purified SRβ GTPase.

3. EXAMINATION OF THE PROPERTIES OF THE SRβ GTPASE

3.1 Introduction

The work presented in chapter 2 established that an intact, functional GTP-binding domain of SRβ is required to participate in a physical interaction with SRα. In this chapter the properties of the isolated SRβ GTPase are examined, and compared with SRβ harbouring a GTPase point mutation at a position predicted to be functionally important, based on observations made in related GTPases.

SRβ bears significant sequence homology to Arf/Sar GTPases, that constitute a sub-family of the Ras superfamily (Miller et al., 1995). These proteins can be distinguished on the basis of residues that line the GTP-binding pocket. Ras-type GTPases contain sequences of conserved residues called G boxes that are arranged at discrete intervals throughout the primary sequence (Dever et al., 1987). Arf family GTPases are distinguished from other Ras-type GTPases by the presence of an aspartic acid instead of a glycine residue in the G1 box (Table 3.1). The identity of this residue within SRβ is not strictly conserved among lower eukaryotes, but higher eukaryotes contain an invariant cysteine in this position (Table 3.2).

Table 3.1: Alignment of G1 box sequences of ras superfamily members

Protein [species]	G1 GTPase box sequence
Ras1p [SC]	GG**G**GVGKS
Ras [RR]	GA**G**GVGKS
Ran [HS]	GD**G**GTGKT
Rac1 [HS]	GD**G**AVGKT
RhoA [HS]	GD**G**ACGKT
ARF-1 [HS]	GL**D**AAGKT
ARF-2 [MM]	GL**D**AAGKT
Sar1p [SC]	GL**D**NAGKT
Sar1 [MM]	GL**D**NAGKT
Sar1a [HS]	GL**D**NAGKT
ARL1 [HS]	GL**D**GAGKT

SC = S. cerevisiae, RR = R. rattus, HS = H. sapiens, MM = M. musculus

Table 3.2: Alignment of G1 box sequences of SRβ orthologues

Organism	Gene/ORF name	G1 GTPase box sequence
S. cerevisiae	Srp102p	GP**Q**NSGKT
S. pombe (putative)	O13950	GP**S**DSGKT
Arabidopsis (putative)	AAD08946	GL**S**DSGKT
C. elegans (putative)	NP_506245	GL**M**DCGKT
M. musculus	SRβ	GL**C**DSGKT
C. familiaris	SRβ	GL**C**NSGKT
H. sapiens	SRβ	GL**C**DSGKT

All data gathered to date on the function of SRβ has been obtained in the context of a SRα-SRβ heterodimer. Attempts to isolate the SRβ GTPase for study involved proteolytic treatment of SR with trypsin or elastase to specifically digest SRα. This releases the GTP-binding domain of SRα from SRβ but leaves an amino-terminal domain of SRα bound to SRβ (Lauffer et al., 1985; Romisch et al., 1989). Therefore, there is no data on the properties of SRβ as an isolated GTPase.

To address this issue directly a soluble version of SRβ, termed SRβΔTM, was expressed and purified from *E. coli*. SRβ harbouring a point mutation that replaces the semi-conserved cysteine with an aspartic acid, $SR\beta_{C71D}\Delta TM$, was also expressed and purified, since the identity of this residue appears to be crucial to the function of other GTPases (Seeburg et al., 1984; Jacquet and Parmeggiani, 1988; Kahn et al., 1995) Using a variety of techniques the GTP binding and hydrolysis properties of both proteins were assessed, and a proposed interaction between SRβ and ribosomes was confirmed. The results of this work reveal that SRβ exhibits properties that are unique among Ras-type GTPases.

3.2 Materials and Methods

3.2.1 Plasmids

Construction of plasmids, sequencing and site directed mutagenesis were performed using standard techniques. All encoded products are under the control of a T7 promoter. The plasmids pMAC191 (containing a modified full-length cDNA sequence of canine SRα), pMAC455 (encoding $SR\beta_{md}$), pMAC1083 (encoding HA-$SR\beta_{XTP}\Delta TM$) and pMAC853 (encoding SRβΔTM, a fusion of the carboxyl-terminal 206 amino acids of canine SRβ with an amino-terminal HA epitope tag) were previously reported (Young et

al., 1995; Legate et al., 2000).

Plasmid pMAC1277 encodes SRβΔTM fused to an amino-terminal His-tag and enterokinase (EK) cleavage site. This plasmid was assembled in two steps. First pMAC701, encoding $SR\beta_{md}$ fused to an amino-terminal His tag and EK cleavage site was generated by removing the SRβ coding sequence from pMAC455 by digestion with *BglII* and *KpnI* and inserting it into pRSETB (Invitrogen) digested with the same enzymes. The sequence encoding SRβΔTM was then excised from pMAC853 using *NcoI* and *EcoRI*, and inserted into pMAC701 digested with *NcoI* and *EcoRI*, thereby replacing the coding region for $SR\beta_{md}$ with that for SRβΔTM.

Plasmid pMAC1623 encodes $SR\beta_{C71G}\Delta TM$ fused to an amino-terminal His tag and EK cleavage site. It was generated from pMAC1277 by the method described in (Hughes and Andrews, 1996). Briefly, the entire plasmid was amplified by PCR using oligo958 (ATGGGCCCCTCG**G**CAACTCTGGGAAAAC, desired mutation in bold) and oligo959 (ATGGGCCCCAACAAGAACAGCTCT). The product was then digested with *ApaI*, and the 3' overhanging ends were blunted by incubation with the Klenow fragment of DNA polymerase, and the linear DNA was circularized by ligation with T4 DNA ligase.

Plasmid pMAC1624 encodes $SR\beta_{C71D}\Delta TM$ fused to an amino-terminal His tag and EK cleavage site, under the control of a T7 promoter. To generate this plasmid pMAC1277 was amplified by PCR using oligo960 (ATGGGCCCCTCG**A**CAACTCTGGGAAAA, desired mutation in bold) and oligo959. The PCR product was digested with *ApaI* and end repaired and ligated as above.

Plasmid pMAC1278 encodes $SR\beta_{XTP}\Delta TM$ fused to an amino-terminal His tag and EK cleavage site. $SR\beta_{XTP}\Delta TM$ was excised from pMAC1083 with *NcoI* and *EcoRI*, and inserted into pMAC701 digested with *NcoI* and *EcoRI*, replacing $SR\beta_{md}$ with $SR\beta_{XTP}\Delta TM$.

Plasmid pMAC1637 encodes $SR\beta_{C71D}\Delta TM$ fused to a carboxyl-terminal His tag. $SR\beta_{C71D}\Delta TM$ was amplified from pMAC1624 using oligo203 (CATGCCATGGCTAAGTTCATCCGGAGCAGA) and oligo976(AGAATTCAATGATGATGATGATGATGGGCGATTTTAGCCAGCCAC) and digested with *NcoI* and *EcoRI*. The digested fragment was inserted into pET16b (Novagen) digested with *NcoI* and *EcoRI*.

3.2.2 Protein purification and gel filtration

Plasmids encoding either His-SRβΔTM or His-$SR\beta_{C71D}\Delta TM$ were expressed in the salt-inducible BL21SI strain by addition of NaCl to 300mM final concentration for 2 hours. All purification steps were carried out at 4°C. Cell pellets were washed once in 50mM Na_2HPO_4, pH 8.0, 1mM PMSF and resuspended in 2.5 mL lysis buffer (50mM Na_2HPO_4, pH 8.0, 500mM NaCl, 5mM $MgOAc_2$, 1mM PMSF, 10% glycerol (v/v)) per gram of cells (wet weight). Cells were lysed in a pressure cell, DNA was precipitated with a final concentration of 0.15% polyethylenamine and lysate was centrifuged at 18 000 *g* for 20 minutes in a Beckman JA-20 rotor. The lysate was further clarified by

centrifuging at 110 000 *g* for 1 hour in a Beckman Ti50.2 rotor prior to loading on Ni-NTA agarose (Qiagen) equilibrated in 50mM Na_2HPO_4, pH 8.0, 300mM NaCl, 5mM $MgOAc_2$, 10% glycerol. The column was washed in 10 volumes of equilibration buffer and His-SRβ was eluted with equilibration buffer +50mM imidazole. Protein containing fractions were detected by BCA assay (Pierce), pooled and dialysed overnight in 40mM Tris-OAc, pH 7.8, 300mM NaCl, 5mM $MgOAc_2$, 1mM DTT, 25% glycerol. Dialysate was diluted with 6 volumes of 40mM Tris-OAc, pH 7.8, 5mM $MgOAc_2$, 1mM DTT, 25% glycerol to reduce the NaCl concentration and loaded immediately onto CM Sepharose equilibrated in 40mM Tris-OAc, pH 7.8, 50mM NaCl, 5mM $MgOAc_2$, 1mM DTT, 25% glycerol. The column was washed with 10 volumes of equilibration buffer and His-SRβ was eluted in a single step in SRβ elution buffer (equilibration buffer +100mM NaCl). Protein containing fractions were detected by Bradford assay (Biorad) and pooled. Protein concentration was determined by absorbance at 280nm as described in (Mach et al., 1992). Aliquots of SRβTM were supplemented with 2 mM $CaCl_2$ final concentration and digested with 0.01 units of enterokinase (Novagen)/10 μg SRβΔTM for 16 hours at 20°C. Reactions were stopped by the addition of EGTA to 5 mM final concentration. Protein was frozen in small aliquots at -80°C; material used for functional studies was thawed once and discarded.

To eliminate the possibility of the epitope tag influencing the properties of SRβ, the SRβΔTM used in all experiments was processed with EK following purification, unless otherwise noted. The EK cleavage site within SRβΔTM was unusually sensitive to enterokinase. Removal of the amino-terminal His_6 tag from 10 μg of SRβΔTM could be accomplished in 16 hours with 0.01 unit of EK, reflecting an activity 20 times higher than the manufacturer's specification (Figure 3.1). The His_6 tag on $SR\beta_{C71D}\Delta TM$ does not include an EK cleavage site; therefore it was not possible to remove the His_6 tag from this protein.

A plasmid encoding SRX2 with a carboxyl-terminal His_6 tag (pMAC1523) was expressed in *E. coli* strain NM522 by addition of 0.5 mM IPTG for 3 hours at 30°C. The cell pellet was resuspended in lysis buffer (40 mM Tris-OAc, pH 7.8, 300 mM KOAc, 10% glycerol (v/v), 1 mM PMSF) and lysozyme was added to a final concentration of 0.25 mg/mL, followed by a 30 minute incubation on ice. Cells were lysed in a pressure cell, DNA was precipitated with a final concentration of 0.15% polyethylenamine and lysate was centrifuged at 18 000 *g* for 20 minutes in a Beckman JA-20 rotor. The lysate was further clarified by centrifuging at 110 000 *g* for 1 hour in a Beckman Ti50.2 rotor prior to the addition of Ni-NTA agarose (Qiagen) equilibrated in lysis buffer -PMSF. Lysate containing a slurry of Ni-NTA agarose was incubated at 4°C for 90 minutes with end-over-end mixing. The slurry was separated from lysate by low speed centrifugation and decanting of the supernatant. The slurry was transferred to a disposable column, washed in lysis buffer -PMSF, and SRX2 was eluted in a single step in lysis buffer -PMSF +100 mM imidazole. The protein-containing peak was determined by BCA assay, peak fractions were pooled and DTT was added to 1 mM.

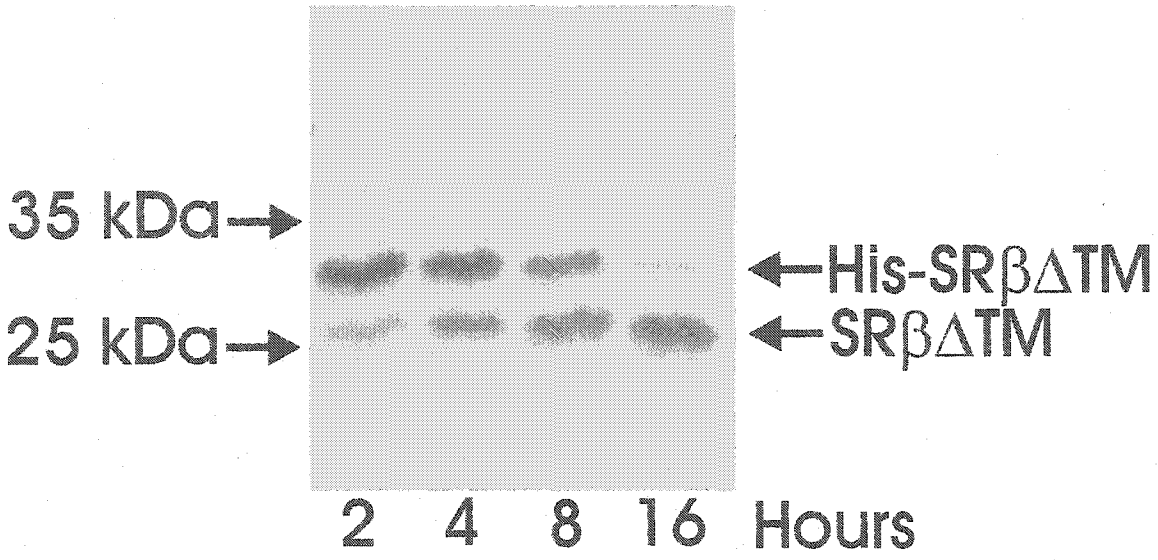

Figure 3.1: Removal of the His_6 tag from SRβΔTM by treatment with enterokinase. 10 μg of SRβΔTM was incubated with 0.01 unit of recombinant enterokinase for an increasing period of time. At the specified times aliquots were removed and resolved by SDS-PAGE followed by Coomassie staining. The positions of 25 kDa and 35 kDa molecular weight standards are indicated.

The following steps were carried out at room temperature. SRX2 was loaded onto a Phenyl Sepharose column equilibrated in 40 mM Tris-OAc, pH 7.8, 300 mM KOAc, 10% glycerol (v/v), 1 mM DTT, washed in this buffer and eluted with a 0.1-0.7% gradient of Triton X-100.

Gel filtration was carried out using a HiPrep 16/60 Superdex 75 FPLC column (Amersham) equilibrated in 40 mM Tris-OAc, pH 7.8, 300 mM KOAc, 5 mM $MgCl_2$, 10% glycerol (v/v) at a flow rate of 0.5 mL/min. Protein was detected by absorbance at 280 nm and plotted using Unicorn 4.00 software (Amersham).

3.2.3 Immunoprecipitation

Proteins were synthesized *in vitro*, quantified and immunoprecipitated as described in sections 2.2.4 and 2.2.5.

3.2.4 HPLC analysis of bound nucleotide

10 nmoles of SRβ were diluted to 250 µL in SRβ elution buffer. An equal volume of 8 M urea, 20 mM Tris-OAc, pH 7.8, 100 mM NaCl was added and the sample was incubated at 37°C for 30 minutes. The sample was centrifuged through a 5 kDa cutoff filter (Millipore) and the filtrate was added to a Bakerbond QUAT 5µm HPLC column (J.T.Baker) in 25 mM triethylamine bicarbonate, pH 7.2. Nucleotide was eluted from the column with a 5-100% gradient of triethylamine bicarbonate. Samples were analysed with 32Karat version 3.0 software (Beckman) and nucleotide was quantified by calculating the area under the curve and comparing to a standard curve of GTP or GDP. A known amount of GMP was used as in internal control in some experiments to determine the nucleotide recovery (90%).

3.2.5 Fluorescence experiments

300 nM SRβ was incubated with 500 nM 2'-(or-3')-*O*-(*N*-methylanthraniloyl)GTP (mant-GTP) in 50 mM Tris-Cl, pH 7.6, 150 mM NaCl, 5 mM $MgOAc_2$, 2 mM DTT and 10% glycerol in a 1cm path length quartz cuvette. All measurements were taken with a fluorometer equipped with a 815 photomultiplier detection system (PTI, London, Ontario, Canada) with a 2 nm exication slit width and a 2 nm emission slit width, and compiled with Felix v 1.4 software (PTI). Samples were excited at 280 nm or 295 nm and emission spectra were obtained by scanning from 300-500 nm in 2 nm increments with an integration time of 0.2 seconds per data point. Emission spectra were corrected by subtracting a buffer blank and peak values were manually selected for further calculation. All calculations and data plots were performed within MS Excel 2002.

3.2.6 Filter binding

100 pmoles of SRβ (1 µM) were incubated at the specified temperatures with 10 µM GTP including 25% ^{3}H-GTP (specific activity 31 Ci/mmol) in 50 mM Tris-OAc, pH 7.8, 200 mM NaCl, 5 mM $MgCl_2$, 10% glycerol, 2 mM DTT. At the appropriate time points samples were withdrawn and diluted to 2 mL in ice cold filter binding buffer (20 mM Tris-OAc, pH 7.8, 200 mM NaCl, 5 mM $MgCl_2$, 10 mM NH_4Cl). Samples were applied to prewashed nitrocellulose discs (Whatman) and the discs were washed with 3x3mL filter binding buffer in a Millipore 1225 Filtration Sampling Manifold

(Millipore). Discs were dried and bound nucleotide was quantified in a scintillation counter.

3.2.7 Nucleotide exchange

Nucleotide exchange reactions were carried out as described in (Koyama and Kikuchi, 2001) and (Wang and Colicelli, 2001). Briefly, SRβΔTM (1 μM) was incubated with 20 mM GTP including 0.2 μM γ-^{32}P-GTP or 20 μM GDP for 10 minutes at 30°C in final buffer conditions containing 20 mM Tris-Cl, pH 7.6, 6 mM $MgCl_2$, 10 mM EDTA, 1 mM DTT, 10% glycerol. After 10 minutes $MgCl_2$ was added to a concentration of 20 mM. The extent of nucleotide exchange was quantified by filter binding. To prepare SRβΔTM for GTPase assays, free nucleotide was separated from bound nucleotide by repurifying SRβΔTM on CM Sepharose using the conditions outlined in section 3.2.2.

3.2.8 UV crosslinking

5 μM SRβ was incubated with 0.5 μM α-^{32}P-GTP and the indicated concentration of unlabelled GTP in crosslinking buffer (50 mM Tris-OAc, pH 7.8, 150 mM KOAc, 5 mM $MgOAc_2$, 2 mM DTT) for 20 minutes on ice, followed by 5 minutes at 24°C. Reactions were placed into a plastic weigh boat on a chilled metal block and irradiated with UV light at 5000 μW/cm^2 for 5 minutes. Samples were precipitated with trichloroacetic acid and washed in ethanol:ether (1:1) to remove free nucleotide, resolved by SDS-PAGE and analysed using a PhosphorImager. K_d estimates were determined from analysing the data in SigmaPlot.

3.2.9 GTPase assay

40 nM nucleotide-bound SRβ or 5.0 OD_{260} units/ml ribosomes was incubated with 83.5 nM γ-^{32}P-GTP in GTPase buffer (50 mM Tris-OAc, pH 7.8, 150 mM KOAc, 5 mM $MgOAc_2$, 2 mM DTT) at 24°C. At the indicated time points samples were removed and quenched by adjusting the EDTA concentration to 50 mM on ice. Samples were spotted onto polyethylenamine cellulose TLC plates and resolved in 0.375 M KH_2PO_4, pH 3.5 for one hour. Plates were dried and exposed to a PhosphorImager screen for quantitative analysis. To generate the Lineweaver-Burk plot, reactions were supplemented with cold GTP to concentrations up to 5 μM and the reaction was monitored using hydrolysis of γ-^{32}P-GTP to estimate hydrolysis of all GTP.

To assess the effect of ribosomes on the SRβ GTPase, 2 nmoles (10 μM) SRβ was incubated with 40 A_{260} units/mL of ribosome-nascent chains (RNCs) (a ratio of 12.5:1 SRβ:RNCs) for 1 hour at 25°C in GTPase buffer. Ribsomes were then removed by centrifugation over a 1 M sucrose cushion in GTPase buffer for 1 hour at 360 000 x g and the top fraction containing SRβ was collected. Nucleotides in this fraction were identified by HPLC as described above.

3.2.10 Ribosome, ribosomal subunit and ribosome-nascent chain (RNC) purification

Canine pancreatic ribosomes and wheat germ RNCs were prepared as described elsewhere (Bacher et al., 1999; Fulga et al., 2001)25 mM HEPES-KOH, pH 7.6, 5 mM MgOAc2, 150 mM KOAc, 1mM DTT (+1 mM cycloheximide for RNCs) and centrifuged in a SW28 rotor for 16 hours at 48 000 *g*. 1 mL fractions were collected by bottom

puncture with monitoring by absorbance at 260 nm. The ribosome peak was centrifuged at 150 000 *g* for 1 hour in a Ti80 rotor and resuspended at a concentration of 100 A_{260} units/mL in 25 mM HEPES-KOH, pH 7.6, 5 mM MgOAc2, 150 mM KOAc, 1mM DTT (+1 mM cycloheximide for RNCs).

Ribosomal subunits were prepared from canine pancreatic ribosomes by raising the EDTA concentration to 10 mM and adding puromycin to 1 mM final concentration, followed by a 15 minute incubation at 25°C. Subunits were separated on sucrose gradients and collected as outlined above. Following the final pelleting step subunits were resuspended in a volume of the above buffer equal to the starting volume and an A_{260} measurement was taken to ensure stoichiometric recovery (0.44 A_{260} units 60S subunit = 0.16 A_{260} units 40S subunit)(Falvey and Staehelin, 1970).

3.2.11 Ribosome binding experiments

5 μM SRβ was incubated with 20 A_{260} units/mL ribosomes or RNCs for 1 hour at 24°C in 25 mM HEPES-KOH, pH 7.6, 5 mM MgOAc2, 150 mM KOAc, 1mM DTT (+1 mM cycloheximide for RNCs) and then added to the top of 30 mL linear 0.3-1.2 M sucrose gradients. The gradients were centrifuged in a SW28 rotor for 16 hours at 48 000 *g*. 1 mL fractions were collected by bottom puncture, protein precipitated with trichloroacetic acid, resolved by SDS-PAGE and analysed by Western blotting using an antibody directed against SRβ.

The nascent chains comprising RNCs were labelled with ^{35}S-methionine to allow the migration position of RNCs to be monitored by autoradiography of the SRβΔTM/RNC Western blot. To monitor the migration position of ribosomes, fractions from a sucrose gradient were extracted with phenol:chloroform and ethanol precipitated to collect rRNA. rRNA was detected by electrophoresis on a 12% polyacrylamide gel and staining with ethidium bromide.

3.2.12 Chemical crosslinking

SRβΔTM (15 pmol) was incubated with 80S ribosomes (0.75 A_{260} units) in a total volume of 25 μL in final buffer conditions of 25 mM HEPES-KOH, pH 7.6, 5 mM MgOAc2, 150 mM KOAc for 15 minutes at 24°C. *bis*-maleimidohexane (Pierce) was added from a freshly prepared stock in DMSO to a final concentration of 20 μM and reactions were incubated for a further 20 minutes. Reactions were quenched by adding an equal volume of SDS-PAGE loading buffer containing 250 mM DTT, and analysed by SDS-PAGE and Western blotting using an anti-SRβ antibody.

3.3 Results

3.3.1 Immunoprecipitation of SRα and SRβ cysteine mutants

In an attempt to identify the importance of the cysteine in the function of SRβ I made two independent mutations at this site. The first, $SR\beta_{C71D}\Delta TM$, replaced the cysteine with aspartic acid, converting SRβ into an Arf family GTPase. The second, $SR\beta_{C71G}\Delta TM$, replaced the cysteine with glycine to resemble other Ras-type GTPases. Coprecipitation was used to assay binding of SRβ molecules to SRα. To permit direct comparison all of the SRβ mutants included an amino-terminal His tag and enterokinase

cleavage site. Following *in vitro* synthesis of SRα, wild-type SRβ, both cysteine point mutants, and another GTPase point mutant, $SR\beta_{XTP}\Delta TM$, previously shown to switch the nucleotide-binding preference from GTP to XTP (Legate et al., 2000; Pool et al., 2002), gel filtration was used to remove nucleotides from some samples (-GTP) and separate reactions containing equimolar amounts of SRα and each of the SRβ variants were incubated together to allow complex formation. Complexes were immunoprecipitated with an antibody against SRα (Figure 3.2). All of the SRβ molecules bound SRα in the presence of nucleotides contributed by the translation mix. As previously reported, nucleotide depletion reduced SRα-binding to the XTP-preferring version of SRβ, since the reduced affinity of $SR\beta_{XTP}\Delta TM$ for GTP allows this SRβ variant to be emptied by gel filtration (Legate et al., 2000). Neither cysteine point mutation was affected by nucleotide depletion demonstrating that, despite the mutation in the G1 box, these molecules retained SRα-binding activity under conditions which appear to empty $SR\beta_{XTP}\Delta TM$ of nucleotide.

3.3.2 Purification of SRβΔTM and $SR\beta_{C71D}\Delta TM$

To examine the isolated SRβ GTPase in greater detail, I expressed a recombinant protein consisting of the cytosolic portion of SRβ fused to an amino-terminal hexahistidine tag (His_6) and enterokinase (EK) cleavage site in *E.coli*. The protein (SRβΔTM) purified to apparent homogeneity in two steps involving nickel-NTA agarose and CM Sepharose (Figure 3.3.A) and the N-terminal His tag was removed by cleavage with EK (Figure 3.1). Gel filtration analysis of the purified product confirmed that SRβΔTM was a monomer in solution (Figure 3.3.C). One of the point mutants, $SR\beta_{C71D}\Delta TM$, was expressed with a carboxyl-terminal His_6 tag and purified using conditions identical to those used to purify SRβΔTM (Figure 3.3.B).

Since it was demonstrated that removal of as few as six amino acids from the carboxyl-terminus of SRβ abolished SRα binding (Figure 2.8) it was possible that the addition of a His_6-tag to the carboxyl-terminus could also disrupt SRα binding. To examine this possibility I used an antibody directed against SRα to immunoprecipitate SRα bound to amino-terminal His_6-tagged $SR\beta_{C71D}\Delta TM$ ($HisSR\beta_{C71D}\Delta TM$) or carboxyl-terminal His_6-tagged $SR\beta_{C71D}\Delta TM$ ($SR\beta_{C71D}\Delta TMHis$)(Figure 3.4). In agreement with the data in Figure 3.2, $HisSR\beta_{C71D}\Delta TM$ bound to SRα (lane 3). $SR\beta_{C71D}\Delta TMHis$ also bound to SRα (lane 4), demonstrating that addition of six histidines to the carboxyl-terminus did not negatively affect the SRα-SRβ binding interaction. More importantly this result confirmed that addition of the His_6-tag to the carboxyl-terminus of SRβ did not grossly perturb the structure of the protein.

3.3.3 Purification of SRX2

Attempts to use the purified SRX2 fragment of SRα to compare the properties of SRβΔTM with the properties of SRβΔTM/SRX2 dimers were ultimately unsuccessful. SRX2 containing a carboxyl-terminal His_6-tag was expressed in *E. coli* but was insoluble in several lysis conditions (Figure 3.5.A). Gel filtration experiments demonstrated that

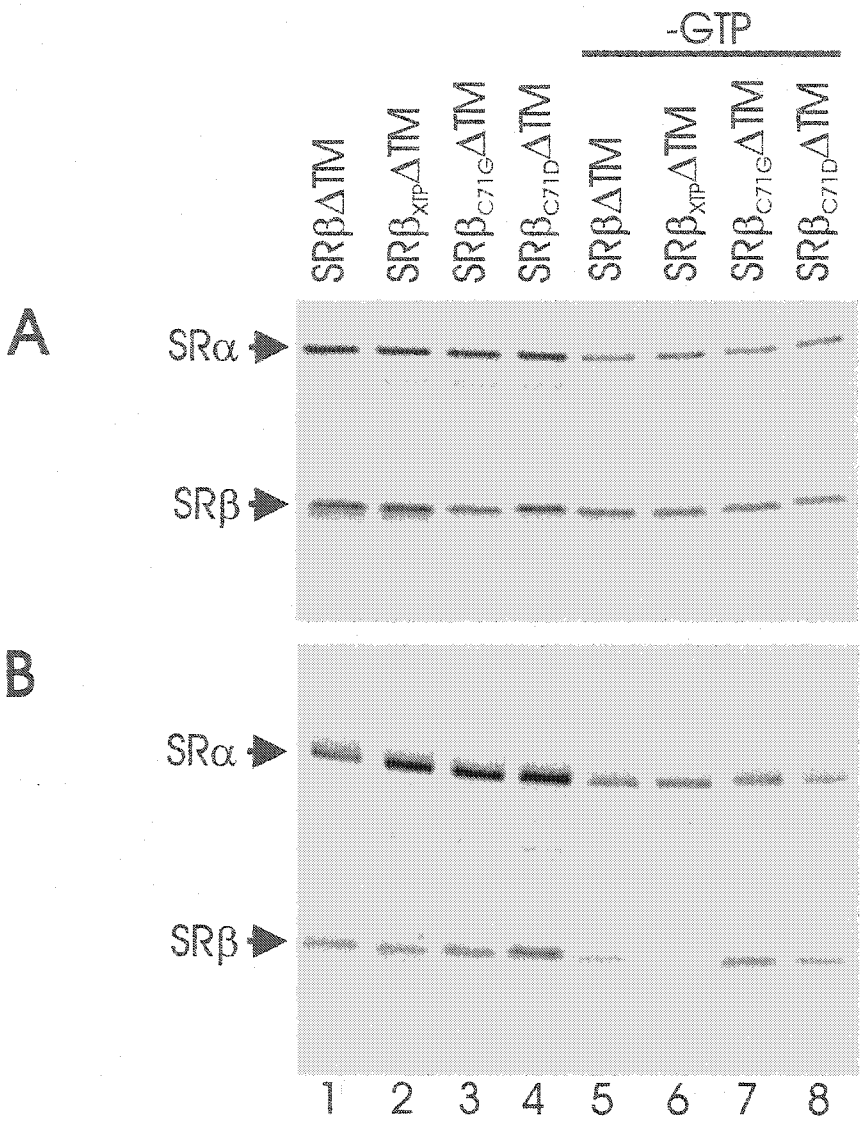

Figure 3.2: Immunoprecipitation of SRα bound to SRβΔTM containing GTPase point mutations. Aliquots of *in vitro* translation reactions containing equimolar amounts of SRα and the specified SRβ GTPase mutation were incubated together prior to immunoprecipitation. Some samples were processed by gel filtration to deplete nucleotides (-GTP) prior to incubation. **A**: Total products prior to immunoprecipitation, **B**: Immunoprecipitation with an anti-SRα antibody. Only $SR\beta_{XTP}\Delta TM$ was unable to bind to SRα in the absence of nucleotide.

Figure 3.3: Purification of His_6-tagged SRβΔTM and $SR\beta_{C71D}\Delta TM$. A: Coomassie stained SDS-PAGE gel of SRβΔTM at each stage of purification. L=clarified lysate, FT=Ni-NTA agarose flow through fraction, Ni=Ni-NTA agarose eluate fraction, CM=CM Sepharose elution fraction. The positions of molecular weight markers are indicated. SRβΔTM migrates to an apparent molecular weight of 30 kDa. **B:** Coomassie stained SDS-PAGE gel of $SR\beta_{C71D}\Delta TM$ at each stage of purification. Lane designations are the same as those in Panel A. $SR\beta_{C71D}\Delta TM$ migrates to an apparent molecular weight of 27 kDa. C: Gel filtration of SRβΔTM on a Superdex 75 FPLC column. Protein was detected by absorbance at 280 nm and plotted vs. elution volume. The position of SRβΔTM and molecular weight calibration standards are indicated.

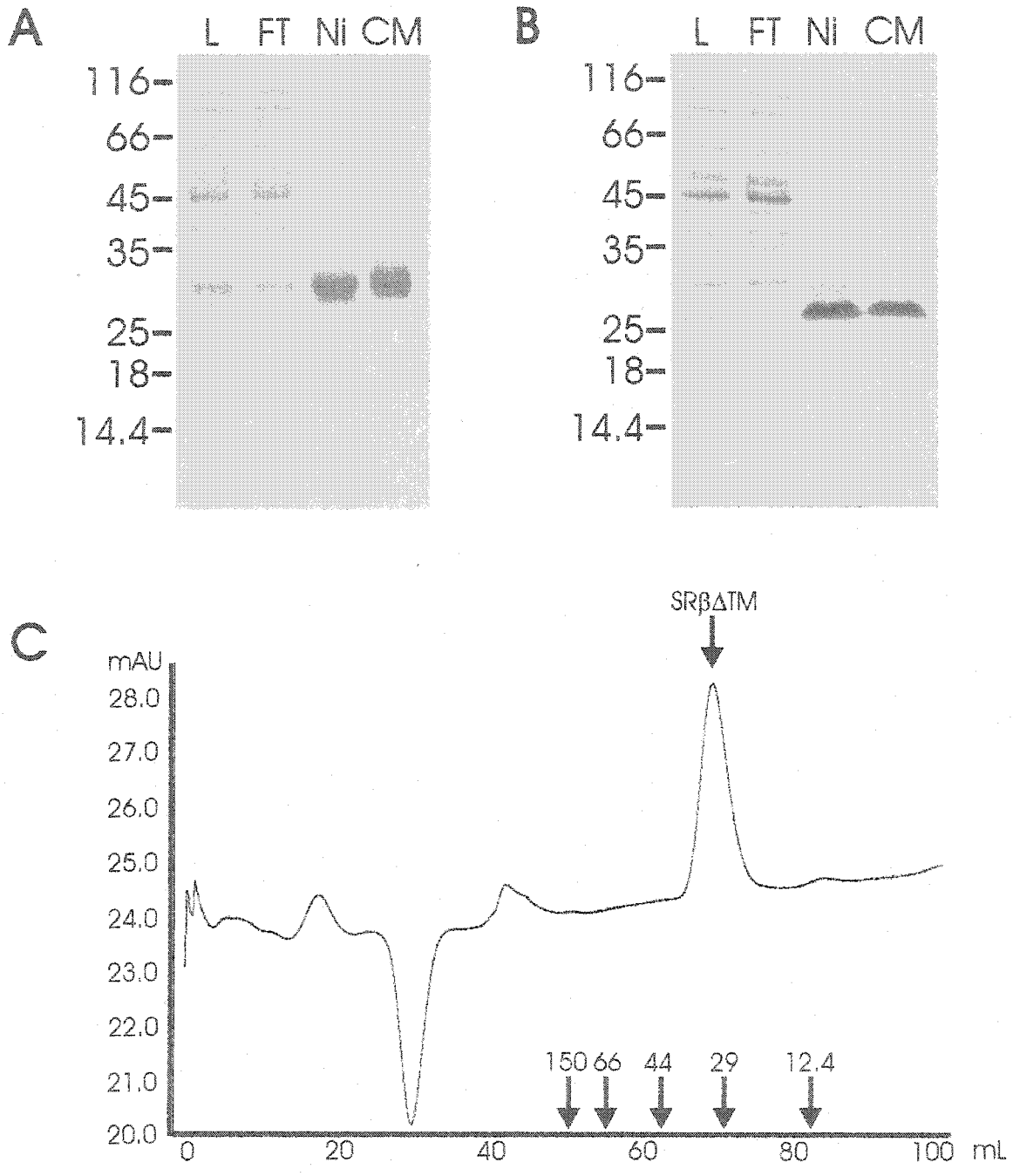
A
L FT Ni CM
116
66
45
35
25
18
14.4
B
L FT Ni CM
116
66
45
35
25
18
14.4
C
SRβΔTM
mAU
28.0
27.0
26.0
25.0
24.0
23.0
22.0
21.0
20.0
150 66 44 29 12.4
0 20 40 60 80 100 mL

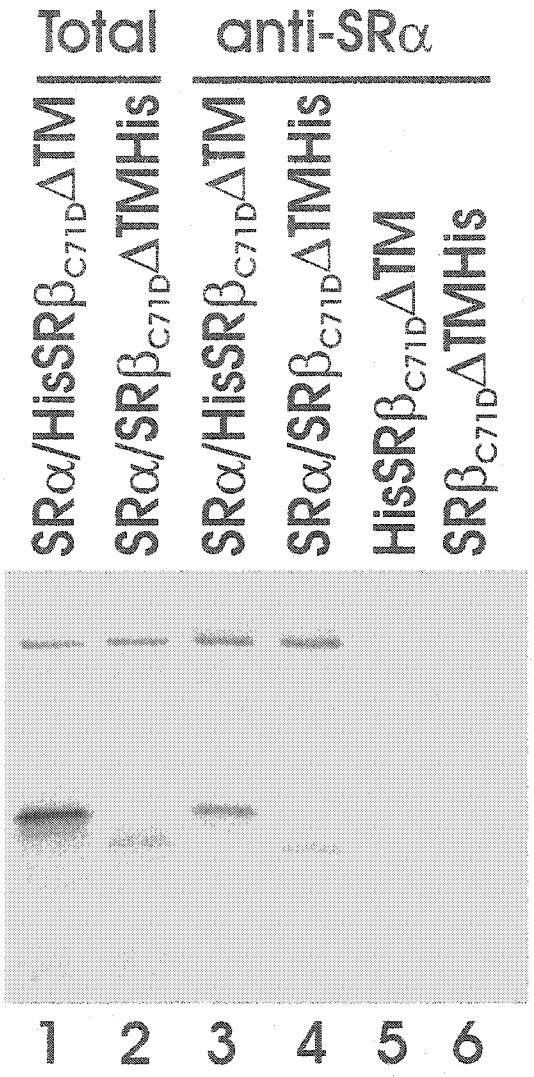

Figure 3.4: Immunoprecipitation of SRα with His_6-tagged versions of $SR\beta_{C71D}\Delta TM$. Aliquots of *in vitro* translation reactions containing SRα and amino-terminal His_6-tagged $SR\beta_{C71D}\Delta TM$ ($HisSR\beta_{C71D}\Delta TM$) or carboxyl-terminal His_6-tagged $SR\beta_{C71D}\Delta TM$ ($SR\beta_{C71D}\Delta TMHis$) were immunoprecipitated with an anti-SRα antibody (lanes 3-4). Lanes 1-2 represent 10% of the starting material. Note that equimolar amounts of each molecule were not used in this assay. Lanes 5-6 contain only SRβ molecules, which do not precipitate with the antibody. The position of the His_6-tag does not affect the ability of $SR\beta_{C71D}\Delta TM$ to bind to SRα.

Figure 3.5: Purification and gel filtration of His_6-tagged SRX2. A: Purification of SRX2 on Ni-NTA agarose. Lanes 1-3 are a Western blot of crude cell lysate using an anti-His_6 antibody. Lanes 1 and 2 represent the supernatant and pellet fractions following cell lysis and low speed centrifugation. Lane 3 represents the supernatant following high speed centrifugation. Most SRX2 was found in the pellet following low speed centrifugation. Lanes 4 and 5 are a Coomassie stain of crude cell lysate following high speed centrifugation, and the elution fraction from Ni-NTA agarose. The migration position of SRX2 is indicated. **B:** Equimolar amounts of SRβΔTM and SRX2 were coincubated prior to gel filtration analysis. Two predominant peaks are observed corresponding to SRβΔTM and SRX2 in Triton X-100 micelles. A Coomassie stain of proteins found in the peak eluting after 40 mLs is shown as an inset. SRX2 is a predominant protein in this peak, but SRβΔTM is not detected.

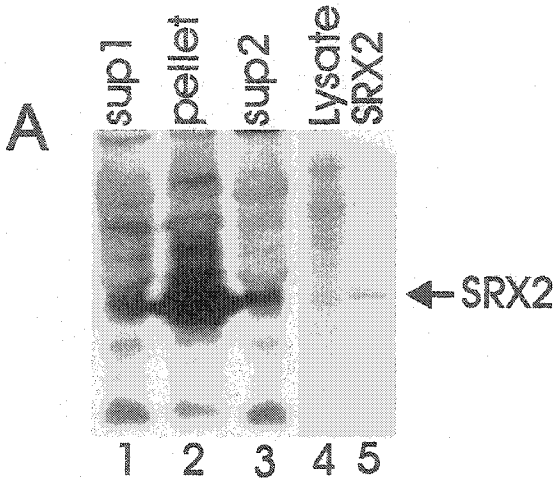
A
sup1
pellet
sup2
Lysate
SRX2
SRX2
1 2 3 4 5

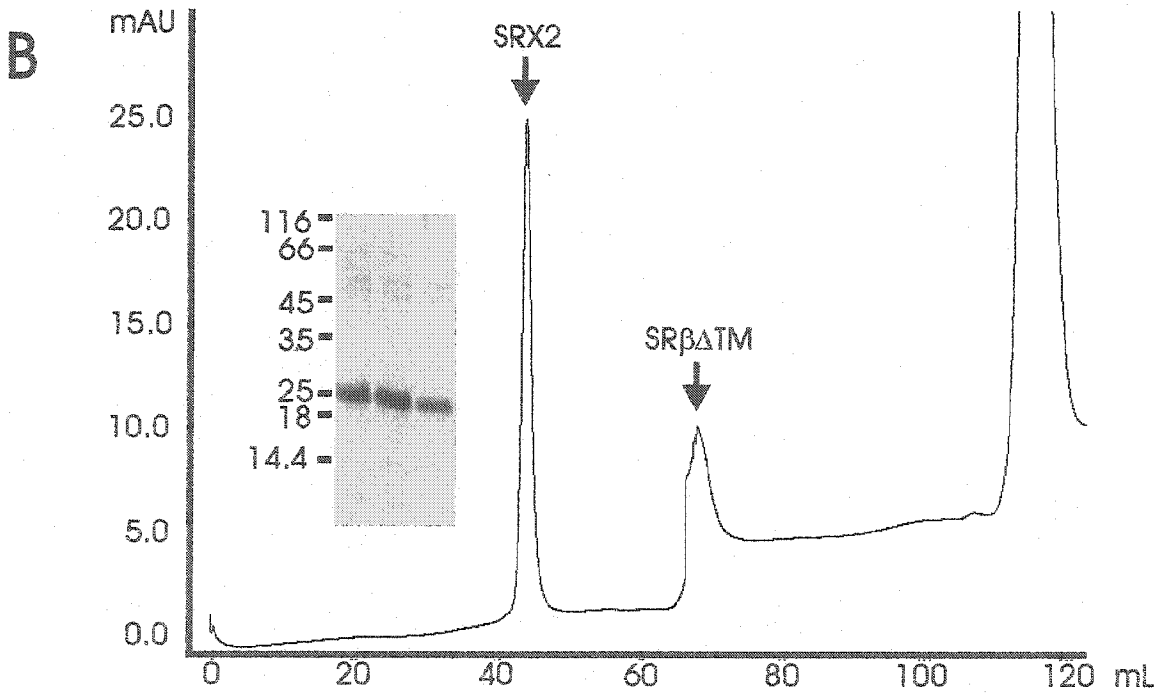
B
mAU
25.0
20.0
15.0
10.0
5.0
0.0
SRX2
SRβΔTM
116
66
45
35
25
18
14.4
0
20
40
60
80
100
120
mL

conditions that retained the solubility of SRX2 did not support SR dimer formation (Figure 3.5.B). As a result of these difficulties this line of experimentation was not pursued further. Therefore, no comparison between isolated SRβ and SRX2-SRβ was possible.

3.3.4 GTP binding characteristics

GTPases are generally purified in the GDP-bound form. This holds true for both tissue-derived proteins as well as recombinant proteins that lack GAP homologues in *E. coli* (Poe et al., 1985; Weiss et al., 1989; Barlowe et al., 1993). Therefore, I expected that purified SRβ would be GDP-bound. To identify and quantify the nucleotide that copurified with SRβ, 10 nmoles of SRβΔTM or $SR\beta_{C71D}\Delta TM$ were denatured in 4M urea to release the bound nucleotide. The denatured protein was removed by filtration and the released nucleotide was analysed by HPLC and compared to standards of GTP and GDP examined in parallel (Figure 3.6). The retention times for GDP and GTP on the HPLC column were 7.9 minutes and 9.6 minutes, respectively (Figure 3.6.A). Surprisingly, the supernatant from denatured SRβ contained a single major peak that eluted at 9.6 minutes, indicating the presence of GTP. A smaller peak was detected at 7.9 minutes, corresponding to a small amount of GDP (Figure 3.6.B). Calculating the area under the curves and comparing these values against values obtained from GTP and GDP standards (and correcting for 10% loss as measured by using GMP as an internal standard) revealed that 72% of SRβΔTM contained bound GTP while only 2% was bound to GDP. Similarly, 71% of purified $SR\beta_{C71D}\Delta TM$ contained GTP and 3% was bound to GDP. Therefore both wild type SRβ and the GTPase point mutant remained bound to GTP throughout purification. The remaining 26% was not bound to nucleotide. This population of SRβ did not bind to GTP in the timescale expected of an active empty GTPase (Feuerstein et al., 1987; Shapiro et al., 1993; see Figures 3.9 and 3.11). Therefore I presume that this population consists of SRβ that became structurally unstable in the absence of bound GTP. A structurally unstable empty state is a common feature of Ras-type GTPases (Feuerstein et al., 1987; John et al., 1990; Mistou et al., 1992). Addition of 10 μM GTP to the buffers used during purification did not decrease the percentage of empty SRβ (Figure 3.7), suggesting that this population did not arise from dissociation of nucleotide during purification.

Two approaches were taken to determine what fraction of recombinant SRβ was able to bind to or exchange bound GTP for exogenous GTP. The first method measured the ability of aromatic amino acids within SRβ to transfer energy to a fluorescent GTP analogue, 2'-(or-3')-*O*-(*N*-methylanthraniloyl)GTP (mant-GTP) (Figure 3.8). Resonance energy transfer (RET) could be measured by monitoring the decrease in fluorescence output of an excited donor molecule (aromatic amino acids) and concomitant increase in acceptor molecule (mant) fluorescence (Figure 3.9.A). Mant fluorescence did not change in a control cuvette lacking protein, nor was there an increase in mant fluorescence attributable to binding to SRβ when the dye was excited directly at 350 nm (Figure 3.9.B, triangles and Figure 3.10.B). Therefore, the increase in mant fluorescence arose solely

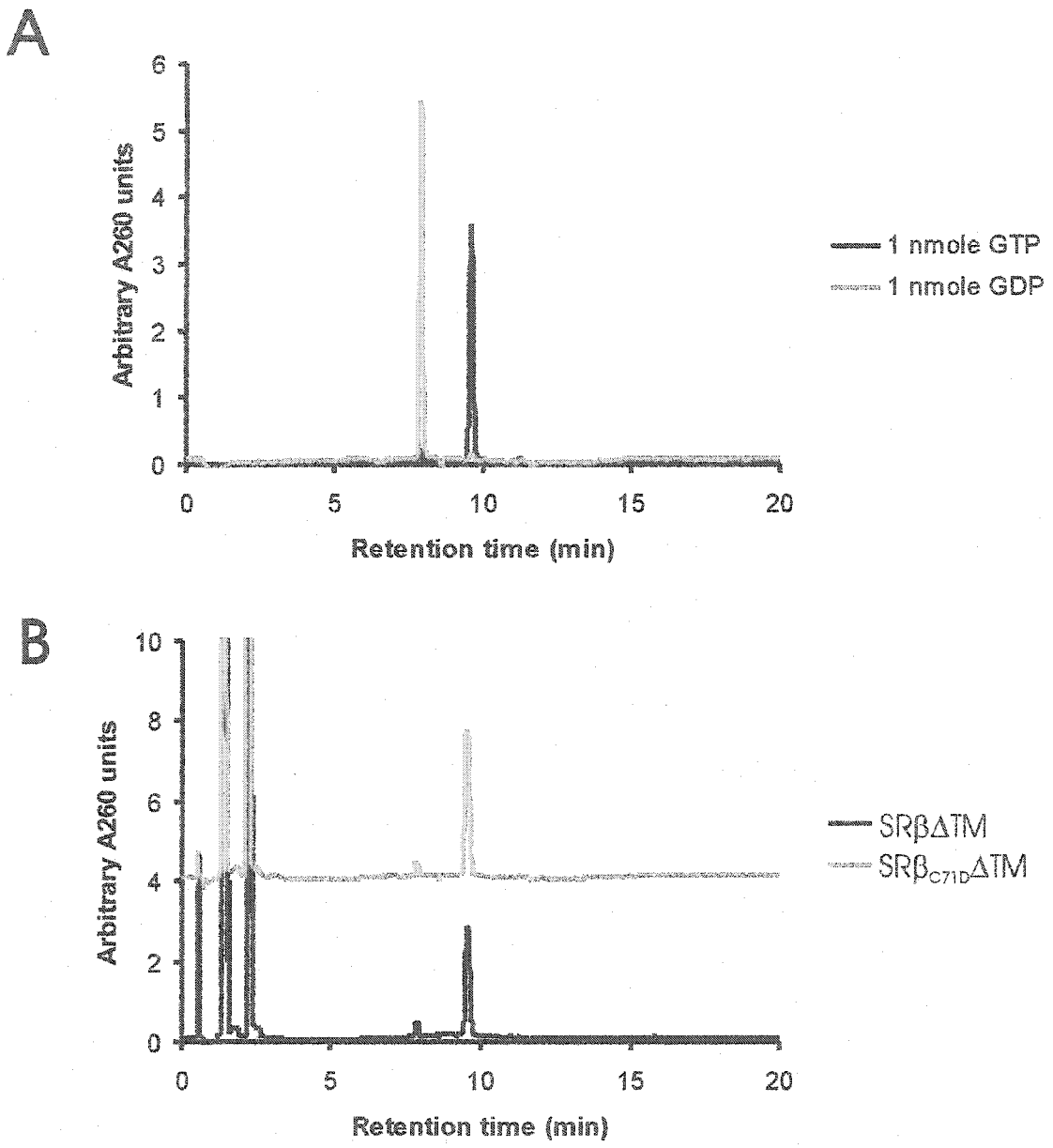

Figure 3.6: Identification of SRβ-bound nucleotide. Samples of SRβΔTM and $SR\beta_{C71D}\Delta TM$ were denatured in urea and the liberated nucleotide was analysed by HPLC by monitoring absorbance at 260 nm. **A:** 1 nmole standards of GTP (black line) and GDP (grey line) show reasonable separation on the HPLC column. **B:** Nucleotide from 4 nmoles of SRβΔTM (black line) and $SR\beta_{C71D}\Delta TM$ (grey line). The predominant nucleotide that binds to both molecules is identified as GTP. The peaks eluting in the flow through fraction arise from contaminants in the urea.

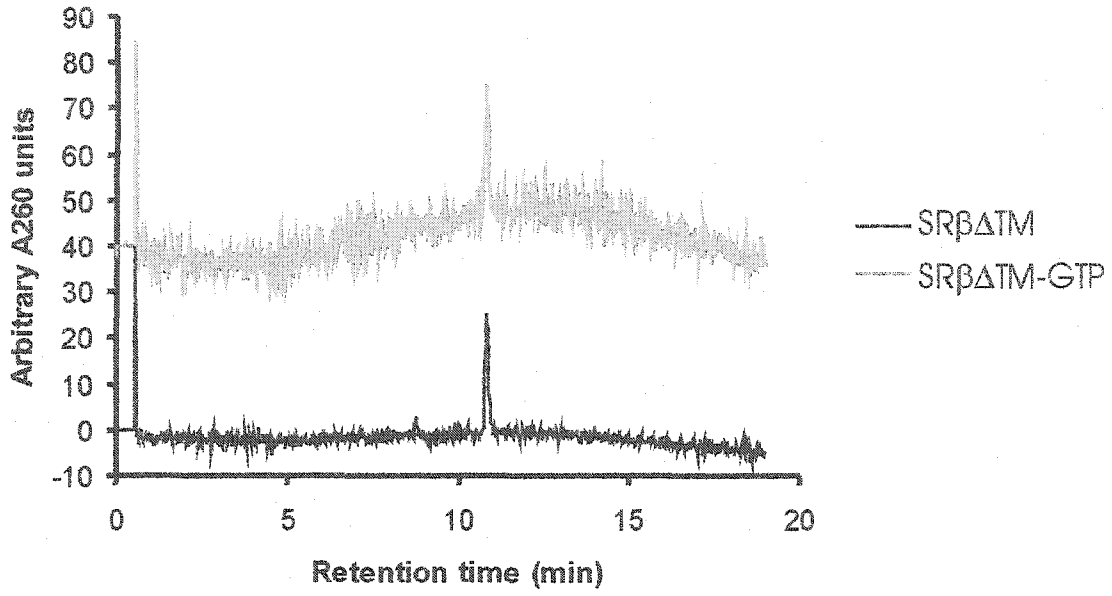

Figure 3.7: Comparison of SRβ-bound nucleotide following purification ±GTP. Samples of SRβΔTM purified in the absence of added GTP (black line) or in the presence of 10 μM GTP (grey line) were denatured in urea and the liberated nucleotide was analysed by HPLC by monitoring absorbance at 260 nm. The amount of GTP liberated from both molecules was identical.

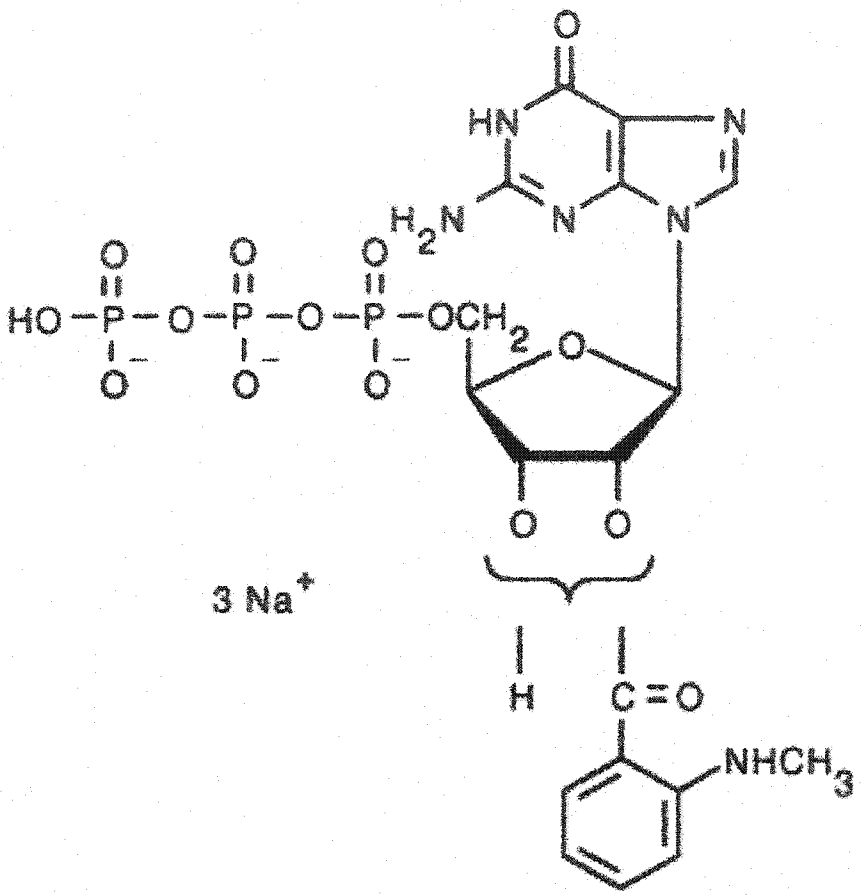

Figure 3.8: Structure of 2'-(or-3')-*O*-(*N*-methylanthraniloyl)GTP (mant-GTP). GTP is equally substituted on the 2' and 3' hydroxyl group of ribose with the *O*-(*N*-methylanthraniloyl) fluorophore. Figure taken from http://www.probes.com/servlets/structure?item=12415.

Figure 3.9: Fluorescence analysis of GTP binding kinetics. 300 nM SRβΔTM or $SR\beta_{C71D}\Delta TM$ were incubated with 500 nM mant-GTP at 24°C and GTP binding was analysed by fluorescence spectroscopy. **A:** Demonstration of resonance energy transfer (RET). Aromatic side chains within SRβ, excited at 280 nm, emit fluorescence with an emission maxima of approximately 330 nm. As mant-GTP binds over time, RET is detected by a decrease in protein fluorescence accompanied by an increase in mant-GTP fluorescence, with an emission maxima of 440 nm. **B:** GTP binding as measured by RET at an excitatory wavelength of 280 nm. The plots for SRβΔTM (◆) and $SR\beta_{C71D}\Delta TM$ (■) represent the increase in mant-GTP fluorescence over time. mant-GTP exposed to 280 nm light in the absence of protein is also shown (▲). **C:** GTP binding as measured by RET at an excitatory wavelength of 295 nm. The plots for SRβΔTM (◆) and $SR\beta_{C71D}\Delta TM$ (■) represent the increase in mant-GTP fluorescence over time. The Y axis in Panels B and C is presented as a fluorescence ratio calculated from the fluorescence intensity at time=X ÷ the fluorescence intensity at time=0. All experiments were performed at least 3 times, with nearly identical results.

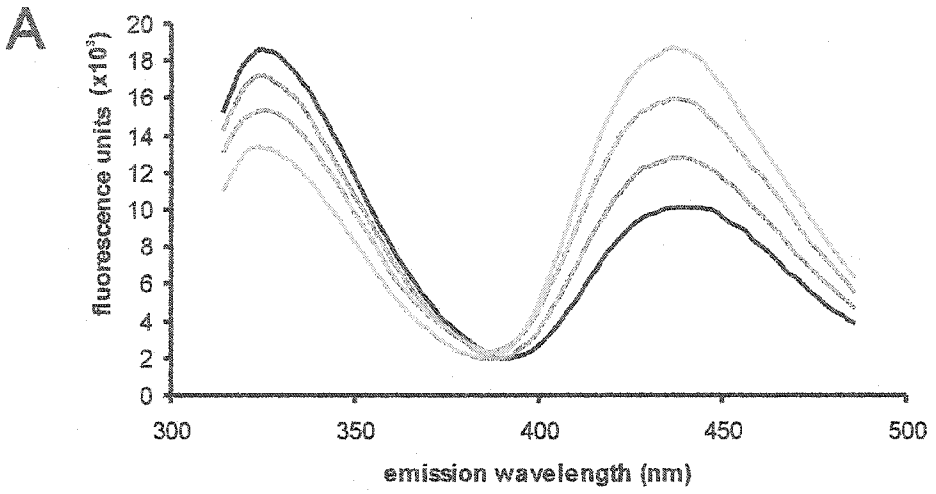
A
fluorescence units (x10³)
20
18
16
14
12
10
8
6
4
2
0
300
350
400
450
500
emission wavelength (nm)

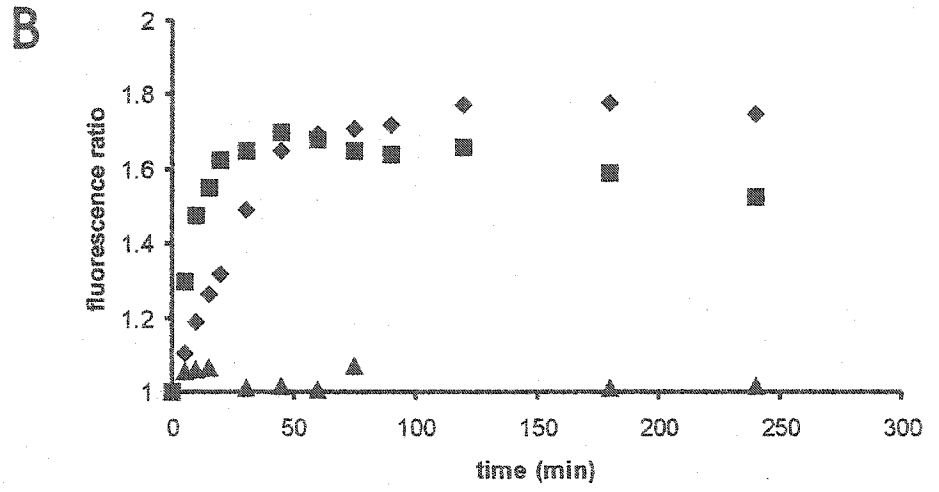
B
fluorescence ratio
2
1.8
1.6
1.4
1.2
1
0
50
100
150
200
250
300
time (min)

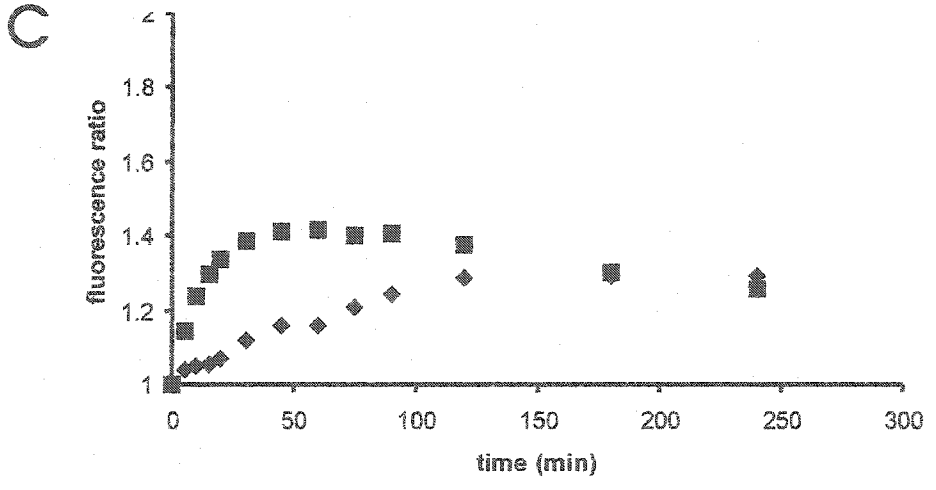
C
fluorescence ratio
1.8
1.6
1.4
1.2
1
0
50
100
150
200
250
300
time (min)

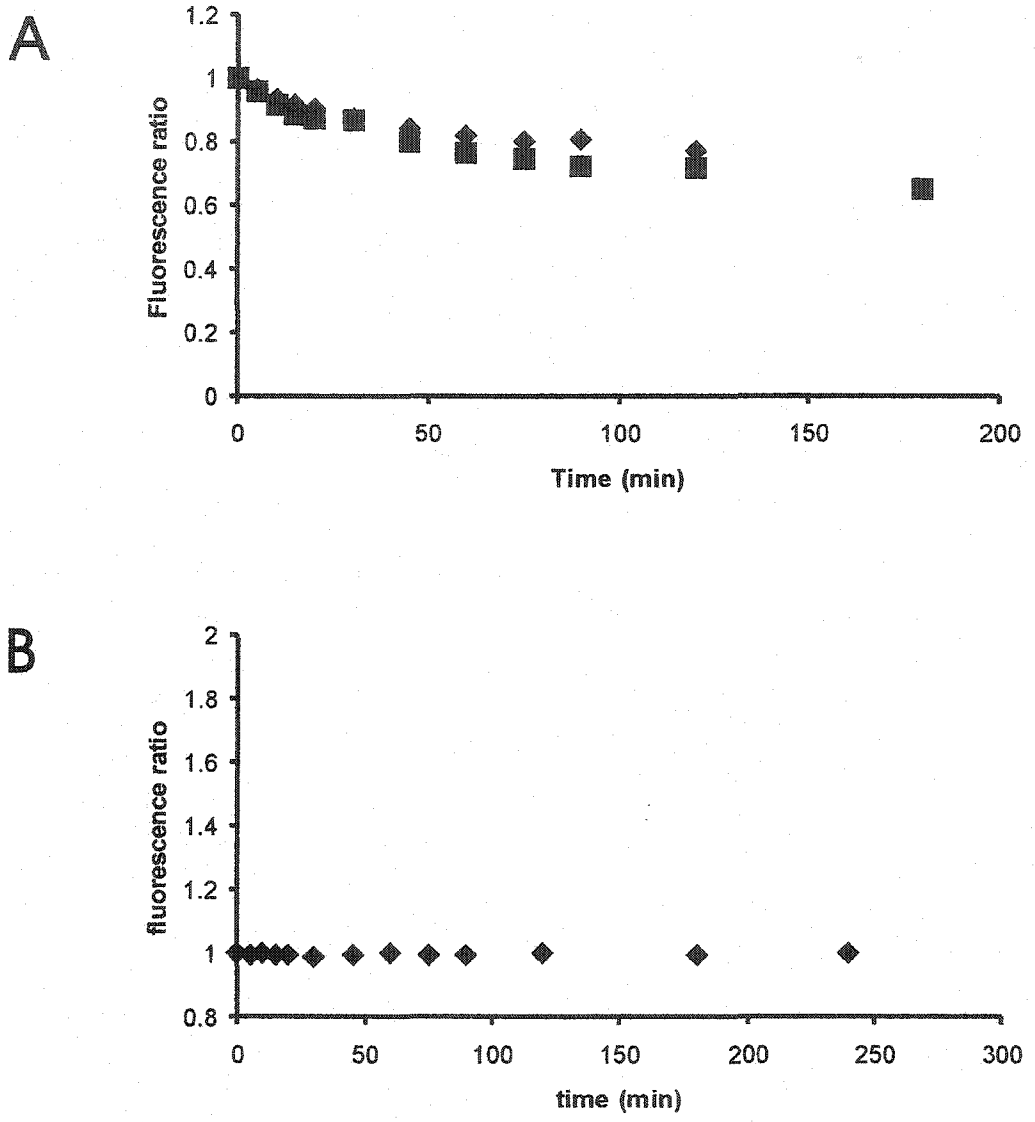

Figure 3.10: Fluorescence spectroscopy control experiments. A: A decrease in fluorescence intensity arising from aromatic residues over time was detected from both SRβΔTM (◆) and $SR\beta_{C71D}\Delta TM$ (■). For this reason the increase in mant-GTP fluorescence over time was used to assay GTP binding kinetics. **B:** Fluorescence change of mant-GTP incubated with SRβΔTM at an excitatory wavelength of 350 nm. There is no change in the fluorescence of mant-GTP upon direct excitation of the fluorophore. Each experiment was performed at least 3 times, with nearly identical results.

from RET between the mant fluorophore and aromatic side chains within SRβ, including a tryptophan near the carboxyl-terminus. GTP binding was quantified using the increase in mant fluorescence since Trp fluorescence decreased over time in the absence of mant-GTP (Figure 3.10.A). I assume this is due to thermal denaturation of the purified protein in the fluorometer cuvette. Whatever the cause, by monitoring the increase in mant fluorescence I would slightly underestimate rather than overestimate the rate of GTP binding. The distance limitations of RET require that mant-GTP is bound to SRβ for energy transfer to occur. Therefore this method provides a sensitive means to compare the rate of GTP-binding to SRβΔTM and $SR\beta_{C71D}\Delta TM$. Reactions containing 300 nM SRβ and 500 nM mant-GTP were excited at 280 nm and energy transfer was monitored by measuring the increase in mant-GTP fluorescence emission at 440 nm (Figure 3.9.B). Both SRβΔTM and $SR\beta_{C71D}\Delta TM$ bound mant-GTP, with SRβΔTM apparently accepting nucleotide with two distinct binding modes. The first mode was complete after 45 minutes; the second mode was slower and took an additional hour to complete. $SR\beta_{C71D}\Delta TM$ showed a single mode of GTP uptake that was complete after 45 minutes. The initial rate of increase in mant fluorescence was greater for $SR\beta_{C71D}\Delta TM$ than for SRβΔTM, indicating that the cysteine mutation permitted mant-GTP more rapid access to the GTP binding site in SRβ.

SRβ contains only one Trp located five amino acids from the carboxyl-terminus. Excitation at 295 nm permitted measurement of RET between this tryptophan and mant-GTP. I observed no change in the apparent kinetics of GTP-binding to $SR\beta_{C71D}\Delta TM$ (Figure 3.9.C). However, SRβΔTM showed a single mode of GTP-binding, that resembled the second mode detected at 280 nm excitation in both slope and duration. Therefore, the first mode arose from RET between one or more of the Tyr (and Phe) residues scattered throughout SRβΔTM, and mant-GTP, while the second mode arose from RET between the carboxyl-terminal Trp residue and mant-GTP.

While fluorescence spectroscopy permitted determination of binding kinetics it did not permit me to determine what fraction of SRβ can bind GTP. Therefore, I used a nitrocellulose filter binding assay to quantify the amount of GTP that could bind SRβ (Figure 3.11). 100 pmoles of SRβΔTM (◆) or $SR\beta_{C71D}\Delta TM$ (■) was incubated with a 10-fold molar excess of GTP, including 25% ^{3}H-GTP, at 24°C for the indicated times. To analyse GTP binding the protein was bound to nitrocellulose filters and washed extensively to remove unbound nucleotide. The nucleotide remaining on the filter, representing the amount of solution GTP retained in a complex with SRβ, was quantified by scintillation counting. At 24°C both proteins showed the same t½ for nucleotide binding as was calculated from fluorescence data. After two hours SRβΔTM bound a maximum of 6.6 pmoles of GTP, reflecting an occupancy of 6.6%. $SR\beta_{C71D}\Delta TM$ bound GTP at a faster rate than SRβΔTM, reaching a maximum of 3.5 pmoles of GTP bound after one hour followed by a steady decline throughout the rest of the experiment. A similar decline in binding was observed during RET experiments (Figure 3.9) and may

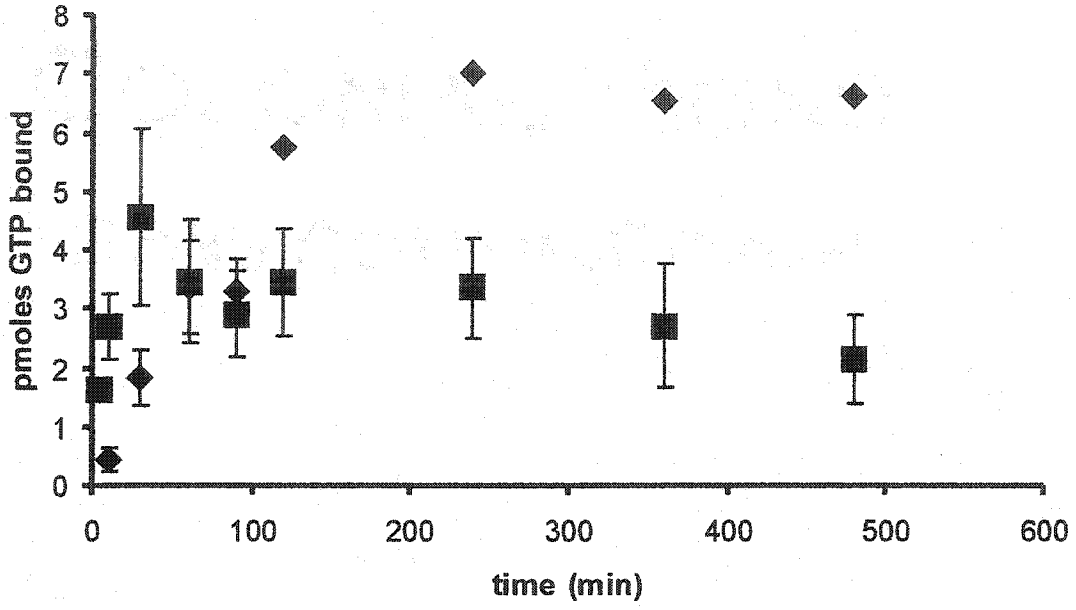

Figure 3.11: Quantification of GTP binding capacity of SRβΔTM and SRβ$_{C71D}$ΔTM. 100 pmoles of SRβΔTM (◆) or SRβ$_{C71D}$ΔTM (■) were incubated with ^{3}H-GTP, and quantification of bound GTP was achieved by binding protein-GTP complexes to nitrocellulose filters followed by scintillation counting. Data points represent the mean of three independent experiments for SRβΔTM, and six independent experiments for SRβ$_{C71D}$ΔTM. Error bars represent the standard deviation. 7% of SRβΔTM can accept exogenous GTP, compared to 3.5% of SRβ$_{C71D}$ΔTM.

reflect structural instability of $SR\beta_{C71D}\Delta TM$ during extended incubation at 24°C. Taken together, the data revealed that <10% of SRβ bound exogenous GTP (de novo or by exchange). Therefore, 90% of SRβ was already tightly bound to nucleotide or in a conformation that was unable to bind nucleotide. Both RET and filter binding experiments indicated that SRβ bound added GTP slowly, consistent with observations made in other GTPases assayed in their nucleotide-bound states (Ferguson et al., 1986; Kahn and Gilman, 1986; Barlowe et al., 1993).

The K_d of SRβ for GTP was reported to range from 1 μM for the purified, solubilized SR dimer (Miller et al., 1995) to 20 nM for the purified SR dimer reconstituted into liposomes (Bacher et al., 1999). To determine the K_d of the 7% of SRβ that accepted exogenous GTP, purified SRβ was crosslinked to α-^{32}P-GTP in the presence of an increasing concentration of non-radiolabelled competitor GTP (Figure 3.12.A, 3.12.B, ■). Binding followed a characteristic sigmoidal curve with the inflection point at 2 μM, demonstrating that recombinant SRβ and solubilized SR (Miller et al., 1995) have similar affinities for GTP. An identical K_d was calculated for $SR\beta_{C71D}\Delta TM$ (Figure 3.12, ▲). Therefore purified recombinant SRβΔTM bound GTP with a similar affinity as native SRβ after solubilization of microsomes, and mutation of the cysteine in the G1 box did not affect the affinity of this protein for GTP. Due to the short incubation period prior to crosslinking this K_d measurement reflected the loose-binding conformation revealed by RET, and not the majority of SRβ that was already bound to GTP.

3.3.5 GTP hydrolysis activity

Since the majority of SRβ remained bound to GTP throughout purification (Figure 3.6.B) it is likely that the intrinsic GTPase activity of SRβΔTM is negligible. To experimentally verify that the SRβ GTPase does not possess intrinsic catalytic activity, SRβΔTM was incubated with γ-^{32}P-GTP and hydrolysis was monitored by quantifying the liberation of the γ-phosphate by thin layer chromatography (Figure 3.13.A). Ribosome-nascent chains (RNCs) treated with N-Ethylmaleimide (NEM), identical to those used in previous attempts to assay the influence of the ribosome on the SRβ GTPase (Bacher et al., 1999), demonstrated that NEM treatment was not sufficient to abolish GTPase activity associated with RNCs (Figure 3.13.A, NEM-RNC). Therefore, initial measurements were made in the absence of ribosomes. After four hours of incubation at 24°C no significant GTP hydrolysis was visually apparent above a control reaction lacking SRβ (Figure 3.13.A, compare SRβ to GTP). To ensure that the assay was sensitive enough to measure even a low basal rate of GTP hydrolysis, the assay was repeated with varying concentrations of GTP and a Lineweaver-Burk plot was generated to estimate a basal GTP hydrolysis rate (Figure 3.13.B). From the plot an estimated K_m of 4.0 μM and k_{cat} of 0.0005 min^{-1} were derived, indicating a negligible rate of GTP hydrolysis for SRβΔTM. The efficiency of crosslinking [α-^{32}P]GTP and [γ-^{32}P]GTP to SRβ were identical (Figure 3.13.C), consistent with the negligible rate of GTPase activity

Figure 3.12: Measurement of GTP binding affinity. SRβΔTM or $SR\beta_{C71D}\Delta TM$ was incubated with α-^{32}P-GTP in the presence of increasing concentrations of unlabelled competitor GTP, and GTP was crosslinked to protein by exposure to UV light. **A:** Crosslinked samples of SRβΔTM separated on SDS-PAGE were detected by autoradiography. The bands arise from the crosslinked radiolabelled GTP. The concentration of unlabelled GTP is indicated across the top of the figure. **B:** Crosslinking data from SRβΔTM (■) and $SR\beta_{C71D}\Delta TM$ (▲) were quantified by PhosphorImager analysis and plotted as arbitrary PhosphorImager units vs the log of the concentration of unlabelled GTP. The measured K_d for both proteins is 2 μM.

A

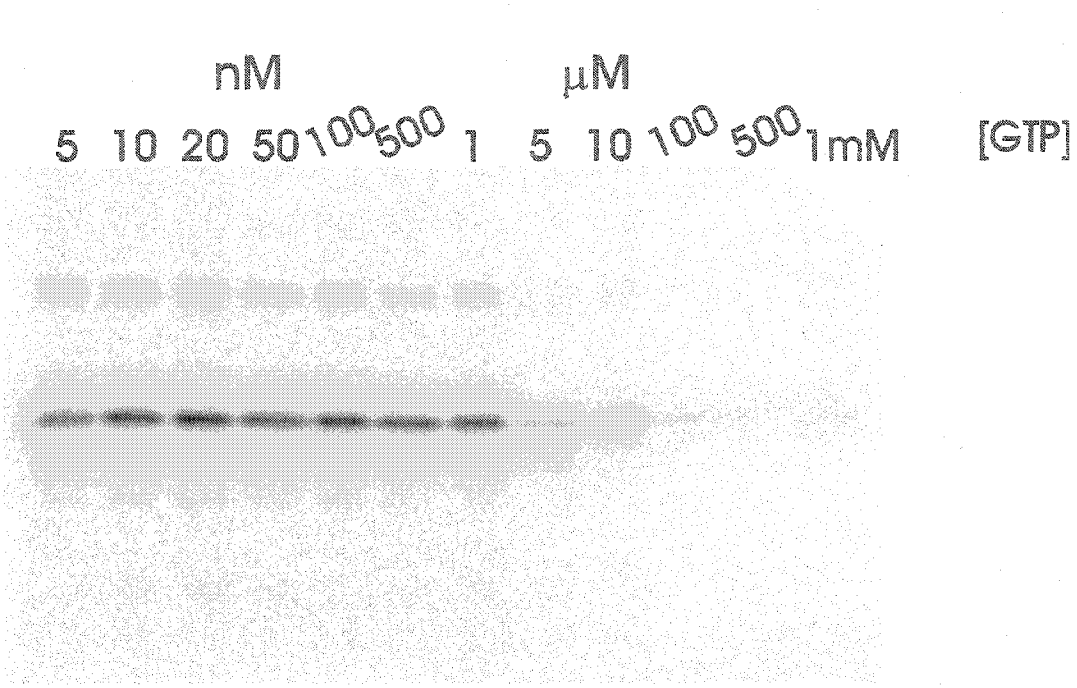
nM
μM
5 10 20 50 100 500 1 5 10 100 500 1mM [GTP]

B

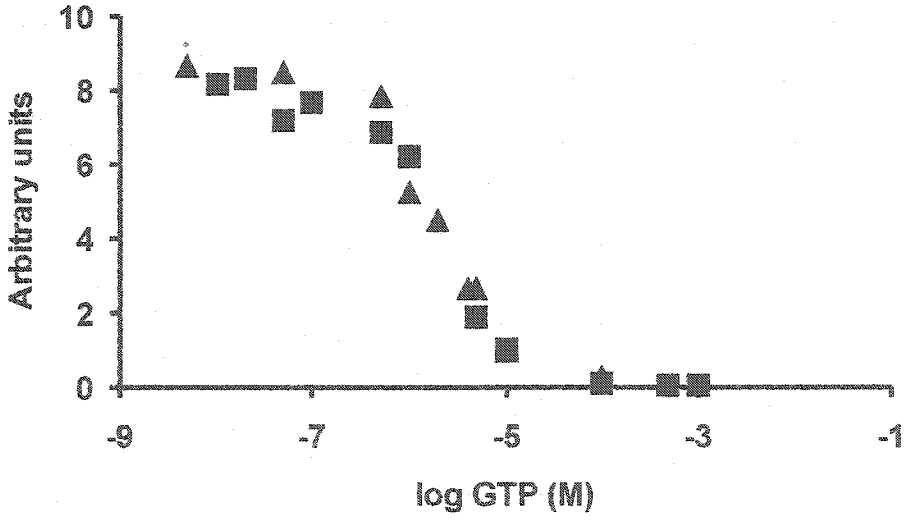
Arbitrary units
10
8
6
4
2
0
-9
-7
-5
-3
-1
log GTP (M)

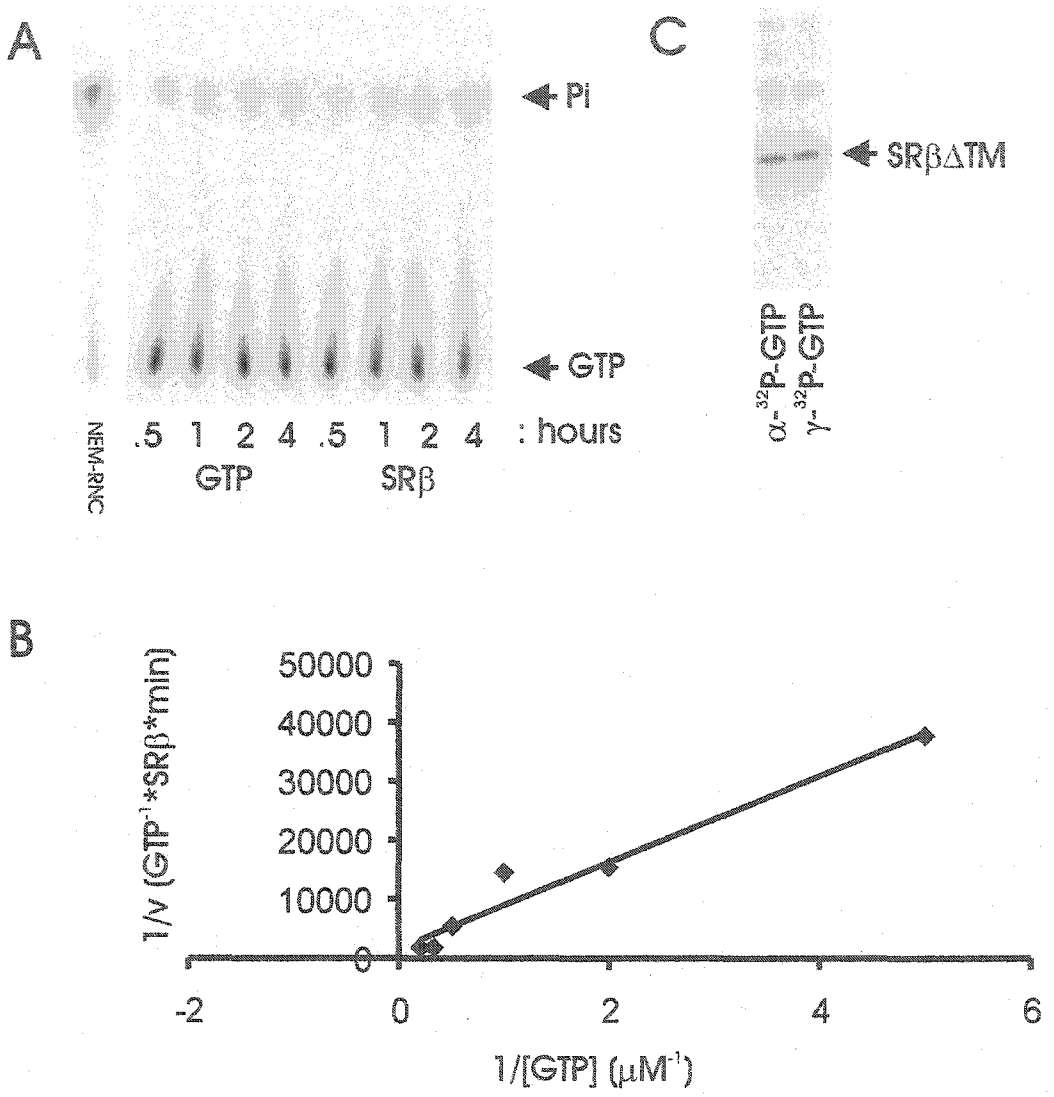

Figure 3.13: Endogenous GTPase activity of SRβΔTM. A: γ-^{32}P-GTP was incubated in the absence (GTP) or presence (SRβ) of SRβΔTM. At the indicated times samples were spotted on TLC plates and developed to assess the hydrolysis of GTP. A sample of *N*-ethylmaleimide-treated ribosome-nascent chains is included as a positive control (NEM-RNC). No significant hydrolysis of GTP by SRβΔTM is detected. The migration positions of γ-^{32}P-GTP and γ-^{32}Pi is indicated. B: A Lineweaver-Burk plot generated from data quantified from TLC plates. The basal rate of GTP hydrolysis estimated from this plot is <0.0005 min-1. C: Crosslinking of α-^{32}P-GTP or γ-$_{32}$P-GTP to SRβΔTM, demonstrating that γ-^{32}P-GTP is not hydrolysed upon binding to SRβ.

obtained using the thin layer chromatography assay. Therefore, unassisted, SRβ was unable to hydrolyse GTP, suggesting a requirement for a GTPase activating protein (GAP) for SRβ.

A candidate GAP for SRβ was recently proposed to reside within the ribosome (Bacher et al., 1999). Since ribosomes are a significant source of GTPase activity, this activity must be abolished to unambiguously assign GTPase activity arising from SRβ in reactions containing both SRβ and ribosomes. The use of alkylating reagents to modify ribosomal proteins reduces, but does not abolish, the activity of ribosome-associated GTPases (Marsh et al., 1975) (see also Figure 3.13.A). Therefore in addition to 80S ribosomes, isolated ribosomal subunits and RNCs were treated with N-ethylmaleimide (NEM) in an attempt to decrease background ribosome-associated GTPase activity enough to detect GTP hydrolysis arising from SRβ. Treatment with NEM had no effect on the GTPase activity of 80S ribosomes or RNCs (Figures 3.13.A, 3.14) but the GTPase activity of isolated 60S subunits, already significantly decreased compared to intact ribosomes, was abolished following treatment with NEM (Figure 3.14). Incubation of SRβ with NEM-treated 60S subunits did not result in any additional GTP hydrolysis above background levels (Figure 3.15).

Although isolated 60S ribosomal subunits did not stimulate the SRβ GTPase, it is possible that ribosome associated GAP activity requires an intact 80S ribosome. The GTPase activity of 80S ribosomes precluded analysis with exogenous nucleotide, therefore I took advantage of the fact that 72% of SRβΔTM purified with bound GTP and assessed the effect of the ribosome on the GTP bound to SRβ. If a protein within the ribosome acts as a SRβ GAP then incubation of SRβ with ribosomes in the absence of added GTP should result in the hydrolysis of SRβ-bound GTP to GDP. If the ribosome functions as a guanine nucleotide release factor (GRF) then incubation of SRβΔTM with ribosomes should lead to the release of the GTP or GDP bound to SRβΔTM. GTP released from SRβ would then be hydrolysed by the ribosome-associated GTPases. To examine these possibilities SRβΔTM or $SR\beta_{C71D}\Delta TM$ was incubated with purified RNCs in the absence of exogenous GTP. The RNCs were removed by centrifugation through high density sucrose and I assayed the top fraction by HPLC to quantify the extent of GTP hydrolysis (Figure 3.16). RNCs alone did not release nucleotide into the solution (Figure 3.16.A), so all nucleotide in the top fraction was assumed to originate from SRβ. Samples of nucleotide from SRβ incubated in the presence of RNCs were identical in the amount and proportion of GTP and GDP as SRβ incubated in the absence of ribosomes (compare Figure 3.16.B with Figure 3.6.B).

Since there was a 12.5-fold excess of SRβ in the previous experiment, there was a possibility that a small but significant amount of GTP hydrolysis could not be detected using an HPLC-based assay. If the interaction between SRβ and the ribosome is catalytic (ie. SRβ and the ribosome dissociate following GTP hydrolysis) then the above assay is valid. However, if in the absence of an intact translocation pathway there is a one-to-one

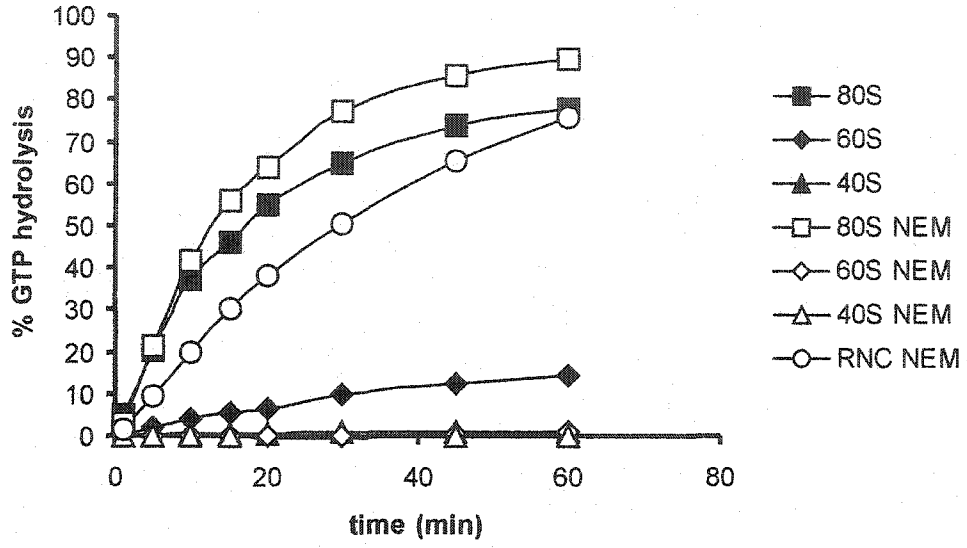

Figure 3.14: GTP hydrolysis by ribosomes. Purified ER-derived ribosomes, ribosomal subunits and RNCs were treated with N-ethylmaleimide, or left untreated, and incubated with γ-^{32}P-GTP for the indicated times. Hydrolysis of GTP was assessed by thin layer chromatography and Phosphorimager analysis. Data was presented as %GTP hydrolysis over time.

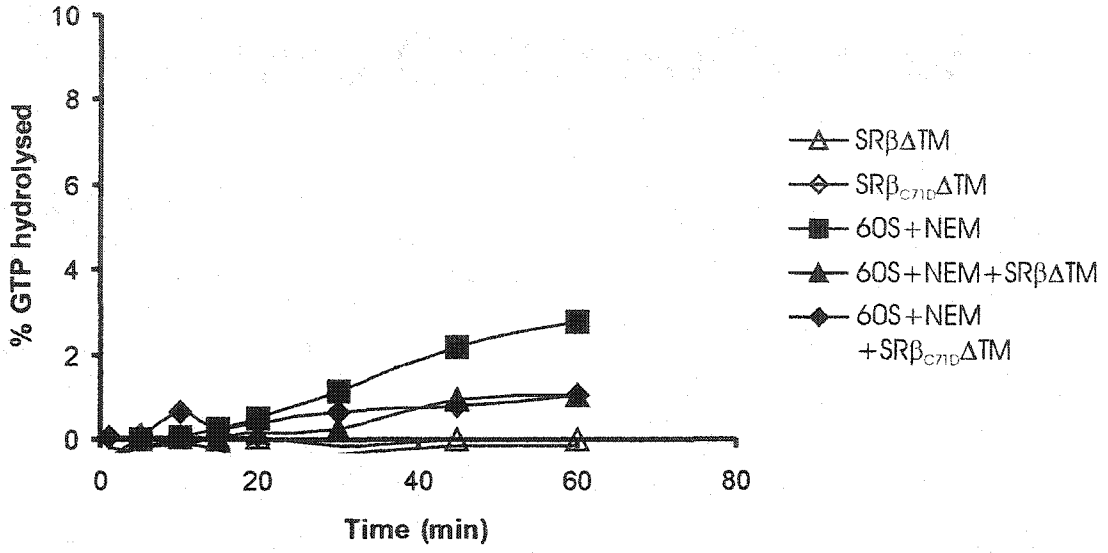

Figure 3.15: The effect of NEM-treated 60S ribosomal subunits on SRβ GTPase activity. SRβΔTM or $SR\beta_{C71D}\Delta TM$ were incubated with purified NEM-treated 60S ribosomal subunits and hydrolysis of γ-^{32}P-GTP was assessed by thin layer chromatography. 60S ribosomal subunits had no effect on the GTPase activity of either protein.

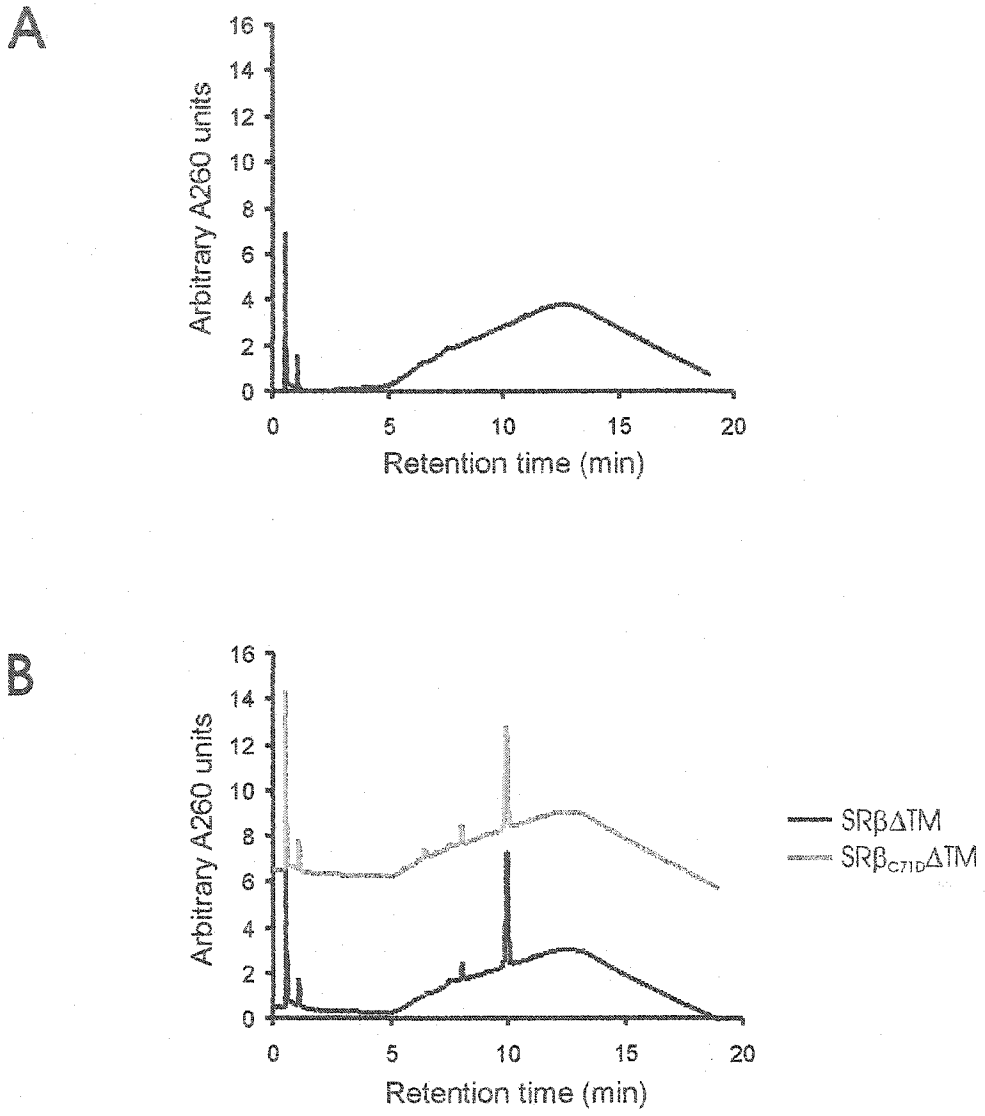

Figure 3.16: The effect of ribosome-nascent chains on SRβ GTPase activity. SRβΔTM or $SR\beta_{C71D}\Delta TM$ was incubated with RNCs for one hour. RNCs were removed by centrifugation, SRβ molecules were denatured in urea and liberated nucleotide was detected by HPLC. A: A sample of RNCs alone, demonstrating that ribosomes do not contribute to the nucleotide content. B: Liberated nucleotide from SRβΔTM (black line) or $SR\beta_{C71D}\Delta TM$ (grey line). Material eluting in the flow through fraction arises from a contaminant in the urea; the "hump" present during elution arises from a contaminant in the triethylamine elution buffer.

interaction between SRβ and the ribosome, the maximum possible hydrolysis would amount to 8% of the total GTP. If the ribosome favours the GDP-bound or empty form of SRβ it is possible that in the presence of excess SRβ no hydrolysis would be detected. To obtain a more sensitive readout of GTP hydrolysis, SRβ was loaded with γ-^{32}P-GTP by sequential treatment with EDTA and magnesium (Koyama and Kikuchi, 2001; Wang and Colicelli, 2001). The total amount of SRβ that exchanged with exogenous GTP under these conditions was 6%, in agreement with the data presented in Figure 3.10. Free nucleotide was separated from bound nucleotide by repurification of SRβ on CM Sepharose, SRβ was incubated with >2-fold molar excess of ribosomes and GTP hydrolysis was monitored using TLC (Figure 3.17). As expected there was no measurable GTP hydrolysis when SRβ was incubated alone. Moreover, the presence of ribosomes did not stimulate the GTPase activity of SRβΔTM. Therefore I conclude that the ribosome exerts no influence upon the GTPase activity of GTP bound SRβ.

In addition to proposing that a ribosomal component acts as a SRβ GAP, Bacher et al. measured a decreased affinity between SRβ and guanine nucleotides in the presence of ribosomes, suggesting that a ribosomal component also behaves as a GRF (Bacher et al., 1999). However, if the ribosome is a GRF for SRβ then some GTP would dissociate from SRβ during the incubation with RNCs and become available for hydrolysis by the ribosome. Since I did not observe any GTP hydrolysis I conclude that the GTP remained tightly bound to SRβ throughout the incubation with RNCs.

3.3.6 Ribosome binding activity

Chemical crosslinking experiments yielded a specific crosslink between SRβ and a protein within the 60S ribosomal subunit, suggesting that there is a physical association between SRβ and ribosomes (Fulga et al., 2001). However, these experiments were performed in the context of SRα/SRβ dimers, which raises the possibility that I did not detect an influence of the ribosome on SRβ because the ribosome was unable to bind SRβ in the absence of SRα. To test this possibility SRβ binding to 80S ribosomes and RNCs was assessed by sedimentation in sucrose density gradients. SRβΔTM or $SR\beta_{C71D}\Delta TM$ was incubated with purified 80S ribosomes or RNCs and ribosome-bound SRβ was separated from unbound SRβ by centrifugation on a 10-40% sucrose gradient. Fractions were collected and analysed by Western blotting with an antibody against SRβ (Figure 3.18). Both SRβΔTM and $SR\beta_{C71D}\Delta TM$ formed a stable complex with both untranslating ribosomes and RNCs, as revealed by their comigration in sucrose (Figure 3.18.B-E). Prolactin, which is not expected to interact with ribosomes, remained at the top of the gradient (Figure 3.18.F). This data demonstrated that although the ribosome was unable to stimulate the SRβ GTPase, a stable interaction between the two could still occur. It should be noted that SRβ was present in a 12.5-fold molar excess over ribosomes in these experiments, so it is not possible to estimate the percentage of SRβ that was able to bind to ribosomes from this figure. When this experiment was repeated using equimolar amounts of SRβΔTM and ribosomes, 22% of the SRβ was recovered in

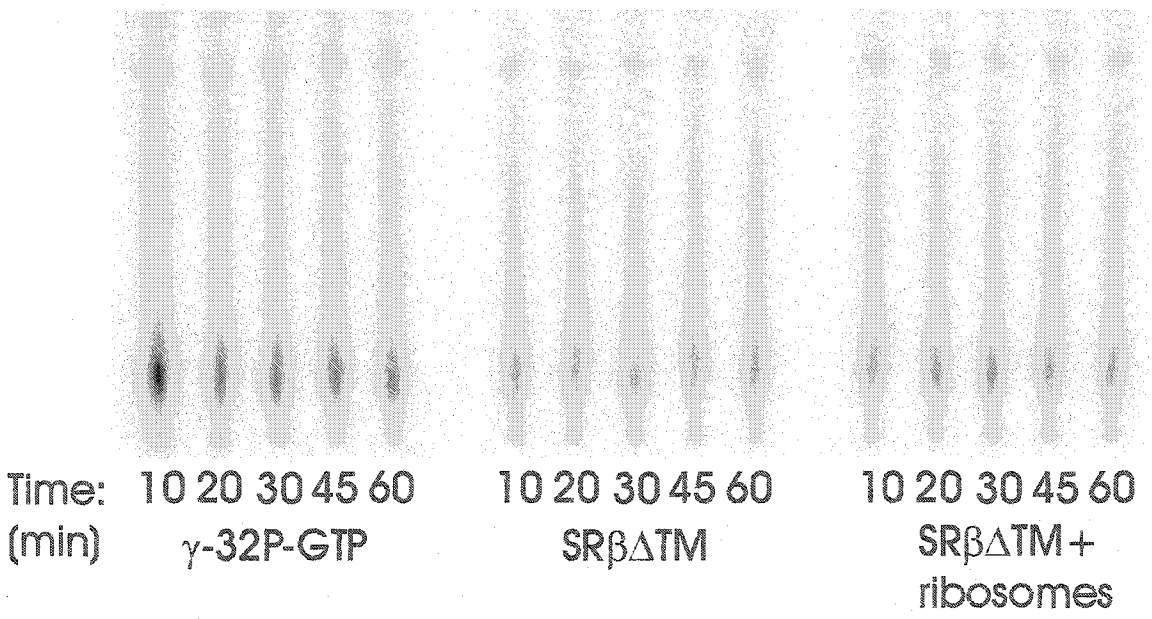

Figure 3.17: The effect of 80S ribosomes on SRβ GTPase activity. SRβΔTM was loaded with exogenous GTP including 1% γ-^{32}P-GTP by incubation with EDTA followed by addition of Mg^{2+}. >2-fold molar excess of 80S ribosomes was added to one sample. Samples were incubated at 37°C, aliquots were removed at the indicated time points and resolved by TLC to assess the extent of GTP hydrolysis. The results from PhosporImager exposure of the TLC plate are shown. In each case less than 0.05% of the GTP was hydrolysed.

Figure 3.18: Binding of SRβΔTM and SRβ$_{C71D}$ΔTM to ribosomes. SRβΔTM (Panels A-C), SRβ$_{C71D}$ΔTM (Panels D-E) or prolactin (Panel F) were incubated with ER-derived 80S ribosomes (Panels B, D, F) or RNCs (Panels C, E). Ribosome-bound material was separated from unbound material by sucrose density gradient centrifugation. Samples were collected and analysed by Western blot with an anti-SRβ antibody (Panels A-E) or an anti prolactin antibody (Panel F). Panels are as follows: **A:** SRβΔTM in the absence of ribosomes (negative control); **B:** SRβΔTM plus 80S ribosomes; **C:** SRβΔTM plus RNCs; **D:** SRβ$_{C71D}$ΔTM plus 80S ribosomes; **E:** SRβ$_{C71D}$ΔTM plus RNCs; **F:** prolactin plus 80S ribosomes (negative control); **G:** ribosomal RNA from 80S ribosomes was analysed on a 11% polyacrylamide gel and stained with ethidium bromide; **H:** Radiolabelled nascent chains incorporated into RNCs were visualized by autoradiography. The order of the lanes from left to right represent the top to the bottom of the gradient.

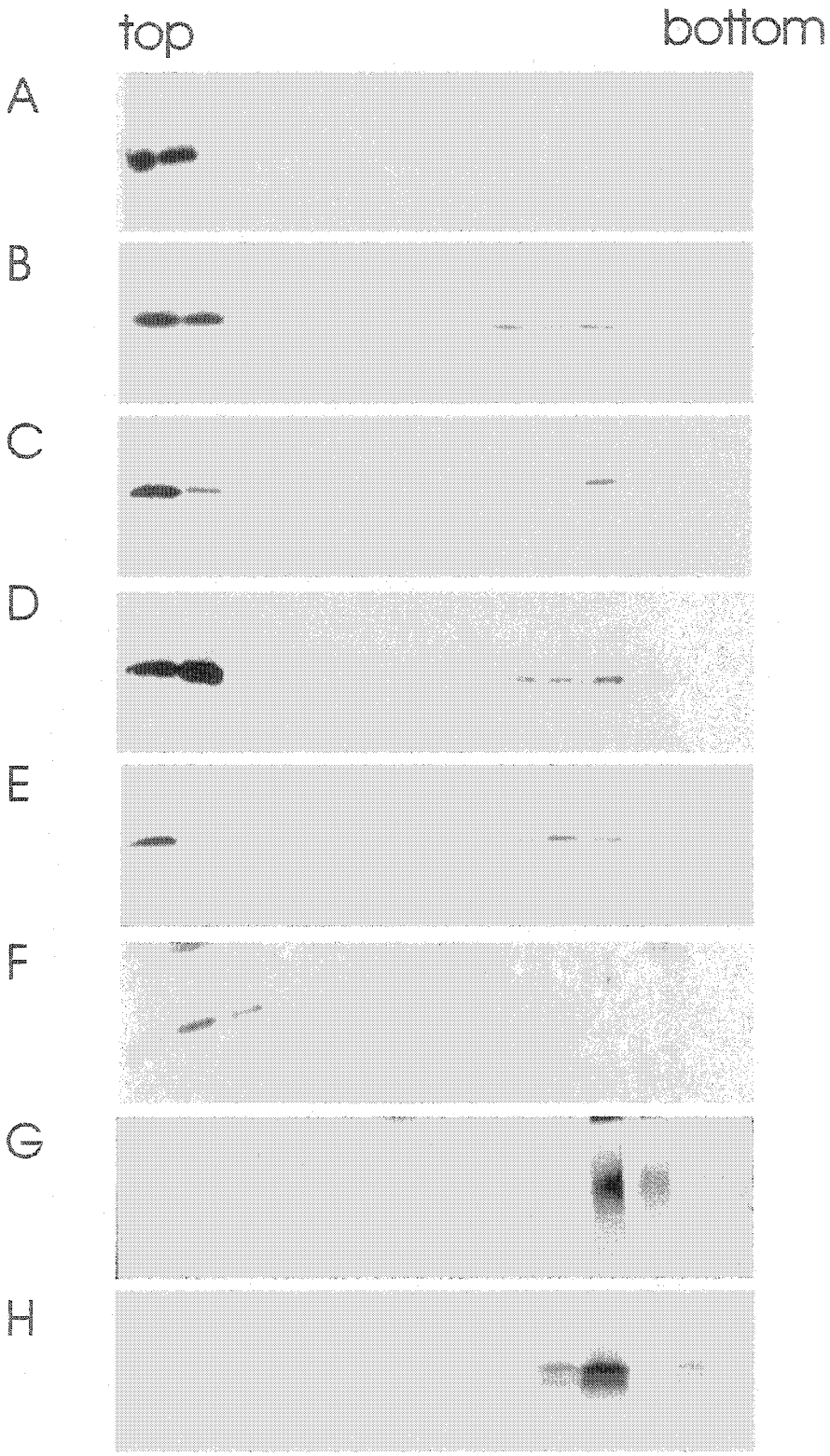
top
bottom
A
B
C
D
E
F
G
H

the ribosome-containing fractions. Although it is not possible to estimate the amount of SRβ that can initially form a complex with ribosomes, the fact that 22% of SRβ remained bound to ribosomes throughout a 16 hour centrifugation step provided evidence for a stable interaction between ribosomes and SRβ.

Since SRβ bound ribosomes in the absence of SRα, crosslinking experiments were performed to determine whether a crosslink similar to that reported previously for SRα-SRβ complexes (Fulga et al., 2001) between SRβ and ribosomal proteins. SRβΔTM and ribosomes were incubated in the presence of 20 μM *bis*-maleimidohexane (BMH), the same homobifunctional cysteine crosslinker used previously to detect a crosslink between SRβ and a 21 kDa ribosomal protein (Fulga et al., 2001) (Figure 3.19). In the absence of ribosomes, discrete crosslinking products representing crosslinks between SRβ molecules were apparent (lane 1). The addition of ribosomes diminished the inter-SRβ crosslinking products but no additional crosslinking products were observed (lane 3). Since Fulga et al. observed a crosslink in the presence of GDP but not in the presence of GTP SRβ was treated with EDTA in the presence of 20 mM GDP, and then Mg^{2+} was added to "lock" the bound nucleotide in place in an attempt to generate SRβ-GDP. No additional crosslinking products were apparent in the presence of GDP (lane 2). There are two possible interpretations of this data: 1. nucleotide exchange in the presence of EDTA was inefficient; since only 6% of SRβ was capable of exchanging bound GTP for γ-^{32}P-GTP, this likely also represents the maximum efficiency for exchange with GDP, although this was not formally tested. Also, the previously reported crosslink between SRβ and the ribosomal protein represented a minor proportion of the total SRβ in the reaction (Fulga et al., 2001). Therefore the combination of inefficient nucleotide exchange with a low degree of crosslinking could result in a crosslink product that is below the detection limit for Western blotting; 2. The nature of the SRβ-ribosome interaction differs from the SRα/SRβ-ribosome interaction in such a way as to negate the possibility of crosslinking with BMH.

3.4 Discussion

Although SRβ was first identified in 1986 (Tajima et al., 1986), the enzymatic properties of SRβ have remained relatively unexplored. The only kinetic parameters reported for SRβ are the binding-specificity for guanine nucleotides and values for GTP-binding affinity of dissociation (K_d) constants, ranging from 20 nM to 1 μM (Young et al., 1995; Bacher et al., 1999). Previous studies used SRα- or SRX2-bound SRβ, and it is not clear whether or not heterodimerization influences the characteristics of SRβ. To examine the properties of the isolated SRβ GTPase, I expressed SRβΔTM and $SR\beta_{C71D}\Delta TM$ in *E. coli*. The transmembrane domain was deleted in both SRβ molecules to increase both the solubility and the yield in the expression system. The deleted region is not believed to contribute to the activity of SRβ, since SRβΔTM rescued translocation function *in vivo* in yeast containing two disrupted SRβ alleles (Ogg et al., 1998).

Recombinant SRβ bound exogenous GTP with a K_d of approximately 2 μM, a

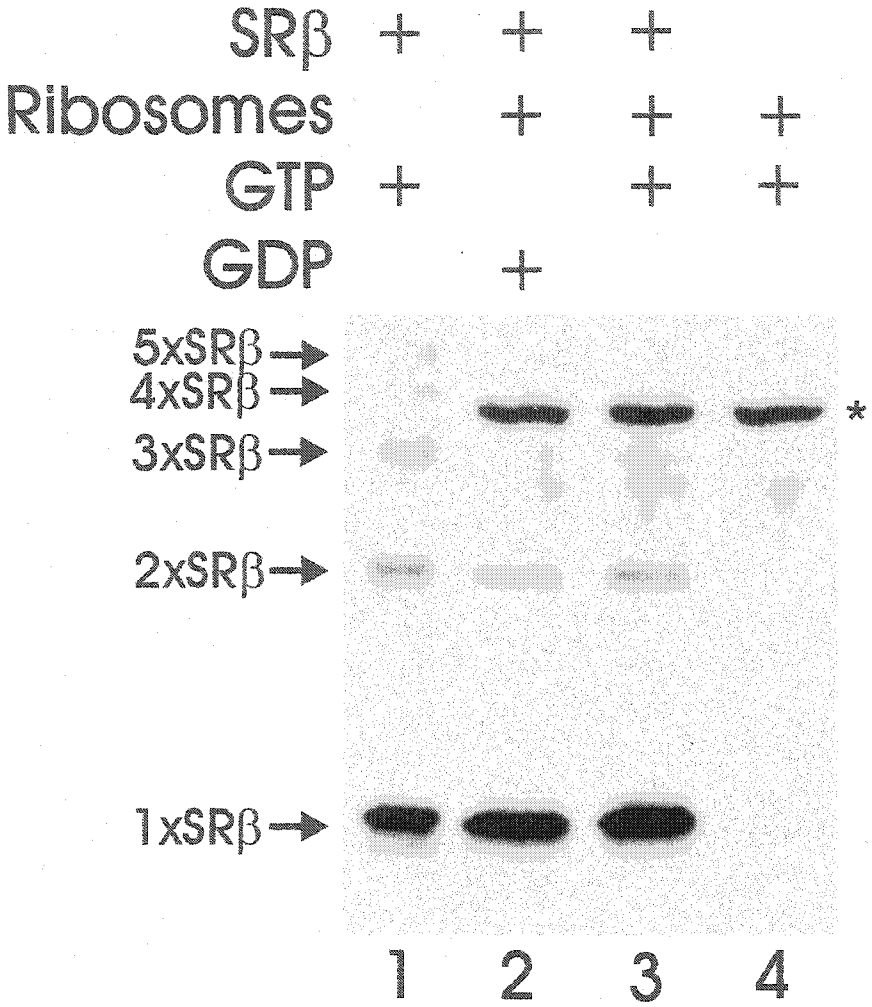

Figure 3.19: Crosslinking of SRβΔTM in the presence of 80S ribosomes. 15 pmol SRβΔTM (lane 1) was incubated with an equal molar concentration of 80S ribosomes (lanes 2 and 3) in the presence of the homobifunctional cysteine crosslinker *bis*-maleimidohexane. Lane 2 contains SRβ "loaded" with GDP, by treatment with EDTA/Mg 2+ in the presence of 20 mM GDP. Reactions were analysed by SDS-PAGE followed by immunoblotting with an anti-SRβ antibody. Discrete crosslinks between SRβ molecules are indicated, and a cross-reacting ribosomal protein is denoted by an asterisk.

value similar to that obtained for detergent solubilized SR (Miller et al., 1995), but much higher than the K_d obtained for SRα-SRβ dimers reconstituted into lipid vesicles (Bacher et al., 1999). It must be noted that for all of these reports the K_d measurement is relevant only to SRβ that was able to bind solution GTP during the assay. In our experiments less than 10% of the SRβΔTM added to the reaction bound to added GTP (Figure 3.11). The affinity for GTP of the larger population (~70%) of SRβ that purified bound to GTP is unknown but it is presumably much higher than 2 μM since there was no appreciable exchange with solution GTP during an eight hour incubation (Figure 3.11). Furthermore, bound GTP was removed during purification of the protein extremely slowly or not at all, despite the absence of solution GTP in the purification buffers. The maximum amount of exchange measured by the filter binding assay (6%) was the same whether SRβ was incubated for long time periods in excess GTP or whether EDTA was added to accelerate nucleotide exchange. For other GTPases time based exchange does not necessarily result in quantitative exchange (Kahn and Gilman, 1986). However, treatment with EDTA/Mg^{2+} resulted in quantitative exchange of bound nucleotide with exogenous nucleotide (Koyama and Kikuchi, 2001; Wang and Colicelli, 2001).

Previous attempts to measure the K_d of SRβ (Miller et al., 1995) did not account for the possibility that much of the SRβ used in the assay may not be able to accept exogenous GTP. It is likely that these early K_d measurements reflected the affinity of the same small population of SRβ that can bind to (or exchange bound nucleotide with) exogenous GTP, and did not reflect the affinity of the majority of SRβ in the assay. It is perhaps significant that 2-3% of SRβ purified from *E. coli* was bound to GDP. My estimates of the fraction of SRβ that bound GTP, 3-6%, are similar enough to 2-3% that I speculate that the GDP bound form of SRβ is what is responsible for the binding activity that I measured. Bacher et al., by incorporating purified SR into proteoliposomes, measured a K_d in close agreement with other Ras-type GTPases (Bacher et al., 1999). It is possible that lipid binding by SRβ led to a conformational change that permitted exchange of tightly bound GTP with exogenous GTP.

The cysteine mutation introduced into SRβ occurs at a position within the G1 GTPase consensus sequence that is highly conserved among family members of Ras-type GTPases (Tables 3.1 and 3.2, mutation site shown in bold). Most Ras homologues contain a glycine at this position that is required for GTPase activity. Mutation of this amino acid in Ras from glycine to any other amino acid except proline leads to cellular transformation of rat fibroblasts, consistent with the loss of GTPase activity in these mutants (Seeburg et al., 1984). Mutation of this residue to Asp or Val locked Ras into the GTP-bound form *in vivo* and induced maturation of *Xenopus* oocytes (Trahey and McCormick, 1987). Likewise, mutation of EF-Tu at this position abolished GTPase activity *in vitro* (Jacquet and Parmeggiani, 1988). Structural analysis of Ras in a complex with Ras-GAP revealed that glycine is the only residue that can be accomodated at this position to prevent steric hindrance of both a key catalytic residue contributed by the GAP, and a glutamine that coordinates the attacking water molecule. Thus, structural data

explains why mutants of Ras at this position demonstrate no GTPase activity (Scheffzek et al., 1997).

Arf-1 and other Arf-like GTPases contain an aspartic acid at this position. Mutants at this position in *S. cerevisiae* Arf-1 lose the ability to bind GTP, and display a recessive loss of function phenotype (Kahn et al., 1995). The crystal structure of Arf6 bound to GTPγS revealed that this aspartic acid hydrogen bonds to residues within the switch 2 region and the α3 helix, and may explain why mutations at this site demonstrate a decreased affinity for GTP (Pasqualato et al., 2001). In contrast to Arf-like GTPases, yeast SRβ contains a glutamine in this position that protrudes into the active site, crowds the catalytic water molecule and hydrogen bonds with the γ-phosphate of GTP (Schwartz and Blobel, 2003) (Figure 2.18 and Figure 3.20.A). Although mammalian SRβ differs from yeast SRβ by containing a cysteine at this position, molecular modelling using the yeast structure as a starting point suggests that the cysteine may also be oriented so as to crowd the active site, which would explain the lack of intrinsic GTPase activity observed with this protein. It is tempting to blame the aspartic acid for the observation that Arf GTPases are also catalytically inert *in vitro* (Kahn and Gilman, 1986; Weiss et al., 1989), but analysis of the available structural data revealed that the aspartic acid does not protrude into the active site. Rather, the side chain is oriented away from the bound nucleotide in both Arf and Sar crystal structures (Figure 2.18). Yeast SRβ appears to be unique in the positioning of this side chain into the active site. The mechanism by which this steric crowding is relieved to allow GTP hydrolysis to proceed may reveal a GAP mechanism that has not been observed for other GTPase-GAP pairs.

The identity of the amino acid at this position in SRβ is somewhat less conserved than other GTPases, suggesting that the identity of the side chain at this position may be less important than its ability to crowd the active site (Table 3.2). To test this hypothesis I constructed $SR\beta_{C71G}\Delta TM$, which replaced a bulky side chain with a hydrogen atom. $SR\beta_{C71G}\Delta TM$ immunoprecipitated SRα to the same extent as SRβΔTM following depletion of nucleotides (Figure 3.1), suggesting that mutation of this amino acid did not decrease the affinity of SRβ for GTP. The properties of the SRβ GTPase in the absence of a bulky side chain at this position could not be tested because His_6-tagged $SR\beta_{C71G}\Delta TM$ expressed poorly in *E. coli* and could not be purified with Ni-NTA agarose.

SRβ exhibits greater sequence homology to Arf GTPases than it does to Ras (Miller et al., 1995). In an attempt to convert SRβ into an Arf-type GTPase the Cys was mutated to Asp and the properties of the mutant were compared to those of the wild type GTPase. However, modelling of an aspartic acid at this position into the yeast SRβ structure revealed that the aspartic acid, like the glutamine in yeast, may orient into the active site (Figure 3.20). $SR\beta_{C71D}\Delta TM$ appeared to bind GTP with faster kinetics than SRβΔTM, suggesting that the conformation of the protein had changed such that GTP had easier access to the binding pocket. The glutamine at this position in yeast SRβ contributes to the binding pocket by hydrogen bonding the γ-phosphate of GTP (Schwartz

Figure 3.20: Cysteine and aspartic acid modelled into the yeast SRβ active site. All models were created by substitution of glutamine with cysteine or aspartic acid at the appropriate position by the mutation function in Swiss PDB viewer (http://ca.expasy.org/spdbv/). Distance approximations were also calculated using this program. GTP is shown in red, the catalytic histidine is shown in green, α-carbon backbone is shown in grey, the coordinating magnesium is shown as a blue sphere representing the van der Waals radius, the catalytic water is shown as a red sphere representing the van der Waals radius and the mutated amino acid is displayed in blue. **A:** The 'wild-type' structure of yeast SRβ. The glutamine is positioned 2.6 Å from the water and 3.22 Å from the γ-phosphate. **B:** Cysteine modelled into the SRβ active site. The cysteine is positioned 2.66 Å from the water and 3.46 Å from the γ-phosphate. **C:** Aspartic acid modelled into the SRβ active site. The Asp is positioned 2.6 Å from the water and 2.48 Å from the γ-phosphate. **D:** The active site of Arf-1 bound to GTPγS is shown for comparison.

A

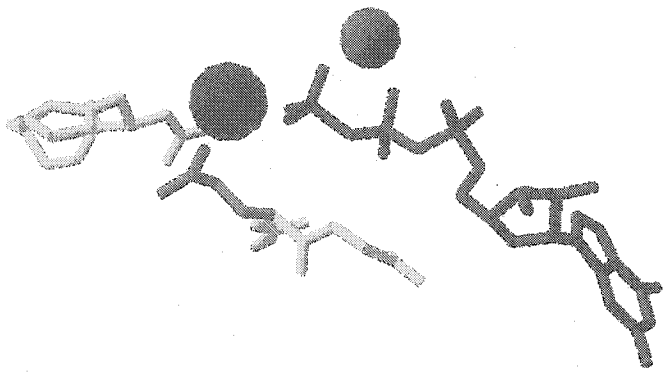

B

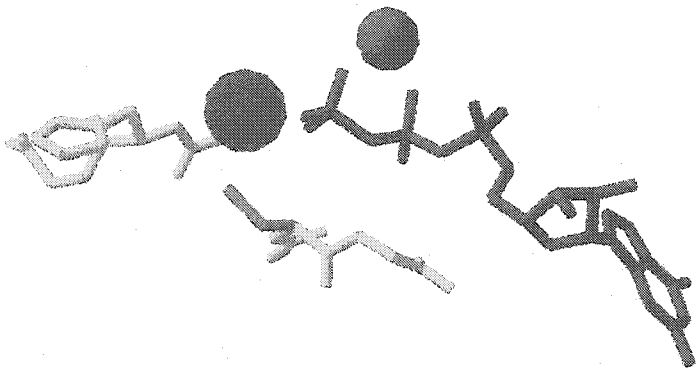

C

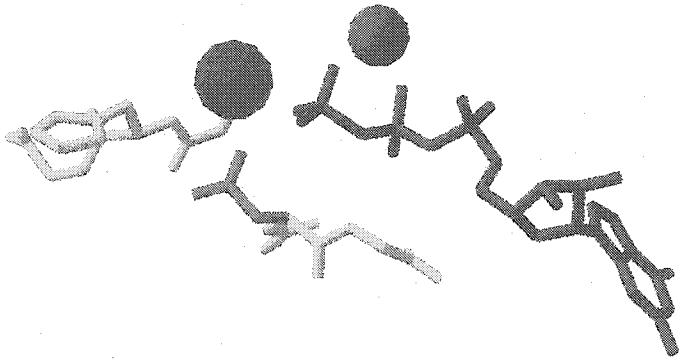

D

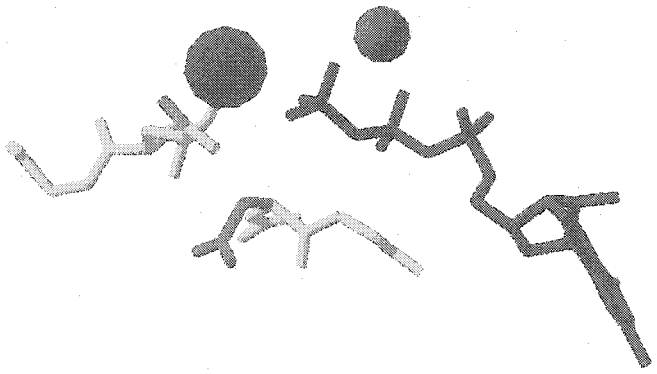

and Blobel, 2003). This residue may contribute to the stability of the protein since at 24°C the mutant protein exhibits a gradual loss of nucleotide binding. (Figures 3.9 and 3.11).

I was unable to distinguish a difference in nucleotide affinity between SRβΔTM and $SR\beta_{C71D}\Delta TM$ for the small fraction of protein that bound exogenous nucleotide. The C71D mutation also does not appear to disrupt binding of SRβΔTM to SRα since coimmunoprecipitation of SRα with $SR\beta_{C71D}\Delta TM$ was identical to coimmunoprecipitation of SRα with SRβΔTM (Figure 3.1). I was unable to detect GTPase activity arising from $SR\beta_{C71D}\Delta TM$ (Figure 3.16) but since I could detect no GTPase activity from wild-type SRβΔTM the role of the cysteine in catalysis remains uncertain. Both cysteine and aspartic acid could be modelled into the active site of the yeast structure, suggesting they may maintain the enzyme in a catalytically inert conformation (Figure 3.20).

The use of fluorescence to study GTP binding to SRβΔTM revealed what appears to be a two-step process (Figure 3.9). The first step is rapid and was detected by monitoring energy transfer between Tyr (and Phe) residues within SRβ and a mant fluorophore incorporated into GTP. The second step is slower and is detected by monitoring energy transfer between a Trp residue located at the carboxyl-terminus of SRβ and the mant fluorophore (Figure 3.21). This second step occurred on the same time scale as GTP binding monitored by a nitrocellulose filter binding assay, a technique that captures tightly bound protein-nucleotide complexes (Figure 3.11).

Taken together these results suggest that the first step involves GTP bound to SRβ in a loose conformation. The filter binding assay did not detect these complexes as loosely-bound GTP was washed away. These complexes are detected by energy transfer between SRβ and mant-GTP. The time scale of the loose-binding interaction is similar to GTP binding by other Ras-type GTPases assayed in their GDP-bound state (Kahn and Gilman, 1986; Barlowe et al., 1993). The second step represents a tight-binding conformation, detected by both filter binding and energy transfer between Trp and mant-GTP. My data suggest that in wild-type SRβΔTM the carboxyl terminus of SRβ reorients such that energy transfer occurs between Trp and mant. I propose that this conformational change stabilizes the tight-binding GTP-SRβΔTM complex. Comparison of the data in Figures 3.11.B and 3.11.C suggests that the increase in RET between the Trp and mant-GTP occurs subsequent to binding. The simplest explanation for the increase in RET between Trp and mant is that SRβΔTM undergoes a conformational change that moves the Trp closer to the GTP binding site. Consistent with a role for the carboxyl-terminus of SRβ in stabilizing the structure of the protein the carboxyl-terminal six amino acids (including the one Trp in SRβ) contributed to a protease-resistant core fragment of SRβ (Figure 2.3).

$SR\beta_{C71D}\Delta TM$ exhibited tight binding of GTP but did not undergo the conformational change that stabilizes the complex. Because the rate of GTP binding was the same whether it was measured by RET or filter binding this mutant bypassed the

Figure 3.21: Position of the tryptophan within SRβ relative to mant-GTP. Two views of SRβ are shown. In both images the α-carbon backbone is displayed in green with the exception of the carboxyl-terminal α-helix, which is shown in black. The top image orients the carboxyl-terminal helix into the page, while the bottom image orients the helix into the page at an angle ~45°. The position of the histidine side chain is shown in red, extending from the carboxyl-terminal helix. GTP is shown as a space-filling model. Either of the ribose oxygens, shown in blue, are the attachment points for the mant fluorophore, as indicated. GTP binds SRβ such that the mant group is oriented into the solvent. The amino (N) and carboxyl (C) termini of SRβ are indicated.

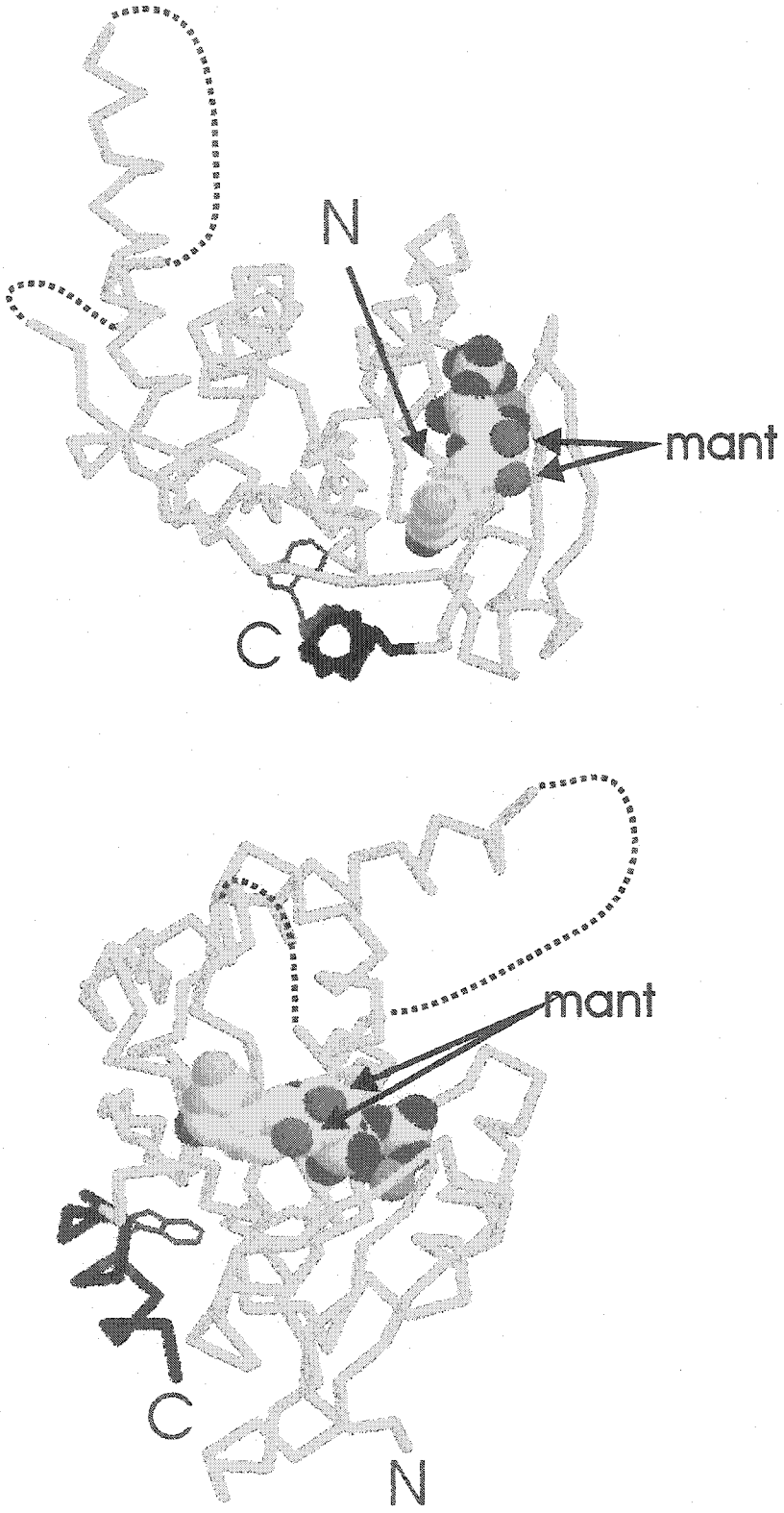
N
mant
C
mant
C
N

loose-binding conformation observed with the wild type GTPase. It may be that access to the GTP binding site is altered in $SR\beta_{C71D}\Delta TM$ in such a way that cannot be predicted by modelling Asp into the GTP binding site (Figure 3.20). The carboxyl-terminus of the yeast SRβ homologue forms an α-helix that is almost certainly conserved in mammalian SRβ since it appears in all crystal structures of related GTPases (Pai et al., 1989; Goldberg, 1998; Huang et al., 2001; Schwartz and Blobel, 2003). Since the tight-binding conformation was detected in the wild type GTPase by an increase in RET between mant-GTP and a carboxyl-terminal Trp residue, it is possible that the presence of a His_6 tag on the carboxyl-terminus of $SR\beta_{C71D}\Delta TM$ could influence the behaviour of the carboxyl-terminus and provide a source of error within the experiments. However, this is unlikely for two reasons. First, histidine favours an α-helical conformation (Levitt, 1978) that would extend the carboxyl-terminal α-helix by approximately 1.7 turns. Second, the length of this α-helix is variable among Arf-type GTPases, ranging from 3 turns in SRβ to 4 turns in Arf-1 (compare black helices in Figure 2.16.B and 3.22.A). Due to the variability in helix length and the likelihood that the addition of histidine residues would not disrupt the structure of the carboxyl-terminus it is unlikely that a His_6 tag in this position affects the biology of $SR\beta_{C71D}\Delta TM$.

The bulk (~70%) of both SRβΔTM and $SR\beta_{C71D}\Delta TM$ are bound to GTP. In contrast, other Ras-type GTPases have all been purified in the GDP-bound state (Poe et al., 1985; Weiss et al., 1989; Barlowe et al., 1993). Even ARF-1 purified GDP-bound, yet it exhibited no measurable GTPase activity *in vitro* (Kahn and Gilman, 1986; Weiss et al., 1989). Ran purified bound to both GTP and GDP, reflecting the equilibrium between the two populations within the cell (Floer and Blobel, 1996). Thus, SRβ is the only Ras-type GTPase confirmed to purify predominantly in the GTP-bound state.

The finding that SRβ binds GTP by default while other Ras-type GTPases bind GDP by default makes some biological sense. GTP-bound SRβ bound to SRα more tightly than when SRβ was loaded with other nucleotides (Figure 2.15; Schwartz and Blobel, 2003). Since SRβ is required to anchor SRα to the ER membrane, and SRα was found exclusively in the membrane fraction (Ogg et al., 1998), unlike other Ras-like GTPases it makes sense for SRβ to favour the GTP-bound state.

It was reported that ribosomes both stimulated the SRβ GTPase and decreased the affinity of SRβ for nucleotides (Bacher et al., 1999). Furthermore, an interaction between SRβ and a 21 kDa ribosomal protein was detected, which may provide the basis for the effect of the ribosome on nucleotide binding by SRβ (Fulga et al., 2001). However, in the absence of SRα, I was unable to detect an influence of ribosomes or ribosomal subunits on the SRβ GTPase. Because SRβ bound to ribosomes in the absence of SRα these results suggest that SRα changes the quality of the interaction between the ribosome and SRβ, either by regulating the structure of SRβ to facilitate GTP hydrolysis or by directly contributing residues that are required for GTP hydrolysis. This suggests an additional role for SRα in translocation as an 'effector' of SRβ. Indeed, SRX was shown to bind the

Figure 3.22: X-ray structures of Arf1 and Sar1. Backbone carbon traces of Arf1 (A) and Sar1 (B) in the GTP (GMPPNP)-bound and GDP-bound states. Two orientations are shown to illustrate the position of the carboxyl-terminal alpha helix (coloured black) relative to the rest of the structure. Bound nucleotide is shown as a space filling model. The tail-like structure at the carboxyl-terminus of Arf1 is a result of additional amino acids present in crystalized Arf1-GMPPNP, and is not evidence of carboxyl-terminal remodelling. PDB accession numbers for Arf1-GDP and Sar1-GDP are 1HUR and 1F6B, respectively.

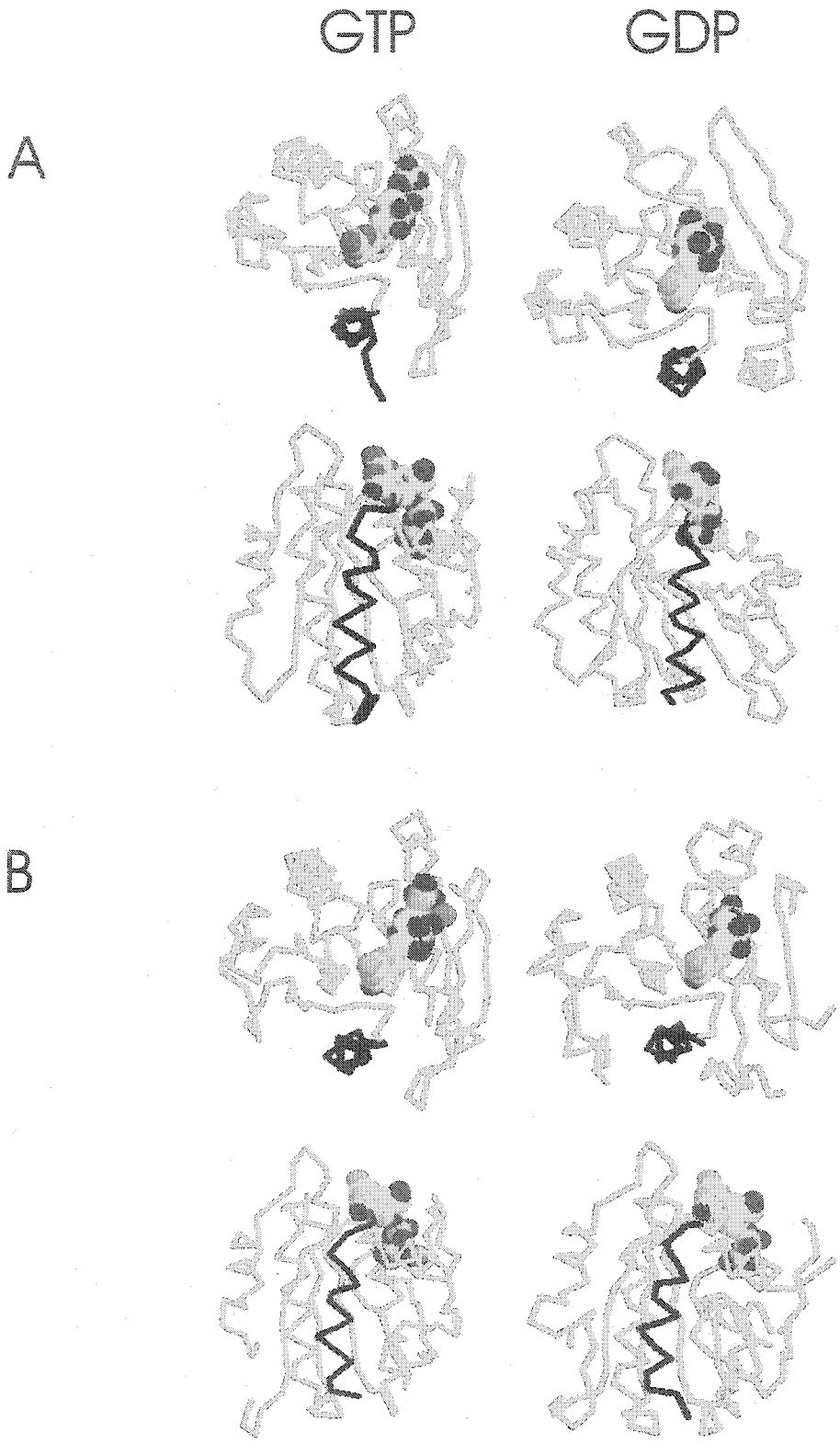
GTP
GDP
A
B

switch 1 region of SRβ, located between the G1 and G2 GTPase consensus sequences (Schwartz and Blobel, 2003)(Figures 2.16 and 2.17). The switch 1 region is the usual binding location for GTPase effector proteins (Vetter and Wittinghofer, 2001; Herrmann, 2003).

In a previous study an increase in GTPase activity of SRβ during incubation of SRα-SRβ complexes with ribosomes was reported, but not quantified (Bacher et al., 1999). The reasons for this may be twofold: first, although the authors claimed to control for residual GTPase activity arising from ribosomes it cannot be ruled out that the observed GTP hydrolysis did not arise from ribosomes. Second, my analysis of the published data suggests that the GTP hydrolysis rate that can be attributed to SRβ is consistent with a one-to-one, non-catalytic interaction between ribosomes and SRβ (Bacher et al., 1999; see Appendix 1). The notion that the ribosome and SRβ do not cycle catalytically was supported by the discovery that the ribosome-SRβ interaction is stable enough to be maintained throughout centrifugation through a sucrose gradient for 16 hours (Figure 3.18). The experiments conducted by Bacher et al. employ purified SR reconstituted into lipid vesicles. These experiments must be extended to include proteoliposomes containing reconstituted Sec61 complex as well as SR to establish whether the Sec61 complex is sufficient to trigger multiple turnover events between SRβ and ribosomes.

Data presented in this thesis has demonstrated that SRα forms a tight physical association with SRβ, and this interaction is nucleotide-dependent and requires the intact GTPase domain of SRβ. These characteristics are consistent with SRα assuming the role of a SRβ effector molecule, a prediction consistent with the observation that yeast SRX binds to SRβ mainly through the switch I region (Schwartz and Blobel, 2003). My finding that the ribosome did not stimulate the GTPase activity of isolated SRβ, together with previous data demonstrating GTPase activity of SRβ only in the context of a SRα-SRβ-ribosome complex (Bacher et al., 1999), leads me to speculate that SRα may regulate the GTPase activity of SRβ. According to the crystal structure of the SRX-SRβ complex it is unlikely that SRα directly influences the mechanism of GTP hydrolysis by contributing residues to the active site(see Figure 2.16). A more likely possibility is that SRα promotes structural changes within SRβ to permit a functional interaction with the GAP, similar to the Ran-RanBP1 interaction (Seewald et al., 2002), or influences the orientation of key residues in the active site to facilitate GTP hydrolysis. The glutamine located proximal to the γ-phosphate of bound GTP crowds the catalytic water molecule, but this glutamine also hydrogen bonds to a serine within SRX (Schwartz and Blobel, 2003). Therefore it is possible that binding to SRX orients this glutamine residue into the active site. A detailed structural comparison between the published SRX-SRβ structure and SRβ alone, and kinetics experiments performed in parallel using both SRX-SRβ and SRβ will be necessary to assess the extent to which binding of SRα regulates SRβ function.

4. DISCUSSION

The process of SRP-mediated protein translocation is evolutionarily conserved. The key protein components (SRP, SRP receptor, and the translocon) are all functionally conserved and a growing body of work suggests that the GTPase-regulated mechanism governing the targeting and nascent-chain transfer steps is also conserved. One striking difference between the SRP pathways of *E. coli* and eukaryotes is the inclusion of a third GTPase, SRβ, in the eukaryotic system. Although the role of SRβ in anchoring SRα to the ER membrane has been established for some time, the regulatory event controlled by the SRβ GTPase domain has remained mysterious. The recent discoveries that the ribosome can stimulate the GTPase activity of SRβ (Bacher et al., 1999) and that SRβ interacts directly with a ribosomal protein (Fulga et al., 2001) provide evidence that the regulatory event controlled by SRβ occurs following the initial targeting step, and is catalyzed by the ribosome itself. Data presented in this thesis suggest that the function of the SRβ GTPase is to dynamically control the interaction between SRα and the membrane; a notion that is further substantiated by gel filtration experiments employing yeast SRX and SRβ, and by the nature of the interface between SRX and SRβ deduced from the crystal data (Schwartz and Blobel, 2003). Furthermore SRβ displays properties that are not shared with other members of the Ras GTPase superfamily. Taken together these data allow the proposal of a new model of protein translocation in which SRβ plays a larger role than previously appreciated.

4.1 Functional consequences of SRα-SRβ dimer regulation

The crystal structure of yeast SRX/SRβ illustrates the binding face between these proteins (Figure 2.16) (Schwartz and Blobel, 2003). SRX binds to SRβ primarily through the switch 1 region of SRβ, consistent with GTPase effector proteins (Herrmann, 2003). GTP-binding by other GTPases causes significant reorganization of the switch I region, allowing for recognition by the effector. Hydrolysis of GTP to GDP reorganizes the switch I region to render it incompatible with effector binding (Herrmann, 2003 see also Figure 3.22). Thus, by analogy with other GTPase-effector pairs, it is predicted that the interaction of SRX with SRβ is favoured when SRβ is bound to GTP, and is disrupted when SRβ is bound to GDP. Biochemical data is consistent with this notion (Figure 2.15 and (Schwartz and Blobel, 2003)), but the effect is more striking *in vitro* when SRβ is forced to adopt the empty state (Figures 2.14 and 2.15).

I have predicted that release of nucleotide from SRβ dissociates the heterodimeric SR on the endoplasmic reticulum membrane, thereby regulating the interaction between SRα and the ER membrane (Legate et al., 2000; Legate and Andrews, 2001). This implies that there is a dynamic interaction between the SR and the membrane. There is a precedent for regulated binding of membranes by SR. In *E. coli*, SR is comprised of a single protein, FtsY, that is found in both the cytoplasm and on the plasma membrane in approximately equal amounts (Luirink et al., 1994). Membrane binding by FtsY is due in part to a direct interaction with phosphatidylethanolamine (PE) (Millman et al., 2001).

However, there is also evidence that FtsY membrane binding is regulated. First, since lipids are in a large molar excess over FtsY, non-regulated binding to lipids is not compatible with the observed distribution of FtsY between membrane bound and soluble pools. Second, a fraction of FtsY was specifically cleaved upon binding to the cell membrane, thereby limiting the total amount of FtsY bound to the membrane (Millman and Andrews, 1999). Finally, evidence was presented that suggested the existence of a membrane bound FtsY receptor (Millman et al., 2001). By using a strain of *E. coli* deficient in PE biosynthesis, it was discovered that FtsY could bind vesicles derived from these cells, but binding was lost if the vesicles were first treated with protease to digest membrane-bound proteins. In contrast, binding of FtsY to vesicles from wild type *E.coli* (which contain PE) was not reduced significantly by pre-treatment of the vesicles with protease, demonstrating that either PE or a membrane-bound protein was sufficient to bind FtsY to vesicles, but loss of both components could no longer support FtsY binding. The identity of the putative membrane-bound receptor for FtsY has not yet been discovered.

Mammalian ER membranes rendered translocation defective by proteolysis of Sec61α accumulated a post-targeting intermediate comprised of the ribosome-nascent chain (RNC) and SR (Song et al., 2000), demonstrating that SR provides a targeting site for RNCs on the ER. The next required step is to transfer the RNC to the Sec61 complex. Taken together with the results presented here, a speculative yet plausible role for regulated dissociation of SR would be to release the ribosome-nascent chain-SRP-SRα complex from SRβ, allowing it to be transferred to the Sec61 complex. Once correct docking of the ribosome to the translocon has occurred, the signal peptide would be released into the translocon, triggering hydrolysis of GTP by SRP54 and SRα. Previously, this hydrolysis step was proposed to release SRP from SR for another round of targeting (Connolly and Gilmore, 1989). According to my model, presented in Figure 4.2, this step releases SRP from SRα, allowing SRP to return to the cytoplasm and SRα to rebind to SRβ.

4.2 Comparison of existing models for GTPase regulation of translocation, and the proposal of a new model

Two recent published models for the GTPase-controlled steps of protein translocation at the ER membrane have been presented (Figure 4.1). The model in Figure 4.1.A was proposed by Dobberstein's lab, based on data demonstrating a crosslink between SRβ and a ribosomal protein and their contention that nascent chain delivery to the translocon is regulated by the GTP bound form of SRβ (Fulga et al., 2001). The model in Figure 4.1.B was proposed by Blobel's lab and is based on their interpretation of the crystal structure of yeast SRX-SRβ, their own biochemical data confirming my discovery that SRα-SRβ dimer formation is favoured by the GTP-bound form of SRβ, and that dimer formation is significantly less efficient when SRβ is bound to GDP (Schwartz and Blobel, 2003). This model also incorporates recent data suggesting that the β subunit of the Sec61 complex may function as the SRβ-GRF (Helmers et al., 2003). My

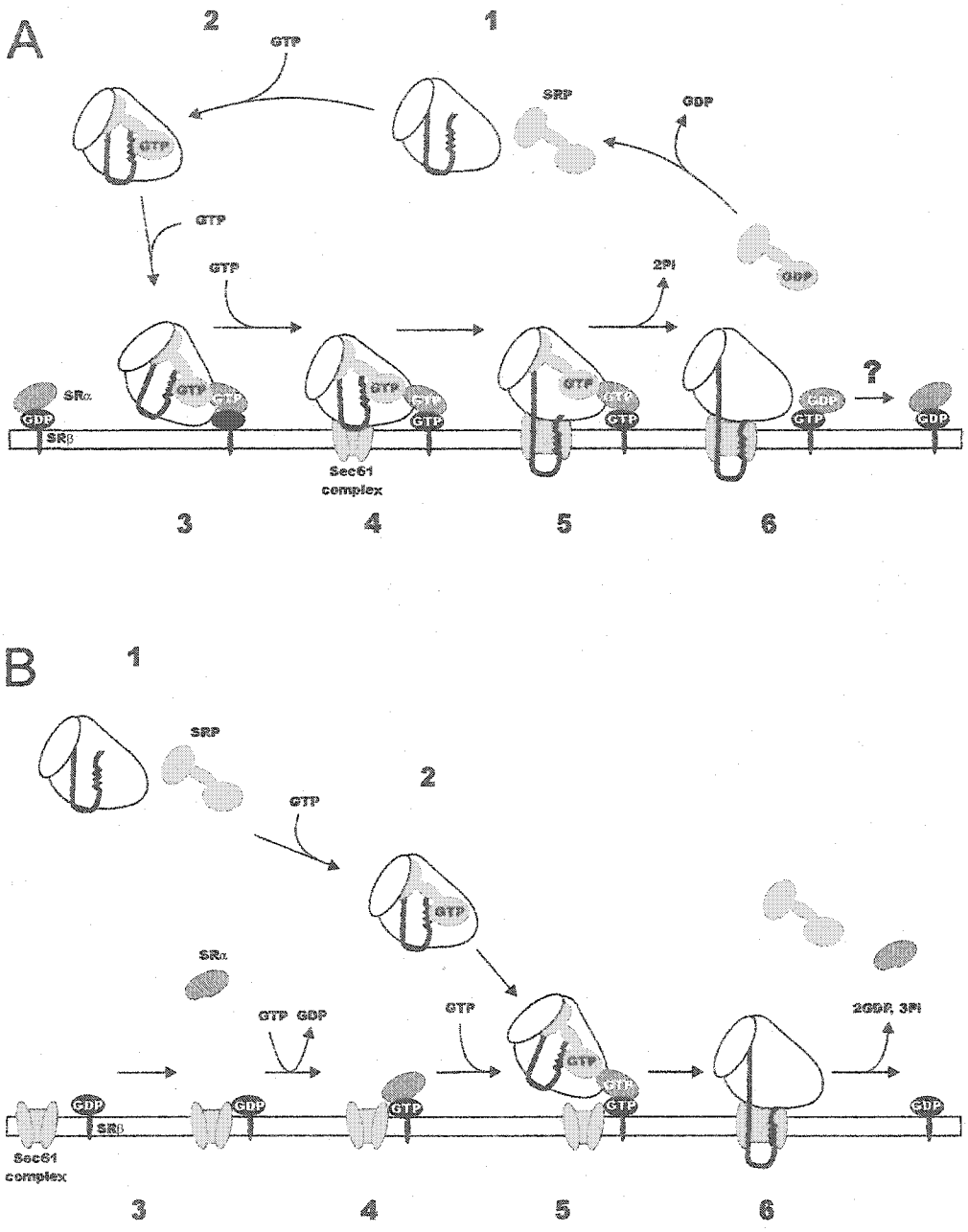

Figure 4.1 Existing models for cotranslational targeting to the ER membrane. A: The model proposed by B. Dobberstein's lab {Fulga 2001}, and B: the model proposed by G. Blobel's lab. {helmers blobel}. Individual components are not drawn to scale. See the text for details.

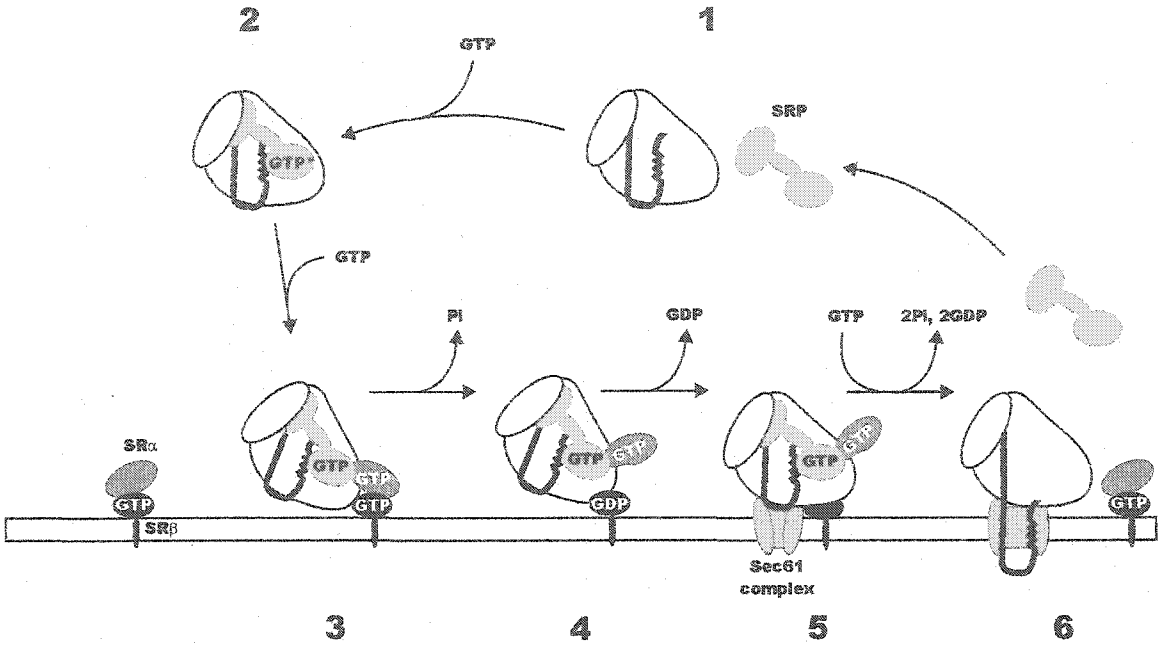

Figure 4.2 A new model for cotranslational targeting to the ER membrane. This model takes into account the results presented in this thesis as well as the data in the published literature. Individual components are not drawn to scale. See the text for details.

data can be reconciled with previously published data in a new model, which differs from previous models primarily by assigning a role for SRβ as the membrane-bound contribution to the post-targeting intermediate (Figure 4.2).

The initial steps in each of these models are the same. Translation of a nascent secretory protein begins in the cytoplasm (step 1). The nascent chain is scanned by SRP and upon encountering an appropriate signal sequence, SRP binds the signal sequence to form the ribosome-nascent chain-SRP ternary complex (step 2) (Ogg and Walter, 1995). SRP 9/14 then elicit a transient pause in translation (Siegel and Walter, 1986; Thomas et al., 1997). The affinity between SRP54 and GTP is increased and SRP54, previously favouring the empty state, now favours the GTP-bound state (Bacher et al., 1996). Therefore, step two of Figures 4.1.A and 4.1.B shows SRP bound to GTP. However, subsequent study has shown that while SRP was capable of binding GTP at this stage, bound GTP remained exchangeable with free GTP until SRP bound to SRα (Rapiejko and Gilmore, 1997). The loose and reversible GTP-bound mode of SRP54 is distinguished with an asterisk in Figure 4.2. In all models the RNC-SRP complex is then targeted to the ER membrane via an interaction between SRP54 and SRα (step 3 in Figure 4.1.A and Figure 4.2, step 5 in Figure 4.1.B). The binding of SRP54 to SRα increases the affinity of both molecules for GTP (Bacher et al., 1996). Bound GTP does not exchange with solution GTP at this stage; therefore both SRP54 and SRα have adopted a GTP-bound, 'active' conformation (Rapiejko and Gilmore, 1997). GTP-binding by both molecules markedly increases their affinity for each other, therefore rendering the targeting step irreversible (Connolly et al., 1991).

The first point of divergence within these models is the depiction of the resting state of SR. The model in Figure 4.1.A portrays SR comprised of empty SRα and GDP-bound SRβ. This configuration is unlikely for two reasons. First, recent data demonstrated that SRX-SRβ complexes purified with SRβ in the GTP-bound state (Schwartz and Blobel, 2003). Secondly, the recent discovery that SRα binds to SRβ through the effector binding region of SRβ suggests that the SRα-SRβ interaction would be governed by the same rules as for other GTPase-effector complexes; that is, effector molecules bind to GTP-bound GTPases, and not to GDP-bound GTPases (Bourne et al., 1990; Schwartz and Blobel, 2003).

The model in Figure 4.1.B also shows SRβ bound initially to GDP. In contrast to the model in Figure 4.1.A, SRβ is not bound to SRα at this stage. Following a guanine nucleotide exchange step that is predicted to be catalysed by Sec61β (Helmers et al., 2003) (step 4) cytosolic SRα binds to GTP-bound SRβ on the ER membrane (step 4). This configuration is unlikely for two reasons. First, I have demonstrated that SRβ purified bound to GTP in the absence of SRα (Figure 3.7). Secondly, although the authors have drawn a parallel between SRα and the bacterial homologue FtsY, which is found both in the cytoplasm and bound to the membrane (Luirink et al., 1994), subcellular fractionation experiments in yeast detected SRα exclusively in the membrane-bound

fraction (Ogg et al., 1998). Therefore, the possibility that eukaryotic SRα spends any significant time in the cytoplasm is not likely.

The model in Figure 4.2 reflects the observations that 1. SRβ purifies bound to GTP when it is in a complex with SRX (Schwartz and Blobel, 2003), and 2. fractionation experiments place SRα on the ER membrane unless membrane binding of SRβ is also disrupted (Ogg et al., 1998). Based on these data, the most likely configuration for resting SR consists of the assembled SR dimer with SRα in the empty state and SRβ in the GTP-bound state.

Although all of the models target the RNC to the membrane via an interaction between SRP54 and SRα, the involvement of SRβ in the steps which follow differs significantly. The model in Figure 4.1.B does not explore the role of SRβ beyond a simple regulator of the interaction between SRα and the membrane. However, recent data suggests that the contribution of SRβ extends beyond a simple regulator of SR dynamics.

The model in Figure 4.1.A displays the ribosome in direct contact with SRβ (step 3), a configuration supported by crosslinking data demonstrating the physical proximity between a 21 kDa ribsomal protein and SRβ in the context of the SR dimer (Fulga et al., 2001), and my own data illustrating the co-fractionation of SRβ and ribosomes on sucrose gradients (Figure 3.20). Furthermore, SRβ is shown in its empty state, consistent with the decrease in affinity between SRβ and nucleotides observed in the presence of ribosomes (Bacher et al., 1999). This observation led the authors to conclude that the ribosome behaves as a guanine nucleotide release factor (GRF) for SRβ, though it must be noted that since the affinity for GDP was not reported it is not clear whether SRβ remains bound to GDP upon binding the ribosome. My own data, and data from others (Helmers et al., 2003) do not support the contention that the ribosome functions as a SRβ-GRF; rather, Sec61β appears to fulfil this role (Helmers et al., 2003). Although nucleotide release from SRβ was inefficient in the presence of Sec61β, the decrease in SRβ-nucleotide affinity detected in the presence of ribosomes may serve to increase the efficiency of Sec61β-mediated nucleotide release from SRβ. The model presented in Figure 4.1.A does not account for the decreased affinity between SRβ and SRα when SRβ is in the empty state (Figures 2.14 and 2.15) (Schwartz and Blobel, 2003).

The model in Figure 4.2 displays a direct physical contact between the ribosome and SRβ, in support of the available data (Figure 3.18) (Fulga et al., 2001). Additionally, it incorporates the finding that the ribosome stimulates SRβ GTPase activity (Bacher et al., 1999). Unlike Figure 4.1.A this model also incorporates the notion that SR dissociates when SRβ is in the GDP-bound state (Figures 2.14 and 2.15) (Schwartz and Blobel, 2003). Since SRα likely dissociates from SRβ once SRβ hydrolyses GTP, the RNC remains tethered to the ER via a physical interaction with SRβ (step 4). This configuration represents the post-targeting intermediate.

Although both models depicting a physical association between the ribosome and SRβ show the interaction occurring concomitantly with SRP54-SRα binding, it is not

clear at what stage a ribosome-SRβ complex is formed. A ribosome-SRβ crosslink could be detected between ribosomes and purified SR reconstituted into proteoliposomes, suggesting that Sec61 is not involved in the ribosome-SRβ interaction (Fulga et al., 2001). This is consistent with the discovery that under conditions whereby limiting amounts of Sec61 were all engaged with RNCs, RNCs continued to accumulate on the ER membrane in a SRα-dependent fashion, but binding to the membrane following the targeting step was both SRα-independent and Sec61-independent (Murphy, III et al., 1997). In fact, Sec61 may disrupt ribosome-SRβ binding, as the crosslink between the ribosome and SRβ was lost when crosslinking experiments were performed using proteoliposomes containing both SR and Sec61 (Fulga et al., 2001). In the absence of Sec61, binding between SRβ and the ribosome is essentially irreversible, as revealed by the ability to resolve ribosome-SRβ complexes on sucrose gradients. Therefore, the most likely candidate for retaining the RNC-SRP complex on the ER membrane as a post-targeting intermediate is SRβ.

Several pieces of recently published data are consistent with a role for SRβ in tethering post-targeting intermediates. Treatment of ER microsomes with protease concentrations that were sufficient to digest Sec61α effectively blocked SRP-mediated translocation of ribosome-nascent chains at the level of the post targeting intermediate (Song et al., 2000) These protease conditions did not affect the integrity of SRβ, although SRα was completely digested. Addition of exogenous SRα to facilitate targeting to these membranes resulted in the detection of post targeting intermediates only when the integrity of SRβ was unaffected. Furthermore, *in vitro*, ribosome-nascent chain complexes were shown to cofractionate with liposomes containing SR from which SRα had been proteolytically removed (Bacher et al., 1999). Taken together with the observation that SRα is dispensable once targeting has occurred (Murphy, III et al., 1997), these results implicate SRβ as the membrane-bound anchor for post targeting intermediates. The model in Figure 4.1.A does not consider this possibility since the SR dimer is presented as a static structure.

The steps leading to transfer of the RNC from SR to Sec61 are a further point of disagreement between the models. Figure 4.2 shows the post-targeting intermediate consisting of a RNC tethered to the ER via binding to SRβ (step 4). Attachment of the RNC to the ER membrane via SRβ may allow the ribosome to remain bound to the membrane until the arrival of an available translocon. In this model, Sec61 itself mediates the transfer of the RNC from a post-targeting intermediate to a pre-translocation intermediate (step 5), consistent with data demonstrating that proteolysis of Sec61 abolished this step (Song et al., 2000). Transfer of the ribosome to Sec61may be mediated by the high affinity interaction between the ribosome and Sec61 (Kalies et al., 1994). The proximity between Sec61 and SRβ during the ribosome transfer step may allow for an interaction between Sec61β and SRβ, catalysing the release of GDP from SRβ (Helmers et al., 2003). GTP binding to SRβ may break the Sec61β-SRβ interaction, consistent with

results obtained from other GRF-GTPase pairs (Boguski and McCormick, 1993).

According to the model in Figure 4.1.A GTP-binding to SRβ regulates the transfer of the RNC to Sec61. The authors reason that since they could detect a crosslink between a 21 kDa ribosomal protein and SRβ in the absence of nucleotide or in the presence of GDP, but not in the presence of GMPPNP, that binding of the ribosome to SRβ did not occur in the presence of GTP (Fulga et al., 2001). However, the failure to detect a crosslink is not proof that a physical interaction did not occur. Clearly, if the ribosome can directly influence the GTPase activity of SRβ, as these researchers had proposed previously (Bacher et al., 1999), a physical interaction between the ribosome and SRβ-GTP must occur.

To further support their model the authors investigated SRβ separately from the other two GTP-binding proteins by using a version of SRβ that prefers XTP over GTP ($SR\beta_{D181N}$) (Fulga et al., 2001). They claim that their data supports a model whereby binding of GTP to SRβ facilitates transfer of the nascent chain to the Sec61 complex. Their hypothesis is derived from the observation that insertion of a preprolactin nascent chain into the translocon (as monitored by crosslinking the nascent chain to either SRP54 (not inserted) or Sec61α (inserted)) occurred readily in the presence of GTP or GMPPNP but was greatly diminished in the presence of excess XDP, conditions that favour $SR\beta_{D181N}$-XDP. However, SRα-SRβ dimer formation was less efficient when SRβ is bound to dinucleotide (Figure 2.15) (Schwartz and Blobel, 2003). Therefore, by using assay conditions that include a high concentration of XDP, favouring the formation of $SR\beta_{D181N}$-XDP over $SR\beta_{D181N}$-GTP, the authors create conditions that favour unstable SR dimers. Their observation that crosslinking between the nascent chain and Sec61α is decreased in the presence of XDP may result from reduced targeting of RNCs to the membrane due to the inability to anchor SRα to the membrane in the presence of XDP, and not due to a direct influence of SRβ on the nascent chain transfer step.

Although the authors did not detect transfer of the nascent chain to Sec61α in the presence of XDP, transfer was detected in the presence of GMPPNP (Fulga et al., 2001). The implication of this result is that hydrolysis of GTP by SRβ is not an absolute requirement for nascent chain transfer to Sec61α.

Although the model in Figure 4.2 proceeds by releasing SRα from SRβ as a result of ribosome-catalysed GTP hydrolysis by SRβ, the discovery that GTP hydrolysis was not required for the insertion of all nascent chains into the Sec61 channel (Fulga et al., 2001) raises questions regarding the importance of SRβ-mediated GTP hydrolysis. It is not clear whether the hydrolysis step is optional for all substrates, or is only required for a subset of secretory proteins. Releasing the nascent chain from a direct connection with the membrane may allow for increased mobility of the nascent chain within the ribosome and allow the RNC the freedom to bind translocons of varying composition. Recent studies demonstrated that a translocon accessory complex called the TRAP complex was required for efficient translocation of a subset of signal peptides (Fons et al., 2003). Furthermore,

the involvement of another translocon accessory factor, TRAM, was required for the efficient translocation of certain substrates (Gorlich et al., 1992a; Gorlich and Rapoport, 1993). The recruitment of accessory factors to the translocon to enable efficient translocation of specific substrates would increase the steric bulk of the translocon. It is conceivable that releasing SRα from SRβ allows the nascent chain to move further away from the point of membrane contact so it can align correctly with a translocon containing a large number of accessory factors. Preprolactin could be translocated by the minimal translocation machinery, consisting only of SR and Sec61 (Gorlich and Rapoport, 1993), so transfer of this substrate to Sec61 *in vitro* may be efficient without a requirement for SRβ-mediated GTP hydrolysis.

Each model presented in Figures 4.1 and 4.2 concludes by returning SRP and SR to their starting configurations. Once the ribosome is correctly aligned with the Sec61 channel the signal peptide is released from SRP and permitted to enter the translocon, and both SRP and SRα hydrolyse GTP and release from one another (Connolly et al., 1991). SRP is recycled to the cytoplasm and SRα returns to the empty state. Figure 4.1.A includes an uncharacterised GTP hydrolysis step to return SRβ to the GDP-bound state. SRβ also hydrolyses GTP to GDP in Figure 4.1.B; this conversion of GTP to GDP causes SRα to release from SRβ and return to the cytoplasm. In contrast, Figure 4.2 concludes with SRβ in the GTP-bound state, in a complex with empty SRα. This is the only configuration that is consistent with both crystal data (Schwartz and Blobel, 2003) and subcellular fractionation data with respect to the localization of SRα on the ER membrane (Ogg et al., 1998).

4.3 Future perspectives

The recent publication of the crystal structure of the SRX-SRβ complex from yeast (Schwartz and Blobel, 2003), together with the model presented in Figure 4.2, allows for the formation of several testable hypotheses. However, considering the significant sequence dissimilarity between the yeast proteins and proteins from higher eukaryotes, particularly among the residues contributing to side chain interactions between SRX and SRβ (see Figure 2.17), the crystal structure of the mammalian homologues is still required to understand the nature of the interaction between SRα and SRβ.

From a structural perspective, there appear to be two binding interfaces on SRβ for three protein-protein interactions including SRα, a 21 kDa ribosomal protein and Sec61β. The published crystal structure reveals that SRα binds SRβ predominantly through the switch I region of SRβ (Figure 2.16) (Schwartz and Blobel, 2003), making this region unavailable to bind to other proteins. Analysis of the interaction between Arf1 and the ArfGRF Arno reveals that Arno binds Arf1 through the switch 1 and 2 regions (Mossessova et al., 1998). The crystal structure of Arf1 with the GRF Sec7 also reveals interactions with the switch regions of Arf1 (Goldberg, 1998). The model in Figure 4.2 is presented such that Sec61β binds SRβ after SRα is released from SRβ. If the interaction

between Sec61β and SRβ is comparable to the interaction between Arf1 and its GRFs, releasing SRα from SRβ could expose the switch 1 region for a potential interaction with Sec61β. *In vitro* immunoprecipitation experiments using radiolabelled Sec61β and SRβ in the presence and absence of SRα may be able to determine whether SRα and Sec61β bind the same region of SRβ.

SRβ diverges significantly from other Ras-type GTPases by a 35 amino acid insertion that extends the α4 helix and contributes to a region of considerable flexibility (since it does not appear in the crystal structure) that could provide a binding surface for the ribosome (Figure 2.16). This region lies on the opposite side of SRβ from the SRα-binding surface, so should be accessible to a binding partner as large as a ribosome. GAPs usually bind GTPases in part through the switch 2 region of the GTPase (Scheffzek et al., 1997; Goldberg, 1999), and this also may be accessible to the ribosome (see red sequence in Figure 2.16.B). One can envision proteins within the ribosome forming extensive contacts with the α4 helix and unstructured loop to enable a stable interaction for membrane-binding, as well as binding to the switch 2 region to enable GTP hydrolysis. Since extensive contacts between the ribosome and SRβ are possible, systematic mutagenesis of the α4 helix and unstructured loop may not be sufficient to disrupt the interaction without introducing large scale changes that may have unpredictable effects on the structure of SRβ. To determine whether this region of SRβ is required for binding the ribosome, it may be possible to conduct peptide inhibition studies using a peptide corresponding to the α4 helix and unstructured loop of SRβ. A decrease in preprotein translocation, loss of ribosome-SRβ crosslinking and sucrose density gradient centrifugation can all be used to assay if a functional interaction between the ribosome and SRβ is lost in the presence of a competing peptide.

Unlike other GTPases, yeast SRβ contains an active site residue that crowds the catalytic water molecule and forms a hydrogen bond with the γ-phosphate of GTP (Schwartz and Blobel, 2003). Arf family GTPases also contain a bulky side chain at this position, but it is oriented away from the active site (Figures 2.18 and 3.20.D). This implies that the GAP mechanism for SRβ may be different from other GTPases, because the crowding at the active site must be relieved before GTP hydrolysis can proceed. To sort out the details of the GTPase mechanism the SRβGAP must be identified, followed by a detailed structural analysis of the SRβ-GAP complex. These goals are still some years away, and identification of the SRβGAP is not likely to be a trivial matter. Although there is little doubt that SRβ contacts a 21 kDa ribosomal protein (Fulga et al., 2001), there is no evidence that this protein is the SRβGAP. Resolving the sequences to which this 21 kDa protein binds by using the deletion mutagenesis and peptide inhibition approaches outlined above will help to resolve its function. Should the binding surface map to the switch 2 region of SRβ, the hypothesis that the 21 kDa protein is the SRβGAP will be strengthened. On the other hand, should the binding surface map distal to the GTP-binding site of SRβ, the possibility that the 21 kDa protein is the SRβGAP will be

diminished.

I did not detect GTP hydrolysis arising from SRβ in the presence of ribosomes. My results differ from previous results, which used SRα-SRβ dimers to assay SRβ GTPase activity (Bacher et al., 1999). The difference between these two systems raises the possibility that binding of SRα is required before SRβ can become catalytically active. Surprisingly, the glutamine residue that crowds the active site of yeast SRβ hydrogen bonds to the terminal phosphate of the bound GTP through the side chain amine, but it also hydrogen bonds to SRX through the side chain oxygen. Therefore it is quite possible that SRX forces the glutamine into the active site, thus preventing untimely GTP hydrolysis. The implication of this proposal is that purified yeast SRβ might have some minimal GTPase activity when SRX is not bound; this possibility has not been tested.

Since the crystal structure of SRX-SRβ is incompatible with the existing GTPase mechanism it is difficult to propose a mechanism for SRβ-mediated GTP hydrolysis based on the mechanism of hydrolysis proposed for other Ras-type GTPases. GAP-catalysed GTP hydrolysis by Ras-type GTPases has been proposed to involve an arginine residue contributed in *trans* by the GAP, that stabilises the transition state by hydrogen bonding to the γ-phosphate of the bound GTP (Mittal et al., 1996; Scheffzek et al., 1997). The presence of a glutamine residue in yeast SRβ at the approximate position where the GAP-contributed arginine would insert renders a homologous GAP-catalysed mechanism incompatible with the published SRX-SRβ structure (Schwartz and Blobel, 2003)(Schwartz and Blobel, 2003). Therefore, a compatible mechanism must be sought elsewhere.

The GTPase mechanism for Gα subunits differs from the mechanism for Ras-type GTPases in that Gα subunits contribute an arginine in *cis* that hydrogen bonds the γ-phosphate of GTP and stabilises the transition state (Coleman et al., 1994; Sondek et al., 1994). A contribution in *cis* of the transition state-stabilising residue is consistent with the SRX-SRβ structure. It is possible that the addition of a GAP to the SRX-SRβ complex could shift the position of the glutamine away from the catalytic water molecule, while allowing the hydrogen bond to the terminal phosphate to be maintained. This would allow the glutamine to stabilise the transition state. The crystal structure of yeast SRX-SRβ will have to be compared to the SRX-SRβ-GAP complex to determine whether this proposed mechanism for GTP hydrolysis by SRβ is correct. There are no crystal structures yet for Arf-family members bound to effectors so it is not known whether the binding of effector proteins reorients the aspartic acid into the active site. As these structures are solved a new general mechanism for GTP hydrolysis may be revealed for Ras-type GTPases that catalyse hydrolysis most efficiently when both effectors and GAPs are allowed to bind simultaneously (ie. Arf and SRβ).

The mechanism of GTP hydrolysis for yeast SRβ may differ from the mechanism for mammalian SRβ, since the active site glutamine is substituted by cysteine in

mammalian SRβ. Unlike glutamine, cysteine is unable to form two hydrogen bonds, so it may either hydrogen bond with the terminal phosphate or with SRX2, but not both. Comparison of the structures of mammalian SRβ, SRX2-SRβ and SRX2-SRβ-GAP may allow the mechanism of GTP hydrolysis by mammalian SRβ to be resolved.

In vitro studies employing an XTP-preferring mutant of SRβ, $SR\beta_{D181N}$, revealed that translocation of preprolactin did not require nucleotide hydrolysis by SRβ (Fulga et al., 2001). I have postulated that GTP hydrolysis by SRβ may only be required for substrates that require translocon accessory factors for efficient translocation, though *in vivo* GTP hydrolysis is likely to occur independent of substrate requirements, unless the ribosome-SR interaction is influenced by the identity of the nascent chain. To address whether GTP hydrolysis is required for translocation of a subset of secretory/membrane proteins a yeast genetic system will likely yield the quickest answer. Based on similar mutations in other Ras-type GTPases (Gideon et al., 1992; Jonak et al., 1994) mutation of the histidine within SRβ that orients the catalytic water molecule (Figure 3.20.C) will create a catalytically dead SRβ that should become incorporated into ER membranes. Transformation of a plasmid construct encoding the mutant SRβ into a yeast strain with the capacity for regulated expression of endogenous SRβ may allow for the enrichment of the mutant SRβ in the ER membrane. Should the mutant SRβ express and become integrated into the ER membrane, purification of membranes containing mutant SRβ will provide a tool that can be used to assay the requirement for GTP hydrolysis by SRβ. By performing translocation assays using substrates with varying requirements for translocon accessory factors the conditions under which SRβ-mediated GTP hydrolysis is required can be assessed. Purification of translocon components and reconstitution of defined components into proteoliposomes may address whether certain accessory factors create a requirement for GTP hydrolysis by SRβ.

A major direction for future studies will be to reconcile the model presented in Figure 4.2 with data obtained from *E. coli*. Most of the factors involved in co-translational protein translocation, and the basic mechanism of translocation, appear to be evolutionarily conserved. The major difference between *E. coli* and eukaryotes lies in the fact that *E. coli* lack an obvious SRβ homologue. There appears to be a protein receptor on the *E. coli* inner membrane that assists in anchoring the SRα homologue, FtsY, to the membrane (Millman et al., 2001) but until it is identified and biochemically characterized it is not known whether this putative receptor regulates the binding of FtsY to the membrane, or binds to ribosomes to serve the same function that I have predicted for SRβ. A biochemical approach is currently being taken to identify the protein receptor, but the techniques of bacterial genetics provide powerful tools that may yield a quicker identification. Previous genetic screens have identified all known proteins in the *E. coli* SRP pathway, none of which fit the description of a FtsY receptor (Tian et al., 2000; Tian and Beckwith, 2002). However, it appears that such a receptor is dispensable as long as the membrane contains PE (Millman et al., 2001). Therefore a genetic screen in a PE-deficient strain of *E. coli* will be necessary to identify this protein using a genetic

approach.

In the last decade, much progress has been made in elucidating the role of SRβ in protein translocation. From being a GTP-binding protein of unknown function it has now become clear that SRβ is the key to regulating membrane attachment of SRα, and evidence is starting to accumulate that SRβ plays a major role in translocation by serving as the post-targeting ribosome receptor on the ER membrane. Developing structural explanations for functional observations will remain a major challenge for the future.

5. REFERENCES

Adams,H., Scotti,P.A., De Cock,H., Luirink,J., and Tommassen,J. (2002). The presence of a helix breaker in the hydrophobic core of signal sequences of secretory proteins prevents recognition by the signal-recognition particle in Escherichia coli. Eur. J. Biochem. *269*, 5564-5571.

Akiyama,Y., Kihara,A., Tokuda,H., and Ito,K. (1996). FtsH (HflB) is an ATP-dependent protease selectively acting on SecY and some other membrane proteins. J. Biol. Chem. *271*, 31196-31201.

Amor,J.C., Harrison,D.H., Kahn,R.A., and Ringe,D. (1994). Structure of the human ADP-ribosylation factor 1 complexed with GDP. Nature *372*, 704-708.

Andrews,D.W., Lauffer,L., Walter,P., and Lingappa,V.R. (1989). Evidence for a two-step mechanism involved in assembly of functional signal recognition particle receptor. J. Cell Biol. *108*, 797-810.

Bacher,G., Lutcke,H., Jungnickel,B., Rapoport,T.A., and Dobberstein,B. (1996). Regulation by the ribosome of the GTPase of the signal-recognition particle during protein targeting. Nature *381*, 248-251.

Bacher,G., Pool,M., and Dobberstein,B. (1999). The ribosome regulates the GTPase of the beta-subunit of the signal recognition particle receptor. J. Cell Biol. *146*, 723-730.

Barlowe,C., d'Enfert,C., and Schekman,R. (1993). Purification and characterization of SAR1p, a small GTP-binding protein required for transport vesicle formation from the endoplasmic reticulum. J. Biol. Chem. *268*, 873-879.

Batey,R.T., Rambo,R.P., Lucast,L., Rha,B., and Doudna,J.A. (2000). Crystal structure of the ribonucleoprotein core of the signal recognition particle. Science *287*, 1232-1239.

Beck,K., Eisner,G., Trescher,D., Dalbey,R.E., Brunner,J., and Muller,M. (2001). YidC, an assembly site for polytopic Escherichia coli membrane proteins located in immediate proximity to the SecYE translocon and lipids. EMBO Rep. *2*, 709-714.

Beckmann,R., Bubeck,D., Grassucci,R., Penczek,P., Verschoor,A., Blobel,G., and Frank,J. (1997). Alignment of conduits for the nascent polypeptide chain in the ribosome-Sec61 complex. Science *278*, 2123-2126.

Bernstein,H.D., Poritz,M.A., Strub,K., Hoben,P.J., Brenner,S., and Walter,P. (1989). Model for signal sequence recognition from amino-acid sequence of 54K subunit of signal recognition particle. Nature *340*, 482-486.

Bessonneau,P., Besson,V., Collinson,I., and Duong,F. (2002). The SecYEG preprotein translocation channel is a conformationally dynamic and dimeric structure. EMBO J. *21*, 995-1003.

Boguski,M.S. and McCormick,F. (1993). Proteins regulating Ras and its relatives. Nature *366*, 643-654.

Bordier,C. (1981). Phase separation of integral membrane proteins in Triton X-114 solution. J. Biol. Chem. *256*, 1604-1607.

Bourne,H.R., Sanders,D.A., and McCormick,F. (1990). The GTPase superfamily: a conserved switch for diverse cell functions. Nature *348*, 125-132.

Bourne,H.R., Sanders,D.A., and McCormick,F. (1991). The GTPase superfamily: conserved structure and molecular mechanism. Nature *349*, 117-127.

Breyton,C., Haase,W., Rapoport,T.A., Kuhlbrandt,W., and Collinson,I. (2002). Three-dimensional structure of the bacterial protein-translocation complex SecYEG. Nature *418*, 662-665.

Brown,J.D., Hann,B.C., Medzihradszky,K.F., Niwa,M., Burlingame,A.L., and Walter,P. (1994). Subunits of the Saccharomyces cerevisiae signal recognition particle required for its functional expression. EMBO J. *13*, 4390-4400.

Brundage,L., Hendrick,J.P., Schiebel,E., Driessen,A.J., and Wickner,W. (1990). The purified E. coli integral membrane protein SecY/E is sufficient for reconstitution of SecA-dependent precursor protein translocation. Cell *62*, 649-657.

Chang,D.Y., Newitt,J.A., Hsu,K., Bernstein,H.D., and Maraia,R.J. (1997). A highly conserved nucleotide in the Alu domain of SRP RNA mediates translation arrest through high affinity binding to SRP9/14. Nucleic Acids Res. *25*, 1117-1122.

Chirico,W.J., Waters,M.G., and Blobel,G. (1988). 70K heat shock related proteins stimulate protein translocation into microsomes. Nature *332*, 805-810.

Ciufo,L.F. and Brown,J.D. (2000). Nuclear export of yeast signal recognition particle lacking Srp54p by the Xpo1p/Crm1p NES-dependent pathway. Curr. Biol. *10*, 1256-1264.

Cleverley,R.M. and Gierasch,L.M. (2002). Mapping the signal sequence-binding site on SRP reveals a significant role for the NG domain. J. Biol. Chem. *277*, 46763-46768.

Coleman,D.E., Berghuis,A.M., Lee,E., Linder,M.E., Gilman,A.G., and Sprang,S.R.

(1994). Structures of active conformations of Gi alpha 1 and the mechanism of GTP hydrolysis. Science *265*, 1405-1412.

Connolly,T. and Gilmore,R. (1989). The signal recognition particle receptor mediates the GTP-dependent displacement of SRP from the signal sequence of the nascent polypeptide. Cell *57*, 599-610.

Connolly,T. and Gilmore,R. (1993). GTP hydrolysis by complexes of the signal recognition particle and the signal recognition particle receptor. J. Cell Biol. *123*, 799-807.

Connolly,T., Rapiejko,P.J., and Gilmore,R. (1991). Requirement of GTP hydrolysis for dissociation of the signal recognition particle from its receptor. Science *252*, 1171-1173.

Craven,R.A., Egerton,M., and Stirling,C.J. (1996). A novel Hsp70 of the yeast ER lumen is required for the efficient translocation of a number of protein precursors. EMBO J. *15*, 2640-2650.

Cristobal,S., Scotti,P., Luirink,J., von Heijne,G., and de Gier,J.W. (1999). The signal recognition particle-targeting pathway does not necessarily deliver proteins to the sec-translocase in Escherichia coli. J. Biol. Chem. *274*, 20068-20070.

Crowley,K.S., Liao,S., Worrell,V.E., Reinhart,G.D., and Johnson,A.E. (1994). Secretory proteins move through the endoplasmic reticulum membrane via an aqueous, gated pore. Cell *78*, 461-471.

Crowley,K.S., Reinhart,G.D., and Johnson,A.E. (1993). The signal sequence moves through a ribosomal tunnel into a noncytoplasmic aqueous environment at the ER membrane early in translocation. Cell *73*, 1101-1115.

De Leeuw,E., te,K.K., Moser,C., Menestrina,G., Demel,R., de Kruijff,B., Oudega,B., Luirink,J., and Sinning,I. (2000). Anionic phospholipids are involved in membrane association of FtsY and stimulate its GTPase activity. EMBO J. *19*, 531-541.

Deshaies,R.J., Koch,B.D., Werner-Washburne,M., Craig,E.A., and Schekman,R. (1988). A subfamily of stress proteins facilitates translocation of secretory and mitochondrial precursor polypeptides. Nature *332*, 800-805.

Deshaies,R.J., Sanders,S.L., Feldheim,D.A., and Schekman,R. (1991). Assembly of yeast Sec proteins involved in translocation into the endoplasmic reticulum into a membrane-bound multisubunit complex. Nature *349*, 806-808.

Dever,T.E., Glynias,M.J., and Merrick,W.C. (1987). GTP-binding domain: three

consensus sequence elements with distinct spacing. Proc. Natl. Acad. Sci. U. S. A *84*, 1814-1818.

Do,H., Falcone,D., Lin,J., Andrews,D.W., and Johnson,A.E. (1996). The cotranslational integration of membrane proteins into the phospholipid bilayer is a multistep process. Cell *85*, 369-378.

Duong,F. and Wickner,W. (1997). Distinct catalytic roles of the SecYE, SecG and SecDFyajC subunits of preprotein translocase holoenzyme. EMBO J. *16*, 2756-2768.

Economou,A., Pogliano,J.A., Beckwith,J., Oliver,D.B., and Wickner,W. (1995). SecA membrane cycling at SecYEG is driven by distinct ATP binding and hydrolysis events and is regulated by SecD and SecF. Cell *83*, 1171-1181.

Economou,A. and Wickner,W. (1994). SecA promotes preprotein translocation by undergoing ATP-driven cycles of membrane insertion and deinsertion. Cell *78*, 835-843.

Falcone,D. and Andrews,D.W. (1991). Both the 5' untranslated region and the sequences surrounding the start site contribute to efficient initiation of translation in vitro. Mol. Cell Biol. *11*, 2656-2664.

Falcone,D., Do,H., Johnson,A.E., and Andrews,D.W. (1999). Negatively charged residues in the IgM stop-transfer effector sequence regulate transmembrane polypeptide integration. J. Biol. Chem. *274*, 33661-33670.

Falvey,A.K. and Staehelin,T. (1970). Structure and function of mammalian ribosomes. I. Isolation and characterization of active liver ribosomal subunits. J. Mol. Biol. *53*, 1-19.

Fekkes,P., Van Der,D.C., and Driessen,A.J. (1997). The molecular chaperone SecB is released from the carboxy-terminus of SecA during initiation of precursor protein translocation. EMBO J. *16*, 6105-6113.

Ferguson,K.M., Higashijima,T., Smigel,M.D., and Gilman,A.G. (1986). The influence of bound GDP on the kinetics of guanine nucleotide binding to G proteins. J. Biol. Chem. *261*, 7393-7399.

Feuerstein,J., Goody,R.S., and Wittinghofer,A. (1987). Preparation and characterization of nucleotide-free and metal ion-free p21 "apoprotein". J. Biol. Chem. *262*, 8455-8458.

Finke,K., Plath,K., Panzner,S., Prehn,S., Rapoport,T.A., Hartmann,E., and Sommer,T. (1996). A second trimeric complex containing homologs of the Sec61p complex functions in protein transport across the ER membrane of S. cerevisiae. EMBO J. *15*, 1482-1494.

Floer,M. and Blobel,G. (1996). The nuclear transport factor karyopherin beta binds stoichiometrically to Ran-GTP and inhibits the Ran GTPase activating protein. J. Biol. Chem. *271*, 5313-5316.

Flower,A.M., Hines,L.L., and Pfennig,P.L. (2000). SecG is an auxiliary component of the protein export apparatus of Escherichia coli. Mol. Gen. Genet. *263*, 131-136.

Fons,R.D., Bogert,B.A., and Hegde,R.S. (2003). Substrate-specific function of the translocon-associated protein complex during translocation across the ER membrane. J. Cell Biol. *160*, 529-539.

Freymann,D.M., Keenan,R.J., Stroud,R.M., and Walter,P. (1997). Structure of the conserved GTPase domain of the signal recognition particle. Nature *385*, 361-364.

Fulga,T.A., Sinning,I., Dobberstein,B., and Pool,M.R. (2001). SRbeta coordinates signal sequence release from SRP with ribosome binding to the translocon. EMBO J. *20*, 2338-2347.

Gavin,A.C., Bosche,M., Krause,R., Grandi,P., Marzioch,M., Bauer,A., Schultz,J., Rick,J.M., Michon,A.M., Cruciat,C.M., Remor,M., Hofert,C., Schelder,M., Brajenovic,M., Ruffner,H., Merino,A., Klein,K., Hudak,M., Dickson,D., Rudi,T., Gnau,V., Bauch,A., Bastuck,S., Huhse,B., Leutwein,C., Heurtier,M.A., Copley,R.R., Edelmann,A., Querfurth,E., Rybin,V., Drewes,G., Raida,M., Bouwmeester,T., Bork,P., Seraphin,B., Kuster,B., Neubauer,G., and Superti-Furga,G. (2002). Functional organization of the yeast proteome by systematic analysis of protein complexes. Nature *415*, 141-147.

Gideon,P., John,J., Frech,M., Lautwein,A., Clark,R., Scheffler,J.E., and Wittinghofer,A. (1992). Mutational and kinetic analyses of the GTPase-activating protein (GAP)-p21 interaction: the C-terminal domain of GAP is not sufficient for full activity. Mol. Cell Biol. *12*, 2050-2056.

Gill,D.R., Hatfull,G.F., and Salmond,G.P. (1986). A new cell division operon in Escherichia coli. Mol. Gen. Genet. *205*, 134-145.

Gilmore,R. and Blobel,G. (1983). Transient involvement of signal recognition particle and its receptor in the microsomal membrane prior to protein translocation. Cell *35*, 677-685.

Gilmore,R., Blobel,G., and Walter,P. (1982a). Protein translocation across the endoplasmic reticulum. I. Detection in the microsomal membrane of a receptor for the signal recognition particle. J. Cell Biol. *95*, 463-469.

Gilmore,R., Walter,P., and Blobel,G. (1982b). Protein translocation across the endoplasmic reticulum. II. Isolation and characterization of the signal recognition particle receptor. J. Cell Biol. *95*, 470-477.

Goldberg,J. (1998). Structural basis for activation of ARF GTPase: mechanisms of guanine nucleotide exchange and GTP-myristoyl switching. Cell *95*, 237-248.

Goldberg,J. (1999). Structural and functional analysis of the ARF1-ARFGAP complex reveals a role for coatomer in GTP hydrolysis. Cell *96*, 893-902.

Gorlich,D., Hartmann,E., Prehn,S., and Rapoport,T.A. (1992a). A protein of the endoplasmic reticulum involved early in polypeptide translocation. Nature *357*, 47-52.

Gorlich,D., Prehn,S., Hartmann,E., Kalies,K.U., and Rapoport,T.A. (1992b). A mammalian homolog of SEC61p and SECYp is associated with ribosomes and nascent polypeptides during translocation. Cell *71*, 489-503.

Gorlich,D. and Rapoport,T.A. (1993). Protein translocation into proteoliposomes reconstituted from purified components of the endoplasmic reticulum membrane. Cell *75*, 615-630.

Gowda,K., Chittenden,K., and Zwieb,C. (1997). Binding site of the M-domain of human protein SRP54 determined by systematic site-directed mutagenesis of signal recognition particle RNA. Nucleic Acids Res. *25*, 388-394.

Gurevich,V.V., Pokrovskaya,I.D., Obukhova,T.A., and Zozulya,S.A. (1991). Preparative in vitro mRNA synthesis using SP6 and T7 RNA polymerases. Anal. Biochem. *195*, 207-213.

Hamman,B.D., Chen,J.C., Johnson,E.E., and Johnson,A.E. (1997). The aqueous pore through the translocon has a diameter of 40-60 A during cotranslational protein translocation at the ER membrane. Cell *89*, 535-544.

Hamman,B.D., Hendershot,L.M., and Johnson,A.E. (1998). BiP maintains the permeability barrier of the ER membrane by sealing the lumenal end of the translocon pore before and early in translocation. Cell *92*, 747-758.

Hanein,D., Matlack,K.E., Jungnickel,B., Plath,K., Kalies,K.U., Miller,K.R., Rapoport,T.A., and Akey,C.W. (1996). Oligomeric rings of the Sec61p complex induced by ligands required for protein translocation. Cell *87*, 721-732.

Hann,B.C., Poritz,M.A., and Walter,P. (1989). Saccharomyces cerevisiae and Schizosaccharomyces pombe contain a homologue to the 54-kD subunit of the signal

recognition particle that in S. cerevisiae is essential for growth. J. Cell Biol. *109*, 3223-3230.

Hann,B.C. and Walter,P. (1991). The signal recognition particle in S. cerevisiae. Cell *67*, 131-144.

Hartl,F.U., Lecker,S., Schiebel,E., Hendrick,J.P., and Wickner,W. (1990). The binding cascade of SecB to SecA to SecY/E mediates preprotein targeting to the E. coli plasma membrane. Cell *63*, 269-279.

Hartmann,E., Sommer,T., Prehn,S., Gorlich,D., Jentsch,S., and Rapoport,T.A. (1994). Evolutionary conservation of components of the protein translocation complex. Nature *367*, 654-657.

Heinrich,S.U., Mothes,W., Brunner,J., and Rapoport,T.A. (2000). The Sec61p complex mediates the integration of a membrane protein by allowing lipid partitioning of the transmembrane domain. Cell *102*, 233-244.

Helmers,J., Schmidt,D., Glavy,J.S., Blobel,G., and Schwartz,T. (2003). The beta-subunit of the protein-conducting channel of the endoplasmic reticulum functions as the guanine nucleotide exchange factor for the beta-subunit of the signal recognition particle receptor. J. Biol. Chem. *278*, 23686-23690.

Herrmann,C. (2003). Ras-effector interactions: after one decade. Curr. Opin. Struct. Biol. *13*, 122-129.

High,S., Andersen,S.S., Gorlich,D., Hartmann,E., Prehn,S., Rapoport,T.A., and Dobberstein,B. (1993a). Sec61p is adjacent to nascent type I and type II signal-anchor proteins during their membrane insertion. J. Cell Biol. *121*, 743-750.

High,S., Gorlich,D., Wiedmann,M., Rapoport,T.A., and Dobberstein,B. (1991). The identification of proteins in the proximity of signal-anchor sequences during their targeting to and insertion into the membrane of the ER. J. Cell Biol. *113*, 35-44.

High,S., Martoglio,B., Gorlich,D., Andersen,S.S., Ashford,A.J., Giner,A., Hartmann,E., Prehn,S., Rapoport,T.A., Dobberstein,B., and . (1993b). Site-specific photocross-linking reveals that Sec61p and TRAM contact different regions of a membrane-inserted signal sequence. J. Biol. Chem. *268*, 26745-26751.

Hortsch,M., Avossa,D., and Meyer,D.I. (1985). A structural and functional analysis of the docking protein. Characterization of active domains by proteolysis and specific antibodies. J. Biol. Chem. *260*, 9137-9145.

Huang,M., Weissman,J.T., Beraud-Dufour,S., Luan,P., Wang,C., Chen,W., Aridor,M., Wilson,I.A., and Balch,W.E. (2001). Crystal structure of Sar1-GDP at 1.7 A resolution and the role of the NH2 terminus in ER export. J. Cell Biol. *155*, 937-948.

Huang,Q., Abdulrahman,S., Yin,J., and Zwieb,C. (2002). Systematic site-directed mutagenesis of human protein SRP54: interactions with signal recognition particle RNA and modes of signal peptide recognition. Biochemistry *41*, 11362-11371.

Hughes,M.J. and Andrews,D.W. (1996). Creation of deletion, insertion and substitution mutations using a single pair of primers and PCR. Biotechniques *20*, 188, 192-188, 196.

Hwang,M.C., Sung,Y.J., and Hwang,Y.W. (1996). The differential effects of the Gly-60 to Ala mutation on the interaction of H-Ras p21 with different downstream targets. J. Biol. Chem. *271*, 8196-8202.

Hwang,Y.W. and Miller,D.L. (1987). A mutation that alters the nucleotide specificity of elongation factor Tu, a GTP regulatory protein. J. Biol. Chem. *262*, 13081-13085.

Jacquet,E. and Parmeggiani,A. (1988). Structure-function relationships in the GTP binding domain of EF-Tu: mutation of Val20, the residue homologous to position 12 in p21. EMBO J. *7*, 2861-2867.

Jagath,J.R., Rodnina,M.V., and Wintermeyer,W. (2000). Conformational changes in the bacterial SRP receptor FtsY upon binding of guanine nucleotides and SRP. J. Mol. Biol. *295*, 745-753.

Janiak,F., Glover,J.R., Leber,B., Rachubinski,R.A., and Andrews,D.W. (1994). Targeting of passenger protein domains to multiple intracellular membranes. Biochem. J. *300 (Pt 1)*, 191-199.

John,J., Sohmen,R., Feuerstein,J., Linke,R., Wittinghofer,A., and Goody,R.S. (1990). Kinetics of interaction of nucleotides with nucleotide-free H-ras p21. Biochemistry *29*, 6058-6065.

Johnsson,N. and Varshavsky,A. (1994). Split ubiquitin as a sensor of protein interactions in vivo. Proc. Natl. Acad. Sci. U. S. A *91*, 10340-10344.

Jonak,J., Anborgh,P.H., and Parmeggiani,A. (1994). Histidine-118 of elongation factor Tu: its role in aminoacyl-tRNA binding and regulation of the GTPase activity. FEBS Lett. *343*, 94-98.

Kahn,R.A., Clark,J., Rulka,C., Stearns,T., Zhang,C.J., Randazzo,P.A., Terui,T., and Cavenagh,M. (1995). Mutational analysis of Saccharomyces cerevisiae ARF1. J. Biol.

Chem. *270*, 143-150.

Kahn,R.A. and Gilman,A.G. (1986). The protein cofactor necessary for ADP-ribosylation of Gs by cholera toxin is itself a GTP binding protein. J. Biol. Chem. *261*, 7906-7911.

Kalies,K.U., Gorlich,D., and Rapoport,T.A. (1994). Binding of ribosomes to the rough endoplasmic reticulum mediated by the Sec61p-complex. J. Cell Biol. *126*, 925-934.

Kalies,K.U., Rapoport,T.A., and Hartmann,E. (1998). The beta subunit of the Sec61 complex facilitates cotranslational protein transport and interacts with the signal peptidase during translocation. J. Cell Biol. *141*, 887-894.

Kihara,A., Akiyama,Y., and Ito,K. (1995). FtsH is required for proteolytic elimination of uncomplexed forms of SecY, an essential protein translocase subunit. Proc. Natl. Acad. Sci. U. S. A *92*, 4532-4536.

Kim,P.K., Janiak-Spens,F., Trimble,W.S., Leber,B., and Andrews,D.W. (1997). Evidence for multiple mechanisms for membrane binding and integration via carboxyl-terminal insertion sequences. Biochemistry *36* , 8873-8882.

Klappa,P., Zimmermann,M., and Zimmermann,R. (1994). The membrane proteins TRAMp and sec61 alpha p may be involved in post-translational transport of presecretory proteins into mammalian microsomes. FEBS Lett. *341*, 281-287.

Koyama,S. and Kikuchi,A. (2001). Ras interaction with RalGDS effector targets. Methods Enzymol. *332*, 127-138.

Kuglstatter,A., Oubridge,C., and Nagai,K. (2002). Induced structural changes of 7SL RNA during the assembly of human signal recognition particle. Nat. Struct. Biol. *9*, 740-744.

Kumamoto,C.A. (1991). Molecular chaperones and protein translocation across the Escherichia coli inner membrane. Mol. Microbiol. *5*, 19-22.

Kusters,R., Lentzen,G., Eppens,E., van Geel,A., van der Weijden,C.C., Wintermeyer,W., and Luirink,J. (1995). The functioning of the SRP receptor FtsY in protein-targeting in E. coli is correlated with its ability to bind and hydrolyse GTP. FEBS Lett. *372*, 253-258.

Laird,V. and High,S. (1997). Discrete cross-linking products identified during membrane protein biosynthesis. J. Biol. Chem. *272*, 1983-1989.

Lauffer,L., Garcia,P.D., Harkins,R.N., Coussens,L., Ullrich,A., and Walter,P. (1985). Topology of signal recognition particle receptor in endoplasmic reticulum membrane.

Nature *318*, 334-338.

Lee,H.C. and Bernstein,H.D. (2001). The targeting pathway of Escherichia coli presecretory and integral membrane proteins is specified by the hydrophobicity of the targeting signal. Proc. Natl. Acad. Sci. U. S. A *98*, 3471-3476.

Legate,K.R. and Andrews,D.W. (2001). Assembly strategies and GTPase regulation of the eukaryotic and Escherichia coil translocons. Biochem. Cell Biol. *79*, 593-601.

Legate,K.R., Falcone,D., and Andrews,D.W. (2000). Nucleotide-dependent binding of the GTPase domain of the signal recognition particle receptor beta-subunit to the alpha-subunit. J. Biol. Chem. *275*, 27439-27446.

Levitt,M. (1978). Conformational preferences of amino acids in globular proteins. Biochemistry *17*, 4277-4285.

Lill,R., Dowhan,W., and Wickner,W. (1990). The ATPase activity of SecA is regulated by acidic phospholipids, SecY, and the leader and mature domains of precursor proteins. Cell *60*, 271-280.

Luirink,J., Hagen-Jongman,C.M., van der Weijden,C.C., Oudega,B., High,S., Dobberstein,B., and Kusters,R. (1994). An alternative protein targeting pathway in Escherichia coli: studies on the role of FtsY. EMBO J. *13*, 2289-2296.

Luirink,J., High,S., Wood,H., Giner,A., Tollervey,D., and Dobberstein,B. (1992). Signal-sequence recognition by an Escherichia coli ribonucleoprotein complex. Nature *359*, 741-743.

Lyman,S.K. and Schekman,R. (1995). Interaction between BiP and Sec63p is required for the completion of protein translocation into the ER of Saccharomyces cerevisiae. J. Cell Biol. *131*, 1163-1171.

Lyman,S.K. and Schekman,R. (1997). Binding of secretory precursor polypeptides to a translocon subcomplex is regulated by BiP. Cell *88*, 85-96.

Mach,H., Middaugh,C.R., and Lewis,R.V. (1992). Statistical determination of the average values of the extinction coefficients of tryptophan and tyrosine in native proteins. Anal. Biochem. *200*, 74-80.

Maegley,K.A., Admiraal,S.J., and Herschlag,D. (1996). Ras-catalyzed hydrolysis of GTP: a new perspective from model studies. Proc. Natl. Acad. Sci. U. S. A *93*, 8160-8166.

Manting,E.H., Van Der,D.C., Remigy,H., Engel,A., and Driessen,A.J. (2000). SecYEG

assembles into a tetramer to form the active protein translocation channel. EMBO J. *19*, 852-861.

Marsh,R.C., Chinali,G., and Parmeggiani,A. (1975). Function of sulfhydryl groups in ribosome-elongation factor G reactions. Assignment of guanine nucleotide binding site to elongation factor G. J. Biol. Chem. *250*, 8344-8352.

Matsumoto,G., Mori,H., and Ito,K. (1998). Roles of SecG in ATP- and SecA-dependent protein translocation. Proc. Natl. Acad. Sci. U. S. A *95*, 13567-13572.

Menetret,J.F., Neuhof,A., Morgan,D.G., Plath,K., Radermacher,M., Rapoport,T.A., and Akey,C.W. (2000). The structure of ribosome-channel complexes engaged in protein translocation. Mol. Cell *6*, 1219-1232.

Meyer,D.I. and Dobberstein,B. (1980). A membrane component essential for vectorial translocation of nascent proteins across the endoplasmic reticulum: requirements for its extraction and reassociation with the membrane. J. Cell Biol. *87*, 498-502.

Meyer,D.I., Krause,E., and Dobberstein,B. (1982a). Secretory protein translocation across membranes-the role of the "docking protein'. Nature *297*, 647-650.

Meyer,D.I., Louvard,D., and Dobberstein,B. (1982b). Characterization of molecules involved in protein translocation using a specific antibody. J. Cell Biol. *92*, 579-583.

Meyer,H.A., Grau,H., Kraft,R., Kostka,S., Prehn,S., Kalies,K.U., and Hartmann,E. (2000). Mammalian Sec61 is associated with Sec62 and Sec63. J. Biol. Chem. *275*, 14550-14557.

Meyer,T.H., Menetret,J.F., Breitling,R., Miller,K.R., Akey,C.W., and Rapoport,T.A. (1999). The bacterial SecY/E translocation complex forms channel-like structures similar to those of the eukaryotic Sec61p complex. J. Mol. Biol. *285*, 1789-1800.

Miller,J.D., Bernstein,H.D., and Walter,P. (1994). Interaction of E. coli Ffh/4.5S ribonucleoprotein and FtsY mimics that of mammalian signal recognition particle and its receptor. Nature *367*, 657-659.

Miller,J.D., Tajima,S., Lauffer,L., and Walter,P. (1995). The beta subunit of the signal recognition particle receptor is a transmembrane GTPase that anchors the alpha subunit, a peripheral membrane GTPase, to the endoplasmic reticulum membrane. J. Cell Biol. *128*, 273-282.

Miller,J.D., Wilhelm,H., Gierasch,L., Gilmore,R., and Walter,P. (1993). GTP binding and hydrolysis by the signal recognition particle during initiation of protein translocation.

Nature *366*, 351-354.

Millman,J.S. and Andrews,D.W. (1999). A site-specific, membrane-dependent cleavage event defines the membrane binding domain of FtsY. J. Biol. Chem. *274*, 33227-33234.

Millman,J.S., Qi,H.Y., Vulcu,F., Bernstein,H.D., and Andrews,D.W. (2001). FtsY binds to the Escherichia coli inner membrane via interactions with phosphatidylethanolamine and membrane proteins. J. Biol. Chem. *276*, 25982-25989.

Mistou,M.Y., Cool,R.H., and Parmeggiani,A. (1992). Effects of ions on the intrinsic activities of c-H-ras protein p21. A comparison with elongation factor Tu. Eur. J. Biochem. *204*, 179-185.

Mittal,R., Ahmadian,M.R., Goody,R.S., and Wittinghofer,A. (1996). Formation of a transition-state analog of the Ras GTPase reaction by Ras-GDP, tetrafluoroaluminate, and GTPase-activating proteins. Science *273*, 115-117.

Montoya,G., Kaat,K., Moll,R., Schafer,G., and Sinning,I. (2000). The crystal structure of the conserved GTPase of SRP54 from the archaeon Acidianus ambivalens and its comparison with related structures suggests a model for the SRP-SRP receptor complex. Structure. Fold. Des *8*, 515-525.

Montoya,G., Svensson,C., Luirink,J., and Sinning,I. (1997). Crystal structure of the NG domain from the signal-recognition particle receptor FtsY. Nature *385*, 365-368.

Morrow,M.W. and Brodsky,J.L. (2001). Yeast ribosomes bind to highly purified reconstituted Sec61p complex and to mammalian p180. Traffic. *2*, 705-716.

Mossessova,E., Gulbis,J.M., and Goldberg,J. (1998). Structure of the guanine nucleotide exchange factor Sec7 domain of human arno and analysis of the interaction with ARF GTPase. Cell *92*, 415-423.

Murphy,E.C., III, Zheng,T., and Nicchitta,C.V. (1997). Identification of a novel stage of ribosome/nascent chain association with the endoplasmic reticulum membrane. J. Cell Biol. *136*, 1213-1226.

Musch,A., Wiedmann,M., and Rapoport,T.A. (1992). Yeast Sec proteins interact with polypeptides traversing the endoplasmic reticulum membrane. Cell *69*, 343-352.

Neumann-Haefelin,C., Schafer,U., Muller,M., and Koch,H.G. (2000). SRP-dependent co-translational targeting and SecA-dependent translocation analyzed as individual steps in the export of a bacterial protein. EMBO J. *19*, 6419-6426.

Newitt,J.A. and Bernstein,H.D. (1997). The N-domain of the signal recognition particle 54-kDa subunit promotes efficient signal sequence binding. Eur. J. Biochem. *245*, 720-729.

NG,D.T., Brown,J.D., and Walter,P. (1996). Signal sequences specify the targeting route to the endoplasmic reticulum membrane. J. Cell Biol. *134*, 269-278.

Nicchitta,C.V., Murphy,E.C., III, Haynes,R., and Shelness,G.S. (1995). Stage- and ribosome-specific alterations in nascent chain-Sec61p interactions accompany translocation across the ER membrane. J. Cell Biol. *129*, 957-970.

Ogg,S.C., Barz,W.P., and Walter,P. (1998). A functional GTPase domain, but not its transmembrane domain, is required for function of the SRP receptor beta-subunit. J. Cell Biol. *142*, 341-354.

Ogg,S.C., Poritz,M.A., and Walter,P. (1992). Signal recognition particle receptor is important for cell growth and protein secretion in Saccharomyces cerevisiae. Mol. Biol. Cell *3*, 895-911.

Ogg,S.C. and Walter,P. (1995). SRP samples nascent chains for the presence of signal sequences by interacting with ribosomes at a discrete step during translation elongation. Cell *81*, 1075-1084.

Padmanabhan,S. and Freymann,D.M. (2001). The conformation of bound GMPPNP suggests a mechanism for gating the active site of the SRP GTPase. Structure. (Camb.) *9*, 859-867.

Pai,E.F., Kabsch,W., Krengel,U., Holmes,K.C., John,J., and Wittinghofer,A. (1989). Structure of the guanine-nucleotide-binding domain of the Ha-ras oncogene product p21 in the triphosphate conformation. Nature *341*, 209-214.

Pai,E.F., Krengel,U., Petsko,G.A., Goody,R.S., Kabsch,W., and Wittinghofer,A. (1990). Refined crystal structure of the triphosphate conformation of H-ras p21 at 1.35 A resolution: implications for the mechanism of GTP hydrolysis. EMBO J. *9*, 2351-2359.

Panzner,S., Dreier,L., Hartmann,E., Kostka,S., and Rapoport,T.A. (1995). Posttranslational protein transport in yeast reconstituted with a purified complex of Sec proteins and Kar2p. Cell *81*, 561-570.

Pasqualato,S., Menetrey,J., Franco,M., and Cherfils,J. (2001). The structural GDP/GTP cycle of human Arf6. EMBO Rep. *2*, 234-238.

Pederson,T. and Politz,J.C. (2000). The nucleolus and the four ribonucleoproteins of

translation. J. Cell Biol. *148*, 1091-1095.

Plath,K. and Rapoport,T.A. (2000). Spontaneous release of cytosolic proteins from posttranslational substrates before their transport into the endoplasmic reticulum. J. Cell Biol. *151*, 167-178.

Plemper,R.K., Bohmler,S., Bordallo,J., Sommer,T., and Wolf,D.H. (1997). Mutant analysis links the translocon and BiP to retrograde protein transport for ER degradation. Nature *388*, 891-895.

Poe,M., Scolnick,E.M., and Stein,R.B. (1985). Viral Harvey ras p21 expressed in Escherichia coli purifies as a binary one-to-one complex with GDP. J. Biol. Chem. *260*, 3906-3909.

Politz,J.C., Yarovoi,S., Kilroy,S.M., Gowda,K., Zwieb,C., and Pederson,T. (2000). Signal recognition particle components in the nucleolus. Proc. Natl. Acad. Sci. U. S. A *97*, 55-60.

Pool,M.R., Stumm,J., Fulga,T.A., Sinning,I., and Dobberstein,B. (2002). Distinct modes of signal recognition particle interaction with the ribosome. Science *297*, 1345-1348.

Poritz,M.A., Bernstein,H.D., Strub,K., Zopf,D., Wilhelm,H., and Walter,P. (1990). An E. coli ribonucleoprotein containing 4.5S RNA resembles mammalian signal recognition particle. Science *250*, 1111-1117.

Powers,T. and Walter,P. (1995). Reciprocal stimulation of GTP hydrolysis by two directly interacting GTPases. Science *269*, 1422-1424.

Prinz,A., Behrens,C., Rapoport,T.A., Hartmann,E., and Kalies,K.U. (2000a). Evolutionarily conserved binding of ribosomes to the translocation channel via the large ribosomal RNA. EMBO J. *19*, 1900-1906.

Prinz,A., Hartmann,E., and Kalies,K.U. (2000b). Sec61p is the main ribosome receptor in the endoplasmic reticulum of Saccharomyces cerevisiae. Biol. Chem. *381*, 1025-1029.

Qi,H.Y. and Bernstein,H.D. (1999). SecA is required for the insertion of inner membrane proteins targeted by the Escherichia coli signal recognition particle. J. Biol. Chem. *274*, 8993-8997.

Qi,H.Y., Hyndman,J.B., and Bernstein,H.D. (2002). DnaK promotes the selective export of outer membrane protein precursors in SecA-deficient Escherichia coli. J. Biol. Chem. *277*, 51077-51083.

Raden,D., Song,W., and Gilmore,R. (2000). Role of the cytoplasmic segments of Sec61alpha in the ribosome-binding and translocation-promoting activities of the Sec61 complex. J. Cell Biol. *150*, 53-64.

Rapiejko,P.J. and Gilmore,R. (1992). Protein translocation across the ER requires a functional GTP binding site in the alpha subunit of the signal recognition particle receptor. J. Cell Biol. *117*, 493-503.

Rapiejko,P.J. and Gilmore,R. (1997). Empty site forms of the SRP54 and SR alpha GTPases mediate targeting of ribosome-nascent chain complexes to the endoplasmic reticulum. Cell *89*, 703-713.

Ribes,V., Romisch,K., Giner,A., Dobberstein,B., and Tollervey,D. (1990). E. coli 4.5S RNA is part of a ribonucleoprotein particle that has properties related to signal recognition particle. Cell *63*, 591-600.

Robinson,C. and Bolhuis,A. (2001). Protein targeting by the twin-arginine translocation pathway. Nat. Rev. Mol. Cell Biol. *2* , 350-356.

Romisch,K., Webb,J., Herz,J., Prehn,S., Frank,R., Vingron,M., and Dobberstein,B. (1989). Homology of 54K protein of signal-recognition particle, docking protein and two E. coli proteins with putative GTP-binding domains. Nature *340*, 478-482.

Romisch,K., Webb,J., Lingelbach,K., Gausepohl,H., and Dobberstein,B. (1990). The 54-kD protein of signal recognition particle contains a methionine-rich RNA binding domain. J. Cell Biol. *111*, 1793-1802.

Samuelson,J.C., Chen,M., Jiang,F., Moller,I., Wiedmann,M., Kuhn,A., Phillips,G.J., and Dalbey,R.E. (2000). YidC mediates membrane protein insertion in bacteria. Nature *406*, 637-641.

Sanders,S.L., Whitfield,K.M., Vogel,J.P., Rose,M.D., and Schekman,R.W. (1992). Sec61p and BiP directly facilitate polypeptide translocation into the ER. Cell *69*, 353-365.

Schatz,P.J., Riggs,P.D., Jacq,A., Fath,M.J., and Beckwith,J. (1989). The secE gene encodes an integral membrane protein required for protein export in Escherichia coli. Genes Dev. *3*, 1035-1044.

Scheffzek,K., Ahmadian,M.R., Kabsch,W., Wiesmuller,L., Lautwein,A., Schmitz,F., and Wittinghofer,A. (1997). The Ras-RasGAP complex: structural basis for GTPase activation and its loss in oncogenic Ras mutants. Science *277*, 333-338.

Schiebel,E., Driessen,A.J., Hartl,F.U., and Wickner,W. (1991). Delta mu H+ and ATP function at different steps of the catalytic cycle of preprotein translocase. Cell *64*, 927-939.

Schwartz,T. and Blobel,G. (2003). Structural basis for the function of the Beta subunit of the eukaryotic signal recognition particle receptor. Cell *112*, 793-803.

Scotti,P.A., Urbanus,M.L., Brunner,J., de Gier,J.W., von Heijne,G., Van Der,D.C., Driessen,A.J., Oudega,B., and Luirink,J. (2000). YidC, the Escherichia coli homologue of mitochondrial Oxa1p, is a component of the Sec translocase. EMBO J. *19*, 542-549.

Seeburg,P.H., Colby,W.W., Capon,D.J., Goeddel,D.V., and Levinson,A.D. (1984). Biological properties of human c-Ha-ras1 genes mutated at codon 12. Nature *312*, 71-75.

Seewald,M.J., Korner,C., Wittinghofer,A., and Vetter,I.R. (2002). RanGAP mediates GTP hydrolysis without an arginine finger. Nature *415*, 662-666.

Shapiro,A.D., Riederer,M.A., and Pfeffer,S.R. (1993). Biochemical analysis of rab9, a ras-like GTPase involved in protein transport from late endosomes to the trans Golgi network. J. Biol. Chem. *268*, 6925-6931.

Siegel,V. and Walter,P. (1986). Removal of the Alu structural domain from signal recognition particle leaves its protein translocation activity intact. Nature *320*, 81-84.

Sigal,I.S., Gibbs,J.B., D'Alonzo,J.S., Temeles,G.L., Wolanski,B.S., Socher,S.H., and Scolnick,E.M. (1986). Mutant ras-encoded proteins with altered nucleotide binding exert dominant biological effects. Proc. Natl. Acad. Sci. U. S. A *83*, 952-956.

Simon,S.M. and Blobel,G. (1991). A protein-conducting channel in the endoplasmic reticulum. Cell *65*, 371-380.

Sondek,J., Lambright,D.G., Noel,J.P., Hamm,H.E., and Sigler,P.B. (1994). GTPase mechanism of Gproteins from the 1.7-A crystal structure of transducin alpha-GDP-AIF-4. Nature *372*, 276-279.

Song,W., Raden,D., Mandon,E.C., and Gilmore,R. (2000). Role of Sec61alpha in the regulated transfer of the ribosome-nascent chain complex from the signal recognition particle to the translocation channel. Cell *100*, 333-343.

Sprang,S.R. (1997). G protein mechanisms: insights from structural analysis. Annu. Rev. Biochem. *66*, 639-678.

Stanley,N.R., Palmer,T., and Berks,B.C. (2000). The twin arginine consensus motif of

Tat signal peptides is involved in Sec-independent protein targeting in Escherichia coli. J. Biol. Chem. *275*, 11591-11596.

Stirling,C.J. and Hewitt,E.W. (1992). The S. cerevisiae SEC65 gene encodes a component of yeast signal recognition particle with homology to human SRP19. Nature *356*, 534-537.

Sung,Y.J., Carter,M., Zhong,J.M., and Hwang,Y.W. (1995). Mutagenesis of the H-ras p21 at glycine-60 residue disrupts GTP-induced conformational change. Biochemistry *34*, 3470-3477.

Suzuki,H., Nishiyama,K., and Tokuda,H. (1998). Coupled structure changes of SecA and SecG revealed by the synthetic lethality of the secAcsR11 and delta secG::kan double mutant. Mol. Microbiol. *29*, 331-341.

Tajima,S., Lauffer,L., Rath,V.L., and Walter,P. (1986). The signal recognition particle receptor is a complex that contains two distinct polypeptide chains. J. Cell Biol. *103*, 1167-1178.

Taura,T., Baba,T., Akiyama,Y., and Ito,K. (1993). Determinants of the quantity of the stable SecY complex in the Escherichia coli cell. J. Bacteriol. *175*, 7771-7775.

Thomas,Y., Bui,N., and Strub,K. (1997). A truncation in the 14 kDa protein of the signal recognition particle leads to tertiary structure changes in the RNA and abolishes the elongation arrest activity of the particle. Nucleic Acids Res. *25*, 1920-1929.

Tian,H. and Beckwith,J. (2002). Genetic screen yields mutations in genes encoding all known components of the Escherichia coli signal recognition particle pathway. J. Bacteriol. *184*, 111-118.

Tian,H., Boyd,D., and Beckwith,J. (2000). A mutant hunt for defects in membrane protein assembly yields mutations affecting the bacterial signal recognition particle and Sec machinery. Proc. Natl. Acad. Sci. U. S. A *97*, 4730-4735.

Topping,T.B. and Randall,L.L. (1997). Chaperone SecB from Escherichia coli mediates kinetic partitioning via a dynamic equilibrium with its ligands. J. Biol. Chem. *272*, 19314-19318.

Trahey,M. and McCormick,F. (1987). A cytoplasmic protein stimulates normal N-ras p21 GTPase, but does not affect oncogenic mutants. Science *238*, 542-545.

Traxler,B. and Murphy,C. (1996). Insertion of the polytopic membrane protein MalF is dependent on the bacterial secretion machinery. J. Biol. Chem. *271*, 12394-12400.

Tyson,J.R. and Stirling,C.J. (2000). LHS1 and SIL1 provide a lumenal function that is essential for protein translocation into the endoplasmic reticulum. EMBO J. *19*, 6440-6452.

Urbanus,M.L., Scotti,P.A., Froderberg,L., Saaf,A., de Gier,J.W., Brunner,J., Samuelson,J.C., Dalbey,R.E., Oudega,B., and Luirink,J. (2001). Sec-dependent membrane protein insertion: sequential interaction of nascent FtsQ with SecY and YidC. EMBO Rep. *2*, 524-529.

Valent,Q.A., Scotti,P.A., High,S., de Gier,J.W., von Heijne,G., Lentzen,G., Wintermeyer,W., Oudega,B., and Luirink,J. (1998). The Escherichia coli SRP and SecB targeting pathways converge at the translocon. EMBO J. *17*, 2504-2512.

Vetter,I.R. and Wittinghofer,A. (2001). The guanine nucleotide-binding switch in three dimensions. Science *294*, 1299-1304.

von Heijne,G. (1985). Signal sequences. The limits of variation. J. Mol. Biol. *184*, 99-105.

von Heijne,G. and Gavel,Y. (1988). Topogenic signals in integral membrane proteins. Eur. J. Biochem. *174*, 671-678.

Walter,P. and Blobel,G. (1980). Purification of a membrane-associated protein complex required for protein translocation across the endoplasmic reticulum. Proc. Natl. Acad. Sci. U. S. A *77*, 7112-7116.

Walter,P. and Blobel,G. (1981). Translocation of proteins across the endoplasmic reticulum III. Signal recognition protein (SRP) causes signal sequence-dependent and site-specific arrest of chain elongation that is released by microsomal membranes. J. Cell Biol. *91*, 557-561.

Walter,P. and Blobel,G. (1982). Signal recognition particle contains a 7S RNA essential for protein translocation across the endoplasmic reticulum. Nature *299*, 691-698.

Walter,P. and Blobel,G. (1983a). Disassembly and reconstitution of signal recognition particle. Cell *34*, 525-533.

Walter,P. and Blobel,G. (1983b). Preparation of microsomal membranes for cotranslational protein translocation. Methods Enzymol. *96*, 84-93.

Walter,P., Ibrahimi,I., and Blobel,G. (1981). Translocation of proteins across the endoplasmic reticulum. I. Signal recognition protein (SRP) binds to in-vitro-assembled polysomes synthesizing secretory protein. J. Cell Biol. *91*, 545-550.

Wang,L. and Dobberstein,B. (1999). Oligomeric complexes involved in translocation of proteins across the membrane of the endoplasmic reticulum. FEBS Lett. *457*, 316-322.

Wang,Y. and Colicelli,J. (2001). RAS interaction with effector target RIN1. Methods Enzymol. *332*, 139-151.

Wattenberg,B. and Lithgow,T. (2001). Targeting of C-terminal (tail)-anchored proteins: understanding how cytoplasmic activities are anchored to intracellular membranes. Traffic. *2*, 66-71.

Watts,C., Wickner,W., and Zimmermann,R. (1983). M13 procoat and a pre-immunoglobulin share processing specificity but use different membrane receptor mechanisms. Proc. Natl. Acad. Sci. U. S. A *80*, 2809-2813.

Weijland,A., Parlato,G., and Parmeggiani,A. (1994). Elongation factor Tu D138N, a mutant with modified substrate specificity, as a tool to study energy consumption in protein biosynthesis. Biochemistry *33* , 10711-10717.

Weiss,O., Holden,J., Rulka,C., and Kahn,R.A. (1989). Nucleotide binding and cofactor activities of purified bovine brain and bacterially expressed ADP-ribosylation factor. J. Biol. Chem. *264*, 21066-21072.

Wilkinson,B.M., Tyson,J.R., and Stirling,C.J. (2001). Ssh1p determines the translocation and dislocation capacities of the yeast endoplasmic reticulum. Dev. Cell *1*, 401-409.

Wittke,S., Dunnwald,M., Albertsen,M., and Johnsson,N. (2002). Recognition of a subset of signal sequences by Ssh1p, a Sec61p-related protein in the membrane of endoplasmic reticulum of yeast Saccharomyces cerevisiae. Mol. Biol. Cell *13*, 2223-2232.

Wittke,S., Lewke,N., Muller,S., and Johnsson,N. (1999). Probing the molecular environment of membrane proteins in vivo. Mol. Biol. Cell *10*, 2519-2530.

Yahr,T.L. and Wickner,W.T. (2000). Evaluating the oligomeric state of SecYEG in preprotein translocase. EMBO J. *19*, 4393-4401.

Yahr,T.L. and Wickner,W.T. (2001). Functional reconstitution of bacterial Tat translocation in vitro. EMBO J. *20*, 2472-2479.

Yang,Y.B., Yu,N., and Tai,P.C. (1997). SecE-depleted membranes of Escherichia coli are active. SecE is not obligatorily required for the in vitro translocation of certain protein precursors. J. Biol. Chem. *272*, 13660-13665.

Yen,M.R., Tseng,Y.H., Nguyen,E.H., Wu,L.F., and Saier,M.H., Jr. (2002). Sequence and

phylogenetic analyses of the twin-arginine targeting (Tat) protein export system. Arch. Microbiol. *177*, 441-450.

Young,B.P., Craven,R.A., Reid,P.J., Willer,M., and Stirling,C.J. (2001). Sec63p and Kar2p are required for the translocation of SRP-dependent precursors into the yeast endoplasmic reticulum in vivo. EMBO J. *20*, 262-271.

Young,J.C. and Andrews,D.W. (1996). The signal recognition particle receptor alpha subunit assembles co-translationally on the endoplasmic reticulum membrane during an mRNA-encoded translation pause in vitro. EMBO J. *15*, 172-181.

Young,J.C., Ursini,J., Legate,K.R., Miller,J.D., Walter,P., and Andrews,D.W. (1995). An amino-terminal domain containing hydrophobic and hydrophilic sequences binds the signal recognition particle receptor alpha subunit to the beta subunit on the endoplasmic reticulum membrane. J. Biol. Chem. *270*, 15650-15657.

Zimmermann,R. and Mollay,C. (1986). Import of honeybee prepromelittin into the endoplasmic reticulum. Requirements for membrane insertion, processing, and sequestration. J. Biol. Chem. *261*, 12889-12895.

Zopf,D., Bernstein,H.D., Johnson,A.E., and Walter,P. (1990). The methionine-rich domain of the 54 kd protein subunit of the signal recognition particle contains an RNA binding site and can be crosslinked to a signal sequence. EMBO J. *9*, 4511-4517.

Appendix 1: Calculation of SRβ GTPase activity in the presence of ribosomes

Based on data from Figure 5 published in Bacher et al. 1999

In this experiment, the authors incubate proteoliposomes (40 nM SRβ) with 0.5 μM α-^{32}P-GTP and 8.4 OD_{260}/ml RNCs (160 nM) for 40 minutes at 25°C. After 40 minutes the reaction is stopped and α-^{32}P-GDP/GTP was determined by TLC.

Assumptions:

1. RNCs do not contribute to GTP hydrolysis,

2. 100% of the SRβ is biologically active,

3. 1 L reaction volume (true reaction volume is not reported, but molar concentrations of reagents are reported, so volume of reaction will not affect the calculations).

The data in Figure 5 is presented as a bar graph with the Y-axis corresponding to % GTP hydrolysis. The column corresponding to SRβ -RNCs shows <1% hydrolysis, the column corresponding to SRβ +RNCs shows ~8% hydrolysis.

Therefore, in a 1 L reaction, the starting material contains 40 nmoles of SRβ and 0.5 μmoles γ-[^{32}P]-GTP.

8% of the GTP is hydrolysed in 40 minutes, representing 0.04 μmoles, or 40 nmoles.

Therefore, there is a 1:1 relationship between SRβ and hydrolysed GTP, suggesting that the interaction between RNCs and SRβ is not catalytic (ie. multiple turnover does not occur).

Appendix 1: Calculation of SRβ GTPase activity in the presence of ribosomes

Based on data from Figure 5 published in Bacher et al. 1999

In this experiment, the authors incubate proteoliposomes (40 nM SRβ) with 0.5 μM α-^{32}P-GTP and 8.4 OD_{260}/ml RNCs (160 nM) for 40 minutes at 25°C. After 40 minutes the reaction is stopped and α-^{32}P-GDP/GTP was determined by TLC.

Assumptions:

1. RNCs do not contribute to GTP hydrolysis,

2. 100% of the SRβ is biologically active,

3. 1 L reaction volume (true reaction volume is not reported, but molar concentrations of reagents are reported, so volume of reaction will not affect the calculations).

The data in Figure 5 is presented as a bar graph with the Y-axis corresponding to % GTP hydrolysis. The column corresponding to SRβ -RNCs shows <1% hydrolysis, the column corresponding to SRβ +RNCs shows ~8% hydrolysis.

Therefore, in a 1 L reaction, the starting material contains 40 nmoles of SRβ and 0.5 μmoles γ-[^{32}P]-GTP.

8% of the GTP is hydrolysed in 40 minutes, representing 0.04 μmoles, or 40 nmoles.

Therefore, there is a 1:1 relationship between SRβ and hydrolysed GTP, suggesting that the interaction between RNCs and SRβ is not catalytic (ie. multiple turnover does not occur).